CENTRAL RESEARCH LIBRARY
DOCUMENT COLLECTION

[redacted]

MARTIN MARIETTA ENERGY SYSTEMS LIBRARIES
3 4456 0360728 3

DECLASSIFIED
CLASSIFICATION CHANGED TO:
BY AUTHORITY OF: AEC 8-26-56
BY: D. Johnstone 11-27-56

ORNL 1796 22A

THE COMBINATION OF HYDROGEN AND OXYGEN IN PLATINUM CATALYZED FLOW REACTORS

H. J. Garber
F. N. Peebles

CENTRAL RESEARCH LIBRARY
DOCUMENT COLLECTION
LIBRARY LOAN COPY
DO NOT TRANSFER TO ANOTHER PERSON
If you wish someone else to see this document, send in name with document and the library will arrange a loan.

OAK RIDGE NATIONAL LABORATORY
OPERATED BY
CARBIDE AND CARBON CHEMICALS COMPANY
A DIVISION OF UNION CARBIDE AND CARBON CORPORATION
UCC
POST OFFICE BOX P
OAK RIDGE, TENNESSEE

[redacted]

This document contains Restricted Data as defined in the Atomic Energy Act of 1946. Its transmittal or the disclosure of its contents in any manner to an unauthorized person is prohibited.

[redacted]

[redacted]

ORNL 1796
This document consists of 80 pages.
Copy 22 of 41 copies. Series A.

Contract No. W-7405, Eng 26
Subcontract S-370
Reactor Experimental Engineering Division

THE COMBINATION OF HYDROGEN AND OXYGEN IN PLATINUM CATALYZED FLOW REACTORS

By

HAROLD J. GARBER
AND
FRED N. PEEBLES
Department of Chemical Engineering
The University of Tennessee

Date Issued OCT 26 1954

OAK RIDGE NATIONAL LABORATORY
Operated By
CARBIDE AND CARBON CHEMICALS DIVISION
Union Carbide and Carbon Corporation
Post Office Box P
Oak Ridge, Tennessee

[redacted]

MARTIN MARIETTA ENERGY SYSTEMS LIBRARIES
3 4456 0360728 3

[redacted]

INTERNAL DISTRIBUTION

1. R. E. Aven
2. J. N. Baird
3. S. E. Beall
4. T. G. Bohlmann
5. R. B. Briggs
6. F. R. Bruce
7. J. S. Culver
8. M. C. Edlund
9. W. R. Gall
10. C. B. Graham
11. J. A. Lane
12. R. N. Lyon
13. E. C. Miller
14. W. C. Moore
15. H. F. Poppendiek
16. W. L. Ross
17. I. Spiewak
18. J. A. Swartout
19. A. M. Weinberg
20. C. E. Winters
21. Biology Library
22. Central Research Library
23. Chemistry Library
24. Health Physics Library
25. Metallurgy Library
26. Physics Library
27. Reactor Experimental Engineering Library
28. Training School Library
29.-31. Laboratory Records

EXTERNAL DISTRIBUTION

32.-33. Argonne National Laboratory
34.-35. AEC, Washington
36.-37. Los Alamos Scientific Laboratory
38.-39. North American Aviation
40.-41. TIS, Oak Ridge

[redacted]

RESTRICTED DATA

This document contains restricted data as defined in the Atomic Energy Act of 1954. Its transmission or the disclosure of its contents in any manner to an unauthorized person is prohibited.

TABLE OF CONTENTS

	Page
LIST OF TABLES	4
LIST OF FIGURES	5,6
ABSTRACT	7
MOTIVATION	9
INTRODUCTION	9,10,12,13,14
BASIC RELATIONSHIPS	14,15,16,17
CONSIDERATION OF VARIOUS RECOMBINATION MECHANISMS	17,18,19,20,21, 22,23,24,25
Case I. Oxygen Diffusion Controls The Recombination Rate	
Case II. Hydrogen Diffusion Controls The Recombination Rate	
Case III. Oxygen And Hydrogen Diffusion Each Control For A Portion Of The Bed	
Case IV. Langmuir Mechanism, Oxygen Diffusion Controls With Surface Restricted	
Case V. Dual-Langmuir Mechanism, Both Oxygen And Hydrogen Diffusion Control With Surface Restricted	
EVALUATION OF THE MASS TRANSFER COEFFICIENTS	25,26,27,28,36, 39,41,48,53,54
Relationship Between The Mass Transfer Coefficients For The Two Zones	
Justification Of The Application Of The Gamson Correlation	
Characteristics Of The Recombiner Bed	
Calculated Mass Transfer Coefficients And Dimensionless Groups	
Temperature Rise Accompanying The Recombination Reaction	
EVALUATION OF TRANSPORT AND RELATED PROPERTIES	54,55,56,62,63, 64,66,67
Calculation Of Viscosities Of Gas Mixtures	
Calculation Of Diffusivities	
Calculation Of Gas Mixture Densities	
CONSIDERATION OF THE GAS FLOW VELOCITY PROFILE	67,70,71
RECOMMENDATIONS FOR FUTURE EXPERIMENTATION	74,75
REFERENCES CITED	76
TABLE OF SYMBOLS	77,78,79,80

LIST OF TABLES

Number	Description	Page
I	Observed And Calculated Primary Recombiner Data	29,30,31
II	Calculated Mass Transfer Coefficients And Dimensionless Groups	32,33,34
III	Mean Values Of The Mass Transfer Dimensionless Groups	42
IV	Comparison Of The Observed And Calculated Values Of The Dual-Langmuir Mechanism Mass Transfer Dimensionless Groups	52
V	Values Of The Collision Integrals $W^{(1)}(1;kT/\epsilon)$ And $W^{(2)}(2;kT/\epsilon)$	57
VI	Summary Of Pertinent Quantities Used For Calculating Transport Properties	59
VII	Values Of The Function ψ	62
VIII	Comparison Of Calculated Versus Estimated Viscosities Of Steam-Hydrogen-Oxygen Mixtures	62
IX	Calculated Viscosities Of Superheated Steam At Relatively Low Pressures	63
X	Calculated Binary Diffusion Coefficients At 10 psia	66
XI	Estimated Compressibility Factors Of Steam-Hydrogen-Oxygen Mixtures	67

LIST OF FIGURES

Number	Description	Page
I	Variation Of Instantaneous Mole Ratio Of Oxygen To Hydrogen In The Gas Stream With Fraction Of Completion Of Hydrogen Recombination And Initial Oxygen To Hydrogen Mole Ratio.	11
2	Justification Of The Reynolds Number Dependence Of The Dual-Langmuir Mechanism Mass Transfer Coefficient; Logarithmic Plots Of Data Of Experiments Of May 5, 7, 11, and 12.	35
3	Justification Of The Schmidt Number Dependence Of The Dual-Langmuir Mechanism Mass Transfer Coefficient; Data Of Experiments Of April 21 and 22.	37
4	Justification Of The Schmidt Number Dependence Of The Dual-Langmuir Mechanism Mass Transfer Coefficient; Data Of Experiments Of May 19.	38
5	Significant Details Of The Catalytic Recombiner	40
6	Temperature Dependence Of The Mass Transfer Dimensionless Group For Case I; Oxygen Diffusion Rate Controlling Over Entire Bed.	43
7	Temperature Dependence Of The Mass Transfer Dimensionless Group For Case II; Hydrogen Diffusion Rate Controlling Over Entire Bed.	44
8	Temperature Dependence Of The Langmuir Mass Transfer Dimensionless Group For Case III; Oxygen Diffusion Rate Controlling Over Entire Bed With Catalytic Surface Restricted.	45
9	Temperature Dependence Of The Mass Transfer Dimensionless Group For Case IV; Oxygen And Hydrogen Diffusion Rates Controlling For Separate Portions Of The Bed.	46
10	Temperature Dependence Of The Dual-Langmuir Mass Transfer Dimensionless Group For Case V; Oxygen And Hydrogen Diffusion Rates Controlling For Separate Portions Of The Bed With Catalytic Surface Restricted. Curve Shows Correlation According To Eyring Equation.	47

Number	Description	Page
11	Correlation Of Dependence Of The Dual-Langmuir Mass Transfer Dimensionless Group On Temperature According To Arrhenius Equation.	49
12	Rectification Of The Dual-Langmuir Mass Transfer Dimensionless Group Data In Accordance With The Eyring Equation; Logarithmic Plot Of The Dimensionless Group Divided By Absolute Temperature Versus Reciprocal Of Absolute Temperature.	50
13	Rectification Of The Dual-Langmuir Mass Transfer Dimensionless Group Data In Accordance With The Arrhenius Equation; Logarithmic Plot Of The Dimensionless Group Versus Reciprocal Of Absolute Temperature.	51
14	Values Of The Collision Integrals $W^{(2)}(2;kT/\epsilon)$ As A Function Of kT/ϵ.	58
15	Variation of Y_{ij} With Temperature For The System Steam-Hydrogen-Oxygen.	60
16	Variation Of Z_{ij} With Temperature For The System Steam-Hydrogen-Oxygen.	61
17	Variation Of The Binary Diffusion Coefficients For The System Steam-Hydrogen-Oxygen At 10 psia With Temperature.	65
18	Compressibility Factor For The System Steam-Hydrogen-Oxygen As A Function Of Temperature And Pressure.	68
19	Variation Of The Ratio Of Point To Mean Velocity As A Function Of Radial Position Ratio In A 2 Inch Pipe Packed With 1/4 Inch Cylinders.	69
20	Numerical Solution Of The Catalytic Bed Equation For Run No. 3 Of April 16.	72
21	Calculated Variation Of Discharge Steam Hydrogen Mole Fraction And Dual-Langmuir Point Mass Transfer Coefficient With Radial Position For Run No. 3 Of April 16.	73

ABSTRACT

An extension of the concepts advanced by Langmuir regarding the nature of the platinum catalyzed oxidation of hydrogen and the application of the resulting theory to the experimental data observed by Ransohoff and Spiewak for an HRE type recombiner indicates that their data are correlated by the dimensionless equations *

$$\frac{K_{L_1}/(G/M_m)_1}{(1-v)^{0.2}}\left[\frac{\mu}{D\rho}\right]^{2/3}_{f_1}\left[\frac{D_p G}{\mu\phi(1-v)}\right]^{0.41} = \begin{cases} 2.46 \times 10^{-4}\ T_g\ e^{-933/T_g} \\ 0.426\ e^{-1560/T_g} \end{cases}$$

equally well, with a mean deviation of 3.8 per cent. This expression is recommended as a basis for the design of catalytic recombiners.

The catalytic combination is pictured as consisting of two surface chemical mechanisms, one of which is oxygen diffusion controlled, the other hydrogen diffusion regulated, the mechanism "change-over" occurring at that point in the recombiner where the components are arriving at the catalyst surface by diffusion in stoichiometric proportions. The catalyst volume requirements for these two portions of the bed are shown to be

$$aL_1 = \frac{V_0}{JK_{L_1}}\left[2\,\frac{H_1 - H_2}{1-0.5H_1} - (2O_0 - H_0)\ \ln\frac{1}{1 - \dfrac{0.5(H_0-H_1)}{O_0(1-0.5H_1)}}\right]$$

$$aL_2 = \frac{V_0}{2JK_{L_2}}\left[\frac{(1-0.5H_0)(H_1-H_2)}{(1-0.5H_1)(1-0.5H_2)} + (2O_0-H_0)\ \ln\frac{H_1(1-0.5H_2)}{H_2(1-0.5H_1)}\right]$$

The hydrogen mole fraction at the mechanism "change-over" point is

$$H_1 = \frac{2.02\left[\dfrac{O_0-0.5H_0}{1-0.5H_0}\right]}{\dfrac{D_{12}}{D_{13}} - \left[1 - \dfrac{O_0 - 0.5H_0}{1-0.5H_0}\right]}$$

And the relationship between the two mass transfer coefficients is

$$K_{L_2} = 0.5\ K_{L_1}\left[\frac{Sc_1}{Sc_2}\right]^{2/3}\left[\frac{\mu_2}{\mu_1}\right]^{0.41}_{g}$$

* See page 78 for Table Of Symbols

Methods for evaluating the necessary transport properties of the ternary system steam-hydrogen-oxygen for carrying out design calculations are summarized, and the significant parameters are tabulated and plotted to facilitate these calculations.

The question of non-uniform velocity profiles in packed bed flow systems, as it applies to the recombiner problem, is considered, and it is indicated that small scale test data may be used directly as a basis for designing large units.

Finally, some of the questionable aspects of the analysis of the problem are reviewed, and further experiments that should be performed to settle the doubtful points are suggested.

Harold J. Garber

Fred N. Peebles

THE COMBINATION OF HYDROGEN AND OXYGEN IN PLATINUM CATALYZED FLOW REACTORS

By

HAROLD J. GARBER
AND
FRED N. PEEBLES
Department of Chemical Engineering
The University of Tennessee

MOTIVATION

The work described in this report was carried out during the period January-August 1954 under a research and consulting subcontract (No. W7405-eng 26, S-370, Supplemental Agreements No. 3 and 4) of the Oak Ridge National Laboratory. The motivation was the desire to evolve a satisfactory basis for making engineering design estimates for packed tube catalytic hydrogen-oxygen recombiners. The basis for testing proposed design equations are the experimental data presented in Progress Report 1583 of ORNL by Ransohoff and Spiewak (11)* for a small supported platinum catalyst type recombiner capable of handling the off-gases of the HRE when operating under low and full power.

INTRODUCTION

Of the two modes of approach possible, confining this investigation specifically to the catalytic bed used by Ransohoff and Spiewak, as opposed to treating platinum beds in general, the latter and broader plan was adopted. Consequently, in this report the final correlations of the data are made in terms of dimensionless groups containing the various mass transfer constants. This differs from the procedure of Ransohoff and Spiewak in that their analyses are in terms of the derived mass transfer coefficients. Based upon the existing data which are severely limited in that they are confined to one experimental bed, one specific catalyst pellet size, relatively narrow ranges of concentration for the reactive gases, and only small variation in gas feed rate, the justification for a generalized treatment of the data may not appear to be too strong. Nevertheless, this approach is followed since inherently it possesses merit.

Employing primarily empirical but nevertheless persuasive arguments, recently Gamson (3) has shown how diffusion controlled processes of many types can be given a unified treatment. By inserting appropriate factors to account for different particle shapes, fraction of voids in the bed, surface availability for flow, in addition to the usual quantities thought to be important in mass transfer, he was able to obtain a "grand" correlation of "j-factors" with Reynolds number, in substance a complete generalization of the Colburn procedure. Sufficient

* Numbers in parentheses refer to References Cited, see page 76.

evidence can be extricated from the data of Ransohoff and Spiewak to indicate that the diffusional aspects of the recombination reaction are essentially in line with the features of purely physical mass transfer, and hence a modification of the Gamson procedure should apply. This is considered adequate justification for the more generalized method of dealing with the mass transfer data in terms of dimensionless groups.

Another manner in which the treatment given here differs from that of Ransohoff and Spiewak is that it incorporates appropriate terms to account for the dependence of the recombination rate on the gas stream temperature. Ransohoff and Spiewak acknowledged that within the scatter of their derived mass transfer coefficients a temperature dependence, particularly for the lower temperature experiments, could be discerned, but they did not pursue this point further. This dependence is stronger than can be accounted for by failure to allow for variation of the Schmidt number of the diffusion film with temperature. In the development given in this report it is shown that the temperature dependence of the recombination rate is associated with the adsorption phenomena and surface reactions occurring on the platinum catalyst.

One of the basic ideas advanced by Ransohoff and Spiewak in their analysis is borrowed and extended in this investigation. For initial feed gas streams containing an excess of hydrogen ($O_0/H_0 < 0.5$)*, they picture the mechanism to be such that the rate of diffusion of oxygen through the boundary layer to the catalyst governs the recombination rate. On the other hand, for an initial gas stream containing a large oxygen excess ($O_0/H_0 >> 0.5$) they postulate that the recombination rate should be entirely hydrogen diffusion controlled. Within these two extremes, and particularly with a mild oxygen excess in the feed stream ($O_0/H_0 > 0.5$), they picture two reaction zones to exist in the recombiner bed. In the first portion, even though present in the gas stream in less than the stoichiometric ratio, hydrogen by virtue of its higher molecular or diffusion velocity is more abundant at the catalyst than is oxygen, so the recombination rate for this first portion should be oxygen diffusion regulated. But with recombination withdrawing hydrogen and oxygen molecules in the ratio 2:1, the hydrogen excess at the catalyst drops off with passage down the bed, and eventually a point is reached at which the hydrogen and oxygen arrive at the catalyst in the stoichiometric ratio. At this point a mechanism "change-over" occurs, and farther down the bed oxygen rather than hydrogen is the more abundant reactant with the consequence that the second portion of the bed is hydrogen diffusion controlled. Thus a feed gas containing the stoichiometric ratio ($O_0/H_0 = 0.5$) would be expected to develop only the oxygen diffusion controlled zone.

Figure 1 shows how the oxygen to hydrogen mole ratio (O/H) in the instantaneous gas stream (not within the diffusion or boundary layer) varies with the fraction of completion of recombination of hydrogen (f) and the initial oxygen to hydrogen mole ratio. The plausibility of the Ransohoff-Spiewak conjecture regarding the existence of two reaction zones is emphasized by this figure which demonstrates strikingly how a mild excess of oxygen is converted into a hugh excess at large percentages of completion of recombination.

* See page 77 for Table Of Symbols.

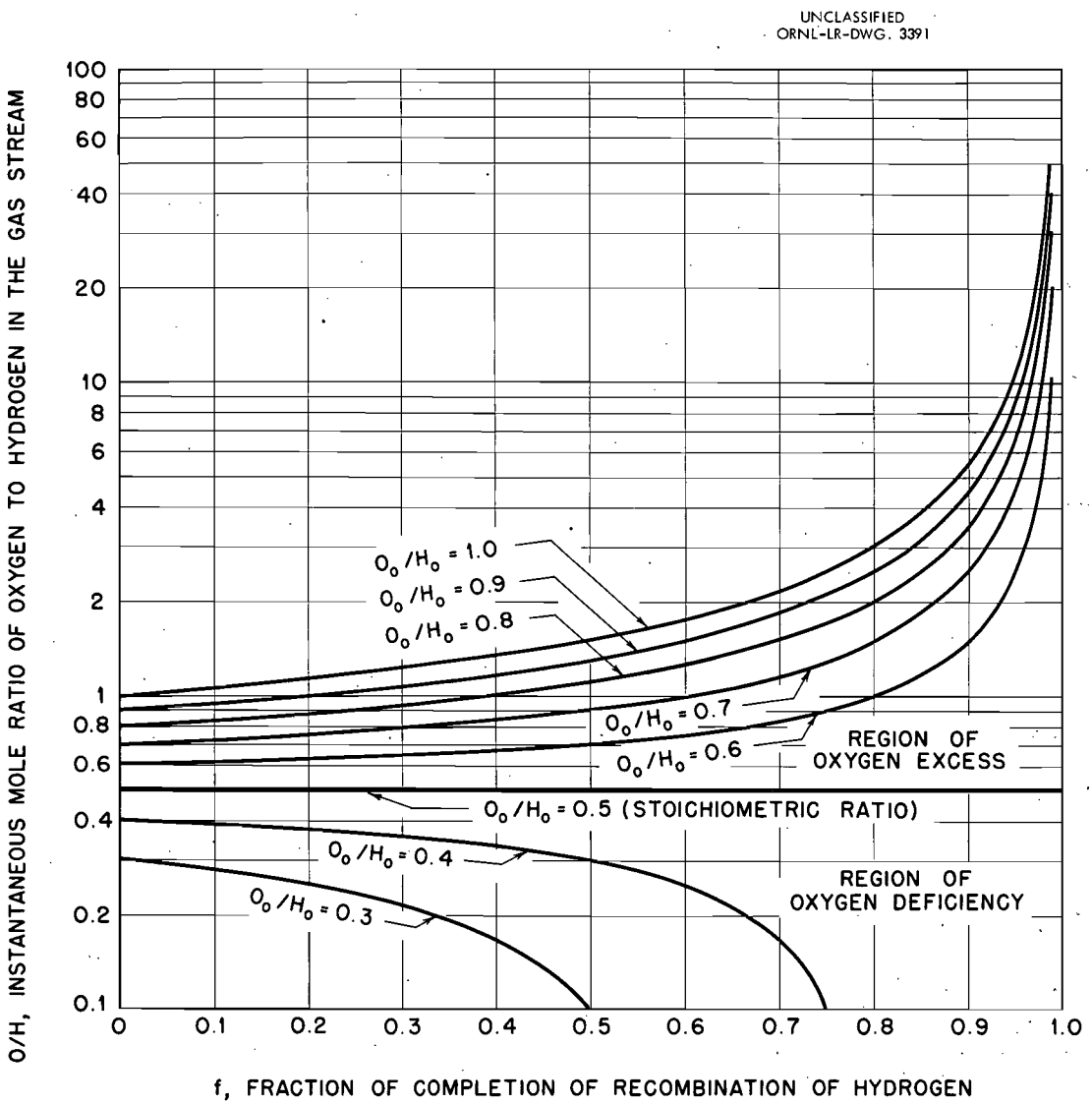

Figure 1

Variation Of Instantaneous Mole Ratio Of Oxygen To Hydrogen In The Gas Stream With Fraction Of Completion Of Hydrogen Recombination And Initial Oxygen To Hydrogen Mole Ratio.

As a consequence of examining several simplified recombination mechanisms and testing these with the data obtained by Ransohoff and Spiewak to discern which one best fits the existing facts, it is recommended that the "Dual-Langmuir" formulation, as developed in this report, be used as the basis for designing catalytic recombiners. Subsequently it will be indicated that additional improvements can be incorporated into this formulation, but these are contingent upon the completion of several additional sets of experiments designed to elucidate additional features of the surface reactions on the catalyst, particularly for the hydrogen diffusion controlled zone.

Although the main contribution of this investigation is the disclosure that the "Dual-Langmuir" formulation fits the observed recombiner data better than any of the other simple recombiner equations, for the sake of completeness these other developments are also presented in this report. Tabulations of the mass transfer coefficients derived from the same data according to the different mechanisms are also included here. Specifically, the separate mechanisms considered in testing the data are:

1. Oxygen diffusion is the rate governing step over the entire bed. All of the catalyst surface is available for oxygen temporary adsorption and activation.

2. Hydrogen diffusion is the rate governing step over the entire bed. All of the catalyst surface is available for hydrogen temporary adsorption and activation.

3. The bed consists of two zones, as pictured by Ransohoff and Spiewak. Oxygen diffusion is the rate governing step over the first portion of the bed, whereas hydrogen diffusion is the rate regulating step for the second portion. All of the catalyst surface is available in both zones. The mechanism change-over occurs at the "stoichiometric point" of the catalyst bed.

4. Oxygen diffusion is the rate governing step over the entire bed, but not all of the catalyst surface is available for oxygen temporary adsorption and activation. That fraction of the surface that is occupied by adsorbed hydrogen cannot induce oxygen activation, and the adsorbed hydrogen molecules are non-reactive to oxygen molecules which impinge on them, so that adsorbed hydrogen behaves as a catalyst poison. This mechanism was proposed by Langmuir (9) and is henceforth referred to as the "Langmuir mechanism" in this report.

5. Oxygen diffusion is the rate governing step for the first portion of the bed and hydrogen diffusion is the rate regulating step for the second portion, but only a portion of the catalyst surface is available for the appropriate activation in each zone. The mechanism change-over occurs at the stoichiometric point of the catalyst bed, as in Case 3, and adsorbed hydrogen and oxygen are catalyst poisons in the first and second zones respectively. This is a combination of the concepts of Ransohoff and Spiewak with those of Langmuir and is henceforth referred to as the "Dual-Langmuir" mechanism in this report.

The attitude that has been adopted in carrying out the investigation described in this report is that the final results should be exhibited in forms that are useful immediately to design engineers. Therefore, in conducting the analyses, it was necessary to avoid theoretical speculations that would introduce unknown quantities or factors that had little chance of being extricated from the existing experimental data or from our present meager knowledge concerning the mechanism details by which hydrogen and oxygen molecules combine under the influence of catalytic surfaces. The "elegant" method of approach would have been to write down the partial differential equations describing the diffusion of hydrogen and oxygen toward the catalyst and diffusion of steam away from the catalyst, meanwhile making appropriate allowances for non-isothermality of the system, momentum transfer among the fluid layers, lateral diffusion along the catalyst surface, and peculiarities of the gas velocity profile across the bed, to name a few of the more embarrassing details. Except for very simple situations, and then in a seriously approximated way, such procedures when applied to reaction kinetics problems have seldom been tractable. Considering the short time allotted for this problem, this avenue of approach did not hold out much promise. Further, the data on hand are too limited in many respects to yield answers to questions that would arise from such a detailed analysis.

In the immediate paragraphs that follow the basic equations that result from the stoichiometry of the reaction are tabulated in terms of the instantaneous hydrogen mole fraction (H) and fraction of completion of recombination (f) of the hydrogen. Considering a differential volume of recombiner, the rate of hydrogen recombination [-d(VH)] is stated in terms of a mass transfer coefficient (K), superficial surface of catalyst exposed (JadL), and a mass transfer driving force (Φ). This differential equation, in turn, is solved under steady state conditions for the five specific cases enumerated previously (the form of Φ is specified), and these are given in form best suited for extrication of the appropriate rate constants from the experimental data. At this point the concepts advanced by Gamson are introduced to facilitate treating the cases where two mechanism zones are presumed to exist. Using some of the data of Ransohoff and Spiewak, the application of the Gamson correlations to this problem are justified. Now the stage is set for evaluating the mass transfer coefficients as they are generated for the five different cases from the data of the 104 experiments, and the resulting mass transfer coefficients are tabulated as such as well as in terms of dimensionless groups. Plots of the latter (grouped and averaged for runs at the same pressure and temperature) versus mean gas stream temperature strongly suggest that the mass transfer coefficients are temperature dependent (as the Langmuir analysis has already indicated), and the temperature dependence for the Dual-Langmuir mechanism case is evaluated in terms of both the Eyring and Arrhenius equations. The proposed design formulations that result from this analysis are then shown to fit the Ransohoff-Spiewak data more than adequately (mean deviation of 3.8 per cent) for design purposes. This concludes the principal part of this report. The remainder is devoted to the following items:

1. A tabulation of the procedures used to determine the transport and related properties of the system is given, taking into account changes in composition, temperature, and pressure. The properties in question are viscosity, diffusivity, and density. In this connection, the ideas set forth recently by Hirschfelder (1, 6, 7) and his coworkers were employed.

2. A cursory examination of the influence of a non-uniform gas velocity profile through the catalyst bed, as related to the question of the validity of applying the small bed correlations to large beds having relatively flat velocity profiles, is made. It is shown that small bed data may be applied with confidence to the design of large bed recombiners.

3. The report concludes by pointing out some of the weaknesses that exist in the present analysis and suggests additional experiments that should be performed. These stem from the desire to increase our understanding of the catalytic mechanism and its connection with the diffusional aspects of the problem. More important from a practical standpoint, however, is the determination of the possible pressure dependence of the recombination rate for the second portion of the bed where the rate of hydrogen diffusion is the rate regulating step. This is important in contemplating designs for operation at very high pressure. The data of Ransohoff and Spiewak suggest a small and possibly negligible pressure effect in the range 30-110 psia. Speculations concerning catalyst surface conditions lead to a possible pressure effect, but to preserve simplicity these have been overlooked. Consequently, there exists a possibility that this conclusion cannot be extrapolated to high pressure operations such as 1000 psi. The incomplete status of the present theory does not permit taking a firm stand concerning extrapolation to high pressure operation of recombiners.

Adhering to the principle that this report is of interest primarily to design engineers, no mathematical embellishments are included. Except where pertinent to exposition of important concepts, derivation steps have been cut to the bone.

BASIC RELATIONSHIPS

Of the three components encountered in the system, hydrogen is selected as the compound of interest. Accordingly, all mass transfer coefficients reported here are stated as moles of hydrogen reacting per unit time per unit surface per unit driving force. The instantaneous mole fraction of hydrogen in the gas stream (H) or the fraction of completion of recombination of hydrogen at some variable location in the bed (f) is regarded as the independent variable. In dealing with transport properties, the subscripts 1, 2, and 3 affixed to quantities will refer to steam, hydrogen, and oxygen respectively.

As a result of the stoichiometry of the recombination reaction, the following relationships exist:

Total gas mole flow rate: $$V = \frac{V_0(1-0.5H_0)}{1-0.5H} \tag{1}$$

Mole fraction of oxygen: $$O = 0.5H + \frac{O_0-0.5H_0}{1-0.5H_0}(1-0.5H)$$

or $$O = \alpha + 0.5(1-\alpha)H \tag{2}$$

where

$$\alpha = \frac{O_0 - 0.5H_0}{1 - 0.5H_0} \tag{3}$$

and

H_0 = mole fraction of hydrogen in the feed stream
H = mole fraction of hydrogen in the flowing stream
O_0 = mole fraction of oxygen in the feed stream
O = mole fraction of oxygen in the flowing stream
V_0 = total gas feed rate, moles/time
V = variable gas flow rate, moles/time

Defining the fraction of completion of recombination of hydrogen (f) as the ratio of moles of hydrogen to the initial moles of hydrogen fed, i. e.,

$$f = \frac{V_0H_0 - VH}{V_0H_0} = \frac{H_0 - H}{H_0(1 - 0.5H)} \tag{4}$$

the following relationships also apply

$$V = V_0(1 - 0.5H_0f) \tag{1a}$$

$$O = \frac{O_0 - 0.5H_0f}{1 - 0.5H_0f} \tag{2a}$$

$$H = \frac{H_0(1-f)}{1 - 0.5H_0f} \tag{5}$$

For those cases where a change in mechanism occurs and the catalytic bed is pictured as comprising two distinct portions, the subscript 1 affixed to a quantity is used to denote the value of that quantity at the mechanism change-over point. In this connection it is expedient to introduce the abbreviations

$$\beta = \frac{H_0 - H_1}{1 - 0.5H_1} \tag{6}$$

$$\gamma = \frac{H_0 - H_2}{1 - 0.5H_2} \tag{7}$$

where

H_1 = mole fraction of hydrogen in the gas stream at the mechanism change-over point
H_2 = mole fraction of hydrogen in the recombiner discharge stream.

In passing through a differential length (dL) of catalyst bed, a differential change in the mole flow rate of hydrogen [-d(VH)] occurs as a consequence of recombination, and this is equal to the product of the mass transfer coefficient (K), the superficial surface of catalyst exposed (JadL), and the mass transfer driving force (Φ). Symbolically this is given by

$$-d(VH) = -V_0(1 - 0.5H_0)\frac{dH}{(1 - 0.5H)^2} = KJa\Phi dL \tag{8}$$

where

- a = recombiner cross-sectional area
- J = catalyst superficial specific surface, surface exposed/unit volume of bed, as packed
- K = appropriate overall mass transfer coefficient, moles of hydrogen recombined/(time)(catalyst surface)(driving force)
- L = length of recombiner
- Φ = appropriate mass transfer driving force.

This can also be stated alternatively as

$$V_0 H_0 \, df = KJa \, \Phi \, dL \tag{8a}$$

It is emphasized that equation (8) involves the tacit assumptions of a steady state condition of operation, equal effectiveness of the catalyst over a plane perpendicular to the flow direction, and slugwise flow of the gas stream.

In applying equation (8) to the separate bed zones for those operations involving a mechanism change-over, it will be necessary to estimate the gas stream composition at this change-over point, for the quantity H_1 (or f_1) is one of the integration limits for both zones. The basis for estimating this H_1 is that at the mechanism change-over point the hydrogen and oxygen molecules are arriving at the catalyst surface via diffusion in stoichiometric amounts. A first estimate of H_1 can be obtained by assuming that the hydrogen and oxygen concentrations adjacent to the catalyst at this state are negligible, that the reactive gas concentration profiles are linear with respect to distance removed from the catalyst, and that the diffusion coefficients for hydrogen and oxygen in the film mixture are essentially their respective diffusivities in steam. This stoichiometric criterion for the diffusion currents is

$$D_{12} H_1 \approx 2 \, D_{13} O_1 \approx 2 \, D_{13} \, [\alpha + 0.5(1-\alpha) H_1] \tag{9}$$

and this leads to

$$H_1 \approx \frac{2\alpha}{\frac{D_{12}}{D_{13}} - (1-\alpha)} \tag{10}$$

where

- D_{12} = diffusion coefficient for the system steam-hydrogen, surface/time
- D_{13} = diffusion coefficient for the system steam-oxygen, surface/time.

A slightly better estimate of H_1 can be obtained by replacing D_{12} and D_{13} in equation (9) by the diffusivities of hydrogen (D_{2g}) and oxygen (D_{3g}) in the gas stream, taking into account the dependency of these diffusivities on the gas composition. Hirschfelder (1, 7) and his co-workers have shown that the diffusivity of component i in a multicomponent gas mixture (D_{ig}) is not additive with respect to composition, as has been stated erroniously in some texts, but is given by

$$D_{ig} = \frac{1-x_i}{\sum (x_j/D_{ij})} \, , \; j \neq i \tag{11}$$

where

D_{ig} = diffusivity of component i in a gas mixture, surface/time

D_{ij} = diffusion coefficient for the binary pair i and j, surface/time

x_i = mole fraction of component i in the gas mixture

x_j = mole fraction of component j in the gas mixture.

Thus, taking the mean mole fractions of hydrogen and oxygen in the boundary layer at the mechanism change-over point to be $H_m = 0.5H_1$ and $O_m = 0.5O_1 = 0.5\alpha + 0.25(1-\alpha)H_1$, and noticing that the corresponding mean steam mole fraction is $(1-H_m-O_m) = (1-0.5\alpha)-0.25(3-\alpha)H_1$, the stoichiometric criterion for the diffusion currents requires that

$$\frac{(1-0.5H_1)H_1}{\dfrac{0.5\alpha + 0.25(1-\alpha)H_1}{D_{23}} + \dfrac{(1-0.5\alpha)-0.25(3-\alpha)H_1}{D_{12}}} =$$

$$2\,\frac{[(1-0.5\alpha)-0.25(1-\alpha)H_1][\alpha + 0.5(1-\alpha)H_1]}{\dfrac{0.5H_1}{D_{23}} + \dfrac{(1-0.5\alpha)-0.25(3-\alpha)H_1}{D_{13}}} \qquad (12)$$

Since equation (12) is cubic in H_1, the use of it on a large mass of data represents considerable labor which may not be warranted, considering the nature of the assumptions involved and the current data to which it may be applied. A comparison of some calculated values of H_1 as derived from equation (12) in contrast to equation (10) for several typical and several extreme cases indicates that the first estimates from equation (10) are low by approximately one per cent. Accordingly, to incorporate this slight correction, all H_1 values employed in this work were obtained from the modified form of equation (10)

$$H_1 = \frac{2.018\,\alpha}{\dfrac{D_{12}}{D_{13}} - (1-\alpha)} \qquad (13)$$

CONSIDERATION OF VARIOUS RECOMBINATION MECHANISMS

One of the most remarkable things about the combination of hydrogen and oxygen to form water is our gross ignorance about the mechanistic details of this important reaction. Other than the researches of Langmuir (9) on the platinum catalyzed combustion at low pressures, the technical literature contains little that can be brought to bear upon the recombiner problem. Among the many treatises existing on reaction kinetics, Hinshelwood (5) is one of the few authors who devotes more than a paragraph or two to this subject; most of the others do not even mention this topic.

Because of the paucity of information and ideas concerning the mechanism of the catalytic process, an Edisonian attack on the problem using all of the existing data as a guide, appeared to hold forth the most promise. This point

of view dictated the decision to apply the five simple mechanisms tabulated in the Introduction to the data of Ransohoff and Spiewak to disclose which would coincide with the data better than the others. The formulations that result from such a consideration are developed in the pages that follow. The starting point is equation (8) and the main problem is that of coming to a decision concerning the nature of the driving force Φ.

Case I. Oxygen Diffusion Controls The Recombination Rate

As implied in the Introduction, for this case it is postulated that the catalyst is virtually saturated with an excess of reactive hydrogen. As soon as a molecule of oxygen impinges on this hydrogen, reaction occurs. Thus the recombination rate is presumed to be simply the product of the oxygen diffusion current and the catalyst surface. Consequently the driving force Φ is either O or PO, where P is the total pressure of the system. The small pressure dependence of the recombination rate observed by Ransohoff and Spiewak suggests using the former. Thus

$$\Phi = O = \alpha + 0.5(1-\alpha)H \tag{14}$$

and equation (8) takes on the form

$$-V_0(1-0.5H_0)\frac{dH}{(1-0.5H)^2} = K_O Ja[\alpha + 0.5(1-\alpha)H]\,dL \tag{15}$$

where the subscript O has been affixed to the K to indicate that this is for the oxygen diffusion regulated mechanism. Upon separating variables and integrating equation (15) over the entire bed length L, during which the hydrogen mole fraction drops from H_0 to H_2, the catalyst bed volume requirements develop as

$$aL = \frac{V_0}{K_O J}\left[\gamma + 2(1-O_0)\ln\frac{1}{1-0.5\gamma/O_0}\right] \tag{16}$$

where

$$\gamma = \frac{H_0-H_2}{1-0.5H_2}$$

or alternatively as

$$aL = \frac{V_0}{K_O J}\left[H_0 f_2 + 2(1-O_0)\ln\frac{1}{1-0.5H_0 f_2/O_0}\right] \tag{16a}$$

where f_2 is the final fraction of completion of hydrogen recombination.

Case II. Hydrogen Diffusion Controls The Recombination Rate

The circumstances at the catalyst in this case are precisely as stated in Case I, with hydrogen now playing the role of the oxygen. Thus

$$\Phi = H \tag{17}$$

and

$$-V_0(1-0.5H_0)\ \frac{dH}{(1-0.5H)^2} = K_H JaHdL \tag{18}$$

and the catalyst volume requirements are given by

$$aL = \frac{V_0}{K_H J}\left[0.5\gamma + (1-0.5H_0)\ \ln \frac{H_0(1-0.5H_2)}{H_2(1-0.5H_0)}\right] \tag{19}$$

or by

$$aL = \frac{V_0}{K_H J}\left[0.5H_0 f_2 + (1-0.5H_0)\ \ln \frac{1}{1-f_2}\right] \tag{19a}$$

where K_H is the mass transfer coefficient for the hydrogen diffusion controlled bed. One disturbing feature of this formulation is the complete absence of the initial oxygen concentration.

Case III. Oxygen And Hydrogen Diffusion Each Control For A Portion Of The Bed

This is the mechanism employed (in a more approximated form) by Ransohoff and Spiewak in treating their data, and is a combination of Cases I and II, with the following modifications:

1. For zone 1, $\Phi = O$; H varies from H_0 to H_1; bed length = L_1
2. For zone 2, $\Phi = H$; H varies from H_1 to H_2; bed length = $L-L_1 = L_2$

For this case the catalyst volume requirements for the two portions of the bed are

$$aL_1 = \frac{V_0}{K_1 J}\left[\beta + 2(1-O_0)\ \ln \frac{1}{1-0.5\beta/O_0}\right] \tag{20}$$

$$aL_2 = \frac{V_0(1-H_0)}{K_2 J}\left[\frac{0.5(H_1-H_2)}{(1-0.5H_1)(1-0.5H_2)} + \ln \frac{H_1(1-0.5H_2)}{H_2(1-0.5H_1)}\right] \tag{21}$$

where

$$\beta = \frac{H_0-H_1}{1-0.5H_1}$$

and K_1 and K_2 are the mass transfer coefficients for zones 1 and 2 respectively, and have the meanings

K_1 = moles hydrogen reacted/(time)(surface)(mole fraction oxygen)
K_2 = moles hydrogen reacted/(time)(surface)(mole fraction hydrogen)

Case IV. Langmuir Mechanism; Oxygen Diffusion Controls With Surface Restricted

The mechanism proposed in this case is due to Langmuir (9), and stems from his investigations of the rate of oxidation of carbon monoxide and hydrogen at low pressures on platinum wires. Although Langmuir's experimentation emphasized the reactions of carbon monoxide, his experiences with hydrogen parallel those of Ransohoff and Spiewak. In the low temperature range (below 320° C) he found the catalytic behavior to be somewhat erratic, the activity being apparently dependent upon the history and previous treatment of the catalyst, although at higher temperatures (above 400° C) the activity was good and not contingent upon the previous treatment. Langmuir claims that the hydrogen molecules that are adsorbed on the platinum are relatively inactive to oxygen molecules but "can be brought into a condition which enables the adsorbed hydrogen to react with oxygen". Ransohoff apparently experienced this behavior, for in a discussion (10) with one of the authors (HJG) he indicated that "his bed operated more smoothly when it was pretreated for a half hour with oxygen prior to commencing a series of runs".

Because the concepts advanced by Langmuir are germane to the problem at hand, it is in order to review them at this point in the manner in which they may apply to the recombination surface reaction. It is first postulated that all three species of the molecules involved strike the catalyst surface at a mole rate described by the classical kinetic theory formulation

$$\lambda_i = \frac{Px_i}{\sqrt{2\pi M_i BT}} \tag{22}$$

where

λ_i = moles of species i impinging on unit catalyst surface/time
B = gas constant, energy/(mole)(degree)
M_i = molecular weight of the i-th component ($1 \sim H_2O$; $2 \sim H_2$; $3 \sim O_2$)
P = total pressure of the system
T = absolute temperature of the system
x_i = mole fraction of the i-th component in the gas mixture

It is next conjectured that each component occupies some fraction of the sites on the catalyst surface, Θ_i, and that Θ fraction of the catalyst surface is bare, with the added stipulation that these fractions total unity, i. e.

$$\Theta + \Theta_1 + \Theta_2 + \Theta_3 = 1 \tag{23}$$

Looking at the catalyst surface, it is assumed to have different binding power for each of the three species. Thus for catalyst completely covered with pure component i, it is conjectured that the surface evaporation rate of this component is ν_i moles per unit surface per unit time, whereas ξ_i (surface factor for condensation) represents the fraction of molecules of component i that adhere to the surface out of the total that impinge on the surface.

Since hydrogen is strongly adsorbed to platinum, it appears that random or stray field forces on hydrogen molecules cannot account for this strong binding, which implies that hydrogen must sit down on the catalyst not as molecules, but as pairs of atoms, with each atom paired off against a platinum atom. Thus the condensation of a hydrogen molecule can occur only at two adjacent sites on the catalyst, and since the probability of the existence of such a vacant duplex site is Θ^2 it follows that the

$$\text{rate of condensation of hydrogen moles} = \Theta^2\lambda_2\xi_2$$

On the other hand, the rate of evaporation of hydrogen from the catalyst is directly proportional to the square of the fraction of the catalyst surface covered by hydrogen so that the

$$\text{rate of evaporation of hydrogen moles} = \nu_2\Theta_2^2$$

The adsorbed hydrogen is assumed to be virtually inert insofar as combination which impinging or adsorbed oxygen molecules is concerned. Hence the adsorbed hydrogen can only leave by evaporation, and for the dynamic steady state that is presumed to exist at a particular location in the bed

$$\Theta^2\lambda_2\xi_2 = \nu_2\Theta_2^2 \tag{24}$$

The behavior described here is that for the catalyst in the "non-active state" with respect to hydrogen, a condition more apt to prevail with a hydrogen excess in the gas stream. For an oxygen excess this passive condition may not exist.

Turning the attention to the oxygen molecules, these are also thought to be accomodated atomically on adjacent platinum duplex sites, and triggered into a state capable of immediate reaction with any hydrogen molecule that impinges on them. Evaporation of the adsorbed oxygen molecules per se is considered negligible in systems containing a hydrogen excess, so that $\nu_3 \approx 0$. Consequently adsorbed oxygen can escape from the catalyst only as a result of reaction with hydrogen. Designating the reaction speed as ω moles of hydrogen recombined per unit catalyst surface per unit time, the steady state equation similar to (24) but applying for oxygen is

$$0.5\omega = \Theta^2\lambda_3\xi_3 \tag{24a}$$

Water molecules are not adsorbed appreciably by platinum, so $\Theta_1 \approx 0$ and $\xi_1 \approx 0$. Accordingly, the rate of water evaporation is virtually identical to the rate of water synthesis, and since the mole rate of water production is equal to the product of the molecules of hydrogen striking unit surface per unit time, the fraction of catalyst surface that is covered by adsorbed oxygen, and the surface reaction factor η (fraction of hydrogen-surface oxygen collisions that are fruitful), it follows that

$$\omega = \eta\Theta_3\lambda_2 \tag{25}$$

where $\eta \approx 1$ for high temperatures. All of the factors ξ_i, ν_i, and η should exhibit some temperature dependence. Further, the activation energy for the

catalyzed hydrogen-oxygen combination should be directly related to the energy required to develop a vacant duplex site, i. e., the heat of evaporation of adsorbed hydrogen molecules, if the concepts presented have any real basis.

Upon manipulating equations (24), (24a), and (25), the fraction of the catalyst surface that is bare (Θ), covered with adsorbed hydrogen (Θ_2) and adsorbed oxygen (Θ_3) can be obtained as

$$\Theta = \left[\frac{\omega}{2\xi_3\lambda_3}\right]^{1/2} \tag{26}$$

$$\Theta_2 = \left[\frac{\xi_2\lambda_2\omega}{2\xi_3\lambda_3\nu_2}\right]^{1/2} \tag{27}$$

$$\Theta_3 = \frac{\omega}{\eta\lambda_2} \tag{28}$$

These can be inserted into the catalyst surface conservation equation (23) to produce a quadratic equation in $\omega^{1/2}$ which when solved gives the hydrogen recombination rate per unit surface as

$$\omega = \left[\frac{\eta\lambda_2}{2}\right]^2 \left[\sqrt{\left(\frac{1}{2\xi_3\lambda_3}\right)^{1/2} + \left(\frac{\xi_2\lambda_2}{2\xi_3\lambda_3\nu_2}\right)^{1/2} + \frac{4}{\eta\lambda_2}} - \left(\frac{1}{2\xi_3\lambda_3}\right)^{1/2} - \left(\frac{\xi_2\lambda_2}{2\xi_3\lambda_3\nu_2}\right)^{1/2}\right]^2 \tag{29}$$

The complicated form of this expression tends to disguise what is implied concerning the nature of the surface reaction, so a more communicable approach is made by backing up and re-examining equation (27). If the catalyst surface is densely populated with hydrogen molecules (as it should be considering the strong adsorption of hydrogen, the greater diffusion rate and hence higher impingement rate of hydrogen, particularly when dealing with a system containing stoichiometric or excess hydrogen), then Θ_2 should dominate Θ and Θ_3, whereas $\Theta_2 \approx 1$. For this state of affairs equation (27) implies that the hydrogen recombination rate should be given by

$$\omega \approx \frac{2\xi_3\lambda_3\nu_2}{\xi_2\lambda_2} \tag{30}$$

Meanwhile equation (22) gives the oxygen and hydrogen impingement rates as

$$\lambda_3 = \frac{PO}{\sqrt{2\pi M_2 BT}}$$

$$\lambda_2 = \frac{PH}{\sqrt{2\pi M_2 BT}}$$

This leads to the conclusion that the hydrogen recombination rate should have the form

$$\omega \approx \frac{2\xi_3\nu_2}{\xi_2}\sqrt{\frac{M_2}{M_3}}\,\frac{O}{H} = K_\omega\frac{O}{H} \tag{31}$$

where

K_ℓ = the Langmuir mass transfer coefficient, moles hydrogen recombined/(time)(surface)(O/H mole fraction ratio)

It is evident that for this mechanism the driving force (Φ) is the ratio of oxygen to hydrogen mole fraction in the gas stream, and it is clear how adsorbed hydrogen manifests itself as a catalyst poison. Further, no pressure dependence of the recombination rate is indicated, although a temperature dependence is implied in the individual terms that make up K_ℓ. This formulation fits Langmuir's data and correlates the data of Ransohoff and Spiewak better than the procedure they used (an approximation of Case III), as will be shown subsequently. The main objection to the Langmuir formulations is that it fails to account explicitly and phenomenonologically for the influence of the flow characteristics of the system on the disturbances created in the boundary layer, which in turn modifies the simple molecular diffusion picture. But this is a common defect which is apt to prevail for quite a long time in the theory of surface catalyzed reactions.

It is now in order to evaluate the catalyst volume requirements for the Langmuir mechanism. Thus

$$\Phi = \frac{O}{H} \tag{32}$$

$$-V_0(1-0.5H_0)\ \frac{dH}{(1-0.5H)^2} = K_\ell Ja\frac{O}{H}\ dL \tag{33}$$

$$aL = \frac{V_0}{K_\ell J}\left[\ 2\gamma - (2O_0 - H_0)\ \ln\ \frac{1}{1-0.5\gamma/O_0}\right] \tag{34}$$

$$aL = \frac{V_0}{K_\ell J}\left[\ 2\ H_0 f_2 - (2O_0 - H_0)\ \ln\ \frac{1}{1-0.5\ H_0 f_2/O_0}\right] \tag{34a}$$

Case V. Dual-Langmuir Mechanism; Both Oxygen And Hydrogen Diffusion Control With Surface Restricted

If a catalyst bed is operating on a feed containing an initial excess of oxygen and is sufficiently large to recombine a large percentage of the hydrogen fed, a zone will develop in the bed where oxygen molecules are arriving at the catalyst surface much more frequently than hydrogen molecules, as described for Case III. For this high oxygen concentration zone, previously adsorbed passive hydrogen molecules could be stripped off and the bed might operate as a "souped-up" version of Case IV, insofar as surface availability is concerned in this zone, the slower hydrogen diffusion rate being the overall rate regulating step. On the other hand, excessive oxygen adsorption might lead to a passive state in the same sense that adsorbed hydrogen does for Case IV, which would interchange the roles of hydrogen and oxygen and lead to a driving force Φ = H/O for this zone. This Dr. Jeckel-Mr. Hyde behavior seems entirely plausible when it is realized that the activity of adsorbed material is closely bound up with whether a continuous layer or a series of small adsorption

"islands" is formed. The force fields for these two states of affairs are quite different. These of course are merely speculations, and no existing data are on hand to point out the way for this specific case.

It may afford some comfort to fall back upon equations (23), (24), (24a), and (25), and seek directions, if not information. If the adsorbed hydrogen molecules are indeed stripped off to a considerable extent, then $\Theta_2 \approx 0$, and the application of equation (23) leads to

$$\omega \approx \frac{(\eta\lambda_2)^2}{4\lambda_3\xi_3}\left[1 + \frac{4\xi_3\lambda_3}{\eta\lambda_2} - \sqrt{1 + \frac{8\xi_3\lambda_3}{\eta\lambda_2}}\right] \tag{35}$$

This can also be stated as

$$\omega \approx 2\sqrt{2}\,\frac{\eta^2}{\xi_3}\,\frac{PH^2}{O}\left[1 + \frac{\xi_3}{\eta}\,\frac{O}{H} - \sqrt{1 + 2\,\frac{\xi_3}{\eta}\,\frac{O}{H}}\right] \tag{35a}$$

which indicates a rather complicated state of affairs for a recombination rate. And other speculations are possible, such as $\Theta_2 \approx \Theta_3$, or $\Theta \approx \Theta_2$, which lead to the respective formulations

$$\omega \approx 2\sqrt{2}\,\frac{PH}{O}\left[1 + 2\,\frac{O}{H} - \sqrt{1 + 4\,\frac{O}{H}}\right] \tag{36}$$

$$\omega \approx 4\,\frac{PH^2}{O}\left[1 + \frac{O}{4H} - \sqrt{1 + \frac{O}{2H}}\right] \tag{37}$$

when the additional assumptions are made that $\eta \approx 1$ and $\xi_3 \approx 1$. Equations (35, (36), and (37) predict a pressure dependency, but these forms are unpalatable in that they lead to unwarranted complications. The present data, further, are not capable of making a crucial decision concerning what the order of events are in the second zone for this case. Faced with a dilemma here, the decision is to accept the simpler form $\Phi = H/O$, leaving the course open for future revision. The main justification for this choice, aside from the question of simplicity, is that this treatment correlates the data of Ransohoff and Spiewak very well. Indeed, the final correlation shows much less scattering of points than is ordinarily encountered in heterogeneous reaction kinetics studies.

The dual-Langmuir mechanism presented here then is based upon the premise that

$$\begin{aligned} \Phi &= \frac{O}{H} \quad \text{for the range } H_0 \text{ to } H_1 \\ \Phi &= \frac{H}{O} \quad \text{for the range } H_1 \text{ to } H_2 \end{aligned} \tag{38}$$

The appropriate differential equations are

$$-V_0(1-0.5H_0)\,\frac{dH}{(1-0.5H)^2} = K_{L_1}Ja\,\frac{O}{H}\,dL \tag{39}$$

$$-V_0(1-0.5H_0)\ \frac{dH}{(1-0.5H)^2} = K_{L_2} Ja \frac{H}{O}\ dL \tag{40}$$

and the catalyst volume requirements for the two zones are

$$aL_1 = \frac{V_0}{K_{L_1} J}\left[2\beta - (2O_0 - H_0)\ \ln \frac{1}{1-0.5\beta/O_0}\right] \tag{41a}$$

$$aL_2 = \frac{0.5V_0}{K_{L_2} J}\left[\frac{(1-0.5H_0)(H_1-H_2)}{(1-0.5H_1)(1-0.5H_2)} + (2O_0 - H_0)\ \ln \frac{H_1(1-0.5H_2)}{H_2(1-0.5H_1)}\right] \tag{41b}$$

where K_{L_1} and K_{L_2} are the dual-Langmuir mass transfer coefficients for the two recombination zones.

The forms that have been developed for the five different cases have striking similarities and contain identical groups of terms. This feature reduces the labor of extricating mass transfer coefficients from the data for the various mechanisms proposed considerably.

EVALUATION OF THE MASS TRANSFER COEFFICIENTS

The extrication of the mass transfer coefficients from the experimental data for the cases where the same recombination mechanism is postulated to apply over the entire catalytic bed is a straightforward process. Thus K_O, K_H, and K_L have been calculated by inserting the measured values of H_0, O_0, H_2, V_0, a, J, and L into the appropriate equations. This simple situation does not exist for those cases where a mechanism change-over is presumed to occur, inasmuch as but two equations are on hand which contain as unknown quantities two mass transfer coefficients and a length of one or the other recombiner zones. Thus, values of K_1, K_2, K_{L_1}, and K_{L_2} cannot be extricated by a frontal assault on the data, and a round-about procedure must be adopted. The basis for this procedure is that the K_1 and K_{L_1} are related to K_2 and K_{L_2} respectively through a relationship which accounts for the manner in which the hydrodynamics of the system alter the sizes of the diffusion layer and the momentum and molecular transfer for each zone. Through such a relationship K_2 (or K_{L_2}) can be eliminated in terms of K_1 (or K_{L_1}) which then can be calculated after the catalyst volume requirements for the two zones have been combined. It is to be observed that such a procedure considers the chemical aspects of the recombination process to be subordinate to the diffusional features. The present thinking regards this to be the case, as reflected in the conjecture that $\eta \approx 1$ and $\xi_3 \approx 1$.

Relationship Between The Mass Transfer Coefficients For The Two Zones

Recently Gamson (3) published the results of his efforts to unify the data of many investigators for various mass transfer configurations, among which are included stationary and fluidized beds, different particle shapes (spheres,

cylinders, flakes, partition rings, and Raschig rings), and both gas-solid and liquid-solid transfer systems. That part of Gamson's work which is of interest here is that a generalized Nusselt-type dimensionless equation can be written which correlates all of the existing diffusion controlled rate data in the form

$$\frac{K}{(G/M_m)}\left[\frac{\mu}{\rho D}\right]_f^{2/3} = 1.46\left[\frac{D_p G}{\mu\phi(1-v)}\right]^{-0.41}(1-v)^{0.2} \tag{42}$$

for defined Reynolds numbers in excess of 100, where

- D = diffusivity of the rate controlling component in the mixture, surface/time
- D_p = equivalent spherical diameter of the particles (based on superficial surface), length
- G = superficial mass velocity (for unpacked bed), mass/(time)(area)
- K = overall mass transfer coefficient computed for one diffusant controlling, moles/(time)(surface)(driving force)
- M_m = mean molecular weight of the fluid stream
- v = fraction of voids in the flow system as operated
- μ = fluid viscosity, mass/(time)(length)
- ϕ = surface effectiveness factor (ϕ = 0.91 for cylinders)
- f = subscript referring to the <u>film</u> through which diffusion occurs

The quantities $(\mu/\rho D)_f$ and $[D_p G/\mu\phi(1-v)]$ are the Schmidt and Reynolds numbers for the film and flow system, and for convenience are henceforth abbreviated as Sc and Re respectively in the remainder of this report, i. e.

$$Sc = \left[\frac{\mu}{\rho D}\right]_f \tag{43a}$$

$$Re = \frac{D_p G}{\mu\phi(1-v)} \tag{43b}$$

Hence equation (42) can be stated more succinctly as

$$K = 1.46\,(1-v)^{0.2}\,(G/M_m)(Sc)^{-2/3}\,(Re)^{-0.41} \tag{42a}$$

and this affords a means for possible elimination of K_2 and K_{L_2} in terms of K_1 and K_{L_1} in treating the data for Cases III and V.

Using the subscripts 1 and 2 to denote the properties for the first and second portions of the catalytic bed, it is evident that $G_1 = G_2$, $M_{m_1} \approx M_{m_2}$, $\rho_1 \approx \rho_2$, and the quantities D_p, ϕ, and v are alike throughout the recombiner. Thus K_2 and K_{L_2} can be related to K_1 and K_{L_1} in terms of the film Schmidt numbers $(Sc)_1$ and $(Sc)_2$ and the fluid stream mean viscosities μ_1 and μ_2. However, since the mass transfer coefficients as treated in the developments are both expressed as moles of <u>hydrogen</u> recombined/(time)(surface)(driving force), whereas the Gamson formulations refer to <u>oxygen</u> for zone <u>1</u> and <u>hydrogen</u> for zone <u>2</u>, the stoichiometric factor 2 needs to be applied. This results in the

speculation that the relationships

$$K_2 = 0.5\, K_1\, (Sc_1/Sc_2)^{2/3}\, (\mu_2/\mu_1)^{0.41} \tag{42b}$$

$$K_{L_2} = 0.5\, K_{L_1}\, (Sc_1/Sc_2)^{2/3}\, (\mu_2/\mu_1)^{0.41} \tag{42c}$$

inter-relate the mass transfer coefficients for the two portions of the recombiner.

The use of equations (42b) and (42c) facilitates combination of equation (20) with (21) and equation (41a) with (41b) to yield the following expressions for extricating K_1 and K_{L_1} from the data of Ransohoff and Spiewak

$$K_1 = \frac{V_0}{JaL}\left\{\beta + 2(1-O_0)\ln\frac{1}{1-0.5\beta/O_0} + 2\left[\frac{Sc_2}{Sc_1}\right]^{2/3}\left[\frac{\mu_1}{\mu_2}\right]^{0.41}(1-H_0)\left[\frac{0.5(H_1-H_2)}{(1-0.5H_1)(1-0.5H_2)} + \ln\frac{H_1(1-0.5H_2)}{H_2(1-0.5H_1)}\right]\right\} \tag{44a}$$

$$K_{L_1} = \frac{V_0}{JaL}\left\{2\beta - (2O_0-H_0)\ln\frac{1}{1-0.5\beta/O_0} + \left[\frac{Sc_2}{Sc_1}\right]^{2/3}\left[\frac{\mu_1}{\mu_2}\right]^{0.41}\left[\frac{(1-0.5H_0)(H_1-H_2)}{(1-0.5H_1)(1-0.5H_2)} + (2O_0-H_0)\ln\frac{H_1(1-0.5H_2)}{H_2(1-0.5H_1)}\right]\right\} \tag{44b}$$

Before these deductions are applied they should be justified for the case on hand. This is the intention of the immediate discussion that follows.

Justification Of The Application Of The Gamson Correlation

The justification of the application of the Gamson correlation centers on the demonstration that the forms of equations (44a) and (44b) substantially are valid in that values close to the exponents 2/3 and 0.41 are generated by the Ransohoff-Spiewak data. Unfortunately, the experimental data given in ORNL Progress Report 1583 do not contain what is needed to make a completely satisfactory quantitative justification, although they are adequate for establishing the soundness of the ideas. To cover the points properly, the following types of data are essential:

1. To establish the Reynolds number dependence, a series of isothermal runs with constant Schmidt numbers, but with varied feed rates, is essential. These runs should have the feed composition adjusted such that for each series all of the recombiner bed is operating either as zone 1 or 2, but not both.

2. For establishing the Schmidt number dependence, a series of isothermal runs with constant Reynolds number, but with varied ratios of oxygen to hydrogen in the feed stream, is essential, and a reasonable number of the runs of this series must cause the bed to operate as two zones.

An inspection of Tables I and II, which are tabulations of the original data of Ransohoff and Spiewak and quantities calculated from their data reveals that the requirements for making a completely satisfactory test does not currently exist. However, the data of May 5-7-11-12 are adequate for testing the dependency on Reynolds number whereas those of April 21-22 and May 19 suffice for indicating the Schmidt number dependency.

The establishment of the Reynolds number dependency is a relatively straightforward procedure, involving determination of the slope of a logarithmic plot of the derived mass transfer coefficients versus Re. To test a larger quantity in one fell swoop it is expedient to deal with the dimensionless group $K(Sc)^{2/3}/(G/M_m)(1-v)^{0.2}$ instead of K alone. Such a test was made on the K_1 and K_{L_1} groups, and the results for the latter are shown in Figure 2. This shows a mean value for all of the points (lumped together) of 0.48 instead of the 0.41 Gamson value, and indicates individual values of 0.31, 0.23, 0.28, and 0.39 for the May 5, 7, 11, and 12 runs respectively. A similar treatment in terms of K_1 instead of K_{L_1} leads to the magnitude 0.44 for the exponent on Re. The argument given here may justifiably be criticised as one that travels in circles, since the elimination of K_2 and K_{L_2} involved using in the analysis that which was sought to be proved, that the tests should have been made on untampered data for a bed operated exclusively in one zone or the other. As indicated, such a test is not possible because of the lack of the right kind of data. The fact that the exponent for part of the bed went into the test as 0.41 and came out for the other part of the bed close to 0.41 is considered adequate indication that the use of the Gamson value of 0.41 is justified. The principal reason for the scatter shown of Figure 2 is that the temperature dependency of K_{L_1} has been ignored. The important conclusion to be drawn is that, as a consequence of the K_{L_1} dependency on Re, it has been demonstrated that the reaction is diffusion controlled, and the order of magnitude of the dependency on Re has been established.

The justification of the 2/3 value as the exponent on the Schmidt number is somewhat more involved. In essence, it involves the use of equation (44a) or (44b) as a starting point, replacing the exponent 2/3 on the Schmidt number group by an unknown quantity n, and eliminating H_1 from these equations in terms of its value given in equation (13). The intention is to obtain a form through subsequent manipulation and valid simplification which allows the value of n to appear as a parameter of a linear plot of a group in which the key variable is H_2. If the Ransohoff-Spiewak data generate a value of $n \approx 2/3$, the conclusion to be drawn is that the recombination reaction is indeed diffusion controlled, and the Gamson correlation applies. In the interest of keeping the exposition brief the manipulative details are omitted and only the end result is indicated. Using the abbreviation

$$\delta = D_{12}/D_{13} \tag{45}$$

TABLE I

OBSERVED AND CALCULATED PRIMARY RECOMBINER DATA

Designation	Run No.	t_0 °C	t_b °C	t_2 °C	t_g °C	P psia	F stand cfm	H_0 mole fr	O_0 mole fr	M_0 lb/lb mole	V_0 lb mole/sec	G lb/(sec)(sq ft)	D_{12}/D_{13}	α	H_1 mole fr	H_2 mole fr	O_2 mole fr	f_2	β	γ
⊖	April 15-1	147	352	346	349	50	13.2	0.0447	0.0413	17.9	6.15×10^{-4}	2.13	3.40	0.0194	0.0162	0.0055	0.0221	0.879	0.0287	0.0392
	2	147	348	340	344	50	13.1	0.0445	0.0351	17.8	6.10	2.10	3.40	0.0132	0.0110	0.0064	0.0164	0.858	0.0337	0.0382
	3	148	340	332	336	50	13.1	0.0443	0.0318	17.8	6.08	2.09	3.40	0.0098	0.0082	0.0074	0.0135	0.836	0.0362	0.0370
	4*	145	332	330	331	30	13.2	0.0477	0.0340	17.6	6.12	2.09	3.41	0.0104	0.0087	0.0108	0.0157	0.779	0.0392	0.0371
	5	142	344	338	341	30	13.3	0.0472	0.0388	17.8	6.19	2.14	3.40	0.0156	0.0130	0.0088	0.0195	0.817	0.0344	0.0385
	6	142	350	341	346	30	13.3	0.0474	0.0414	17.8	6.16	2.13	3.40	0.0182	0.0152	0.0081	0.0222	0.831	0.0325	0.0394
	7	151	349	342	346	80	13.3	0.0431	0.0416	17.9	6.19	2.15	3.40	0.0205	0.0171	0.0046	0.0228	0.896	0.0262	0.0386
	8	152	350	345	348	80	13.3	0.0437	0.0360	17.8	6.15	2.12	3.40	0.0145	0.0121	0.0054	0.0171	0.879	0.0318	0.0384
	9	152	345	342	344	80	13.1	0.0442	0.0325	17.8	6.08	2.09	3.40	0.0107	0.0089	0.0061	0.0137	0.864	0.0354	0.0382
	10	163	349	333	341	110	13.2	0.0439	0.0316	17.8	6.13	2.11	3.40	0.0099	0.0083	0.0059	0.0128	0.869	0.0358	0.0381
	11	163	351	334	343	110	13.3	0.0437	0.0366	17.8	6.16	2.13	3.40	0.0151	0.0126	0.0048	0.0175	0.892	0.0313	0.0390
	12	163	353	334	344	110	13.4	0.0435	0.0427	17.9	6.20	2.16	3.40	0.0214	0.0179	0.0043	0.0236	0.902	0.0258	0.0392
⦶	April 16-1	139	435	409	422	30	13.4	0.0630	0.0541	17.8	6.20×10^{-4}	2.14	3.36	0.0233	0.0198	0.0085	0.0275	0.869	0.0436	0.0548
	2	140	421	409	415	30	13.3	0.0635	0.0465	17.7	6.16	2.10	3.36	0.0152	0.0129	0.0112	0.0207	0.828	0.0510	0.0526
	3*	142	412	411	412	30	13.3	0.0647	0.0433	17.6	6.19	2.11	3.36	0.0114	0.0097	0.0143	0.0184	0.784	0.0542	0.0508
	4*	145	435	430	433	50	13.2	0.0645	0.0418	17.6	6.13	2.12	3.36	0.0099	0.0084	0.0103	0.0150	0.845	0.0563	0.0545
	5	146	441	432	437	50	13.3	0.0628	0.0472	17.7	6.16	2.11	3.36	0.0164	0.0139	0.0075	0.0201	0.883	0.0492	0.0554
	6	145	439	430	435	50	13.3	0.0599	0.0539	17.8	6.18	2.13	3.36	0.0247	0.0209	0.0058	0.0275	0.905	0.0395	0.0543
	7	152	445	440	443	80	13.3	0.0585	0.0540	17.8	6.17	2.13	3.36	0.0255	0.0216	0.0046	0.0277	0.923	0.0373	0.0540
	8	152	439	430	435	80	13.2	0.0591	0.0477	17.7	6.13	2.11	3.36	0.0187	0.0159	0.0053	0.0213	0.912	0.0435	0.0539
	9	152	434	426	430	80	13.1	0.0593	0.0433	17.7	6.10	2.10	3.36	0.0140	0.0119	0.0060	0.0170	0.901	0.0477	0.0535
	10	165	427	421	424	110	13.2	0.0607	0.0448	17.7	6.12	2.10	3.36	0.0149	0.0127	0.0059	0.0178	0.905	0.0483	0.0549
	11	164	430	422	426	110	13.2	0.0612	0.0491	17.7	6.10	2.10	3.36	0.0190	0.0161	0.0053	0.0216	0.916	0.0455	0.0561
	12	165	425	420	423	110	13.2	0.0605	0.0542	17.8	6.14	2.12	3.36	0.0247	0.0209	0.0047	0.0269	0.925	0.0401	0.0560
⊕	April 21-1	159	518	488	503	100	13.0	0.0684	0.0681	17.9	6.02×10^{-4}	2.09	3.34	0.0351	0.0298	0.0041	0.0370	0.943	0.0392	0.0645
	2	159	515	487	501	100	13.2	0.0721	0.0580	17.7	6.14	2.11	3.34	0.0228	0.0194	0.0050	0.0252	0.933	0.0532	0.0673
	3	150	515	487	501	100	12.9	0.0723	0.0541	17.6	6.01	2.05	3.34	0.0187	0.0159	0.0054	0.0213	0.927	0.0568	0.0670
	4	149	509	475	492	80	13.0	0.0725	0.0530	17.6	6.05	2.06	3.35	0.0174	0.0149	0.0094	0.0220	0.874	0.0581	0.0634
	5	153	519	490	505	80	12.9	0.0717	0.0550	17.6	6.01	2.05	3.34	0.0199	0.0170	0.0056	0.0226	0.925	0.0552	0.0663
	6	152	519	490	505	80	13.1	0.0700	0.0583	17.7	6.07	2.08	3.34	0.0242	0.0206	0.0044	0.0264	0.939	0.0498	0.0657
	7	150	518	490	504	80	13.2	0.0693	0.0652	17.8	6.11	2.11	3.34	0.0316	0.0269	0.0039	0.0335	0.946	0.0429	0.0655

* No mechanism change over occurred - oxygen diffusion rate controlling throughout.

TABLE I (continued)

Designation	Run No.	t_0 °C	t_b °C	t_2 °C	t_g °C	P psia	F stand cfm	H_0 mole fr	O_0 mole fr	M_0 lb/lb mole	V_0 lb mole/sec	G lb/(sec)(sq ft)	D_{12}/D_{13}	α	H_1 mole fr	H_2 mole fr	O_2 mole fr	f_2	β	γ
⊘	April 22-1	141	508	480	494	30	13.2	0.0747	0.0593	17.7	6.11×10^{-4}	2.09	3.34	0.0228	0.0194	0.0101	0.0278	0.869	0.0558	0.0649
	2	141	501	479	490	30	13.2	0.0720	0.0647	17.8	6.13	2.11	3.35	0.0297	0.0253	0.0090	0.0341	0.879	0.0474	0.0633
	3	142	511	488	500	30	13.1	0.0769	0.0548	17.6	6.10	2.07	3.34	0.0170	0.0146	0.0117	0.0228	0.853	0.0628	0.0657
	4	146	522	500	511	50	13.1	0.0759	0.0544	17.6	6.09	2.07	3.34	0.0171	0.0146	0.0087	0.0214	0.889	0.0617	0.0675
	5	146	522	500	511	50	13.1	0.0740	0.0587	17.7	6.10	2.09	3.34	0.0226	0.0193	0.0071	0.0260	0.908	0.0552	0.0671
	6	145	521	500	511	50	13.3	0.0723	0.0656	17.8	6.19	2.13	3.34	0.0306	0.0260	0.0057	0.0333	0.924	0.0469	0.0668
	7	151	511	490	501	80	13.0	0.0684	0.0650	17.8	6.05	2.09	3.34	0.0319	0.0271	0.0037	0.0337	0.947	0.0418	0.0648
	8	151	509	484	497	80	12.9	0.0686	0.0542	17.7	5.98	2.05	3.34	0.0206	0.0176	0.0046	0.0229	0.935	0.0514	0.0641
	9	152	508	482	495	100	12.8	0.0687	0.0512	17.6	5.96	2.04	3.34	0.0174	0.0149	0.0053	0.0200	0.926	0.0542	0.0636
	10	160	505	470	488	100	13.1	0.0696	0.0504	17.6	6.07	2.07	3.35	0.0161	0.0137	0.0056	0.0188	0.923	0.0563	0.0643
	11	160	510	470	490	100	13.2	0.0683	0.0595	17.8	6.12	2.11	3.35	0.0262	0.0223	0.0041	0.0282	0.942	0.0465	0.0643
⊘	April 23-1	144	242	233	238	30	13.4	0.0259	0.0247	17.9	6.21×10^{-4}	2.16	3.46	0.0119	0.0097	0.0091	0.0164	0.653	0.0163	0.0169
	2*	144	235	230	233	30	13.3	0.0259	0.0225	17.9	6.20	2.16	3.47	0.0096	0.0079	0.0100	0.0146	0.619	0.0160	0.0160
	3*	145	223	224	224	30	13.3	0.0259	0.0206	17.9	6.18	2.14	3.47	0.0077	0.0063	0.0109	0.0131	0.583	0.0151	0.0151
	4*	149	229	226	228	50	13.3	0.0247	0.0202	17.9	6.17	2.14	3.47	0.0080	0.0065	0.0094	0.0127	0.601	0.0153	0.0153
	5*	149	233	228	231	50	13.3	0.0245	0.0232	17.9	6.19	2.15	3.47	0.0111	0.0090	0.0093	0.0157	0.624	0.0153	0.0153
	6*	154	225	227	226	80	13.3	0.0236	0.0208	17.9	6.17	2.14	3.47	0.0091	0.0074	0.0096	0.0138	0.597	0.0141	0.0141
	7*	154	227	229	228	80	13.2	0.0276	0.0208	17.9	6.15	2.13	3.47	0.0072	0.0058	0.0115	0.0129	0.586	0.0162	0.0162
	8*	154	235	230	233	80	13.3	0.0261	0.0246	17.9	6.16	2.14	3.46	0.0118	0.0096	0.0100	0.0167	0.621	0.0162	0.0162
	9*	160	230	235	233	100	13.4	0.0268	0.0236	17.9	6.21	2.16	3.47	0.0104	0.0084	0.0107	0.0156	0.604	0.0162	0.0162
	10	160	230	230	230	100	13.4	0.0268	0.0265	18.0	6.23	2.17	3.47	0.0133	0.0108	0.0107	0.0185	0.604	0.0161	0.0162
⊗	April 24-1*	155	233	255	244	80	16.3	0.0354	0.0297	17.9	7.55×10^{-4}	2.61	3.46	0.0122	0.0100	0.0136	0.0189	0.620	0.0220	0.0220
	2*	156	231	254	243	80	16.2	0.0355	0.0273	17.8	7.53	2.60	3.46	0.0097	0.0080	0.0142	0.0168	0.604	0.0215	0.0215
	3*	155	233	258	246	80	16.3	0.0351	0.0320	17.9	7.56	2.62	3.46	0.0148	0.0112	0.0131	0.0212	0.630	0.0221	0.0221
	4*	161	245	263	254	100	16.4	0.0359	0.0314	17.9	7.62	2.64	3.45	0.0137	0.0112	0.0131	0.0202	0.638	0.0229	0.0229
	5*	160	240	261	251	100	16.5	0.0365	0.0288	17.8	7.65	2.64	3.45	0.0108	0.0088	0.0139	0.0177	0.623	0.0228	0.0228
	6*	150	225	250	238	50	16.2	0.0359	0.0302	17.9	7.51	2.60	3.46	0.0125	0.0102	0.0146	0.0197	0.598	0.0215	0.0215
	7*	149	218	240	229	50	16.1	0.0357	0.0272	17.8	7.48	2.58	3.47	0.0096	0.0078	0.0158	0.0174	0.562	0.0200	0.0200
◓	April 28-1*	143	275	275	275	30	16.2	0.0484	0.0353	17.7	7.50×10^{-4}	2.58	3.44	0.0114	0.0094	0.0202	0.0214	0.588	0.0284	0.0284
	2*	142	287	275	281	30	16.2	0.0474	0.0390	17.8	7.52	2.59	3.43	0.0157	0.0129	0.0179	0.0245	0.627	0.0297	0.0297
	3*	142	292	289	291	30	16.3	0.0482	0.0423	17.8	7.56	2.61	3.43	0.0187	0.0154	0.0188	0.0279	0.615	0.0297	0.0297
	4*	149	302	298	300	50	16.3	0.0453	0.0390	17.8	7.55	2.61	3.42	0.0168	0.0139	0.0149	0.0241	0.677	0.0307	0.0307
	5*	149	295	290	293	50	16.3	0.0451	0.0348	17.8	7.57	2.61	3.43	0.0125	0.0104	0.0158	0.0203	0.655	0.0295	0.0295
	6*	149	290	280	285	50	16.3	0.0497	0.0315	17.7	7.58	2.59	3.43	0.0068	0.0056	0.0203	0.0169	0.597	0.0297	0.0297
	7*	155	295	296	296	80	16.2	0.0462	0.0318	17.7	7.50	2.58	3.43	0.0089	0.0074	0.0165	0.0171	0.649	0.0300	0.0300
	8*	155	310	304	307	80	16.3	0.0450	0.0359	17.8	7.58	2.61	3.37	0.0137	0.0116	0.0146	0.0209	0.680	0.0306	0.0306

* No mechanism change over occurred - oxygen diffusion rate controlling throughout.

TABLE I (continued)

Designation	Run No.	t_0 °C	t_b °C	t_2 °C	t_g °C	P psia	F stand cfm	H_0 mole fr	O_0 mole fr	M_0 lb/lb mole	V_0 lb mole/sec	G lb/(sec)(sq ft)	D_{12}/D_{13}	α	H_1 mole fr	H_2 mole fr	O_2 mole fr	f_2	β	γ
◒	April 30-1	142	422	400	411	35	16.1	0.0646	0.0531	17.7	7.47×10^{-4}	2.57	3.37	0.0215	0.0182	0.0111	0.0269	0.833	0.0469	0.0639
	2*	144	429	410	420	35	16.2	0.0728	0.0454	17.5	7.53	2.55	3.37	0.0093	0.0079	0.0196	0.0190	0.738	0.0537	0.0537
	3*	148	435	420	428	50	16.2	0.0690	0.0433	17.5	7.53	2.56	3.36	0.0091	0.0078	0.0150	0.0165	0.789	0.0545	0.0545
	4	148	435	422	429	50	16.1	0.0614	0.0486	17.7	7.46	2.56	3.36	0.0184	0.0156	0.0097	0.0232	0.846	0.0461	0.0519
	5	154	431	421	426	80	16.0	0.0570	0.0484	17.8	7.42	2.56	3.36	0.0205	0.0173	0.0067	0.0237	0.889	0.0400	0.0505
	6	154	432	426	429	80	16.0	0.0602	0.0433	17.7	7.41	2.54	3.36	0.0136	0.0116	0.0089	0.0180	0.856	0.0489	0.0515
	7	160	432	422	427	100	16.0	0.0576	0.0467	17.7	7.41	2.55	3.36	0.0185	0.0157	0.0060	0.0214	0.899	0.0422	0.0518
	8	159	437	426	432	100	15.9	0.0612	0.0414	17.6	7.40	2.53	3.36	0.0111	0.0095	0.0089	0.0155	0.859	0.0520	0.0526
◐	May 19-1	151	352	320	336	50	9.69	0.0322	0.0332	18.0	4.50×10^{-4}	1.57	3.40	0.0174	0.0145	0.0036	0.0192	0.890	0.0178	0.0286
	2	152	352	319	336	50	9.64	0.0326	0.0273	17.9	4.47	1.55	3.40	0.0112	0.0093	0.0039	0.0131	0.882	0.0234	0.0287
	3*	153	350	315	338	50	9.59	0.0328	0.0220	17.8	4.45	1.53	3.40	0.0057	0.0048	0.0050	0.0082	0.851	0.0279	0.0279
	4	153	352	320	336	50	9.62	0.0327	0.0252	17.8	4.46	1.54	3.40	0.0089	0.0075	0.0042	0.0110	0.872	0.0253	0.0285
	5	153	351	318	335	50	9.60	0.0327	0.0235	17.8	4.46	1.54	3.40	0.0073	0.0061	0.0045	0.0095	0.864	0.0267	0.0283
	6*	153	349	314	332	50	9.58	0.0340	0.0207	17.8	4.45	1.53	3.41	0.0037	0.0031	0.0064	0.0069	0.816	0.0278	0.0278
	7*	153	348	315	332	50	9.60	0.0370	0.0191	17.7	4.46	1.53	3.41	0.0006	0.0005	0.0093	0.0052	0.752	0.0278	0.0278
	8*	153	350	314	332	50	9.59	0.0344	0.0205	17.8	4.45	1.53	3.41	0.0032	0.0028	0.0066	0.0066	0.810	0.0279	0.0279
	9	152	348	310	329	50	9.72	0.0317	0.0358	18.0	4.51	1.57	3.41	0.0203	0.0169	0.0033	0.0219	0.898	0.0150	0.0285
	10†	150	345	315	330	50	9.87	0.0312	0.0513	18.2	4.58	1.62	3.41	0.0362	0.0299	0.0033	0.0378	0.896	0.0013	0.0280
◑	May 11-1	150	401	370	386	50	9.06	0.0408	0.0427	18.0	4.20×10^{-4}	1.46	3.38	0.0228	0.0191	0.0041	0.0248	0.902	0.0218	0.0368
	2	153	400	379	390	50	13.7	0.0453	0.0421	17.9	6.36	2.20	3.38	0.0199	0.0167	0.0068	0.0232	0.853	0.0288	0.0386
	3	155	396	376	386	50	17.1	0.0440	0.0441	17.9	7.94	2.76	3.38	0.0227	0.0191	0.0081	0.0266	0.819	0.0252	0.0360
	4	155	400	379	390	50	20.0	0.0453	0.0438	17.9	9.28	3.22	3.38	0.0217	0.0182	0.0100	0.0266	0.784	0.0274	0.0355
	5	154	379	372	376	50	23.6	0.0471	0.0450	17.9	10.94	3.79	3.39	0.0219	0.0184	0.0119	0.0278	0.751	0.0290	0.0354
○	May 12-1	156	398	350	374	100	8.81	0.0381	0.0420	18.0	4.09×10^{-4}	1.43	3.39	0.0234	0.0196	0.0032	0.0250	0.918	0.0186	0.0349
	2	159	401	354	378	100	12.2	0.0421	0.0432	17.9	5.68	1.98	3.38	0.0226	0.0190	0.0045	0.0248	0.896	0.0234	0.0377
	3	162	399	365	382	100	16.2	0.0421	0.0440	18.0	7.52	2.62	3.38	0.0234	0.0197	0.0050	0.0259	0.883	0.0266	0.0371
	4	162	396	375	386	100	18.7	0.0417	0.0450	18.0	8.69	3.03	3.38	0.0247	0.0207	0.0057	0.0275	0.867	0.0212	0.0361
	5	162	395	368	382	100	20.8	0.0416	0.0442	18.0	9.65	3.36	3.38	0.0239	0.0200	0.0064	0.0270	0.850	0.0218	0.0353
	6	162	398	371	385	100	23.3	0.0438	0.0451	18.0	10.80	3.76	3.38	0.0237	0.0199	0.0076	0.0274	0.830	0.0242	0.0364
○	May 5-1	158	396	382	389	100	21.8	0.0532	0.0477	17.8	10.12×10^{-4}	3.50	3.38	0.0217	0.0182	0.0085	0.0259	0.843	0.0353	0.0449
	2	157	400	378	389	100	16.4	0.0501	0.0487	17.9	7.62	2.64	3.38	0.0243	0.0203	0.0073	0.0278	0.858	0.0301	0.0430
	3	159	401	369	385	100	12.7	0.0505	0.0469	17.9	5.92	2.05	3.38	0.0222	0.0187	0.0061	0.0252	0.883	0.0322	0.0446
	4	159	395	360	378	100	8.25	0.0434	0.0479	18.0	3.83	1.34	3.38	0.0268	0.0224	0.0029	0.0252	0.934	0.0212	0.0405
○	May 7-1	158	405	382	394	100	14.8	0.0535	0.0501	17.9	6.89×10^{-4}	2.38	3.38	0.0240	0.0202	0.0073	0.0276	0.867	0.0337	0.0464
	2	158	401	369	385	100	12.0	0.0522	0.0510	17.9	5.59	1.94	3.38	0.0256	0.0214	0.0059	0.0285	0.889	0.0310	0.0464
	3	157	399	379	389	100	18.2	0.0508	0.0511	17.9	8.43	2.93	3.38	0.0264	0.0221	0.0076	0.0301	0.854	0.0290	0.0434
	4	158	401	362	382	100	8.05	0.0440	0.0491	18.0	3.74	1.30	3.38	0.0277	0.0232	0.0031	0.0292	0.931	0.0210	0.0409

* No mechanism change over occurred - oxygen diffusion rate controlling throughout.

† Hydrogen diffusion rate controlling throughout.

TABLE II

CALCULATED MASS TRANSFER COEFFICIENTS AND DIMENSIONLESS GROUPS

Run No.	t_g °C	P psia	$(G/M_m)_1$	(G/M_m)	$(Sc)_1$	$(Sc)_2$	$(Re)_1$	Re	K_O	$\frac{K_O(Sc)_1^{2/3}(Re)^{0.41}}{(G/M_m)(1-v)^{0.2}}$	K_H	$\frac{K_H(Sc)_2^{2/3}(Re)^{0.41}}{(G/M_m)(1-v)^{0.2}}$	K_ℓ	$\frac{K_\ell(Sc)_1^{2/3}(Re)^{0.41}}{(G/M_m)(1-v)^{0.2}}$	K_1	$\frac{K_1(Sc)_1^{2/3}(Re)_1^{0.41}}{(G/M_m)_1(1-v)^{0.2}}$	K_{L_1}	$\frac{K_{L_1}(Sc)_1^{2/3}(Re)_1^{0.41}}{(G/M_m)_1(1-v)^{0.2}}$
April 15-1	349	50	0.118	0.118	0.754	0.220	3320	3340	3.21×10^{-3}	0.693	5.24×10^{-3}	0.497	1.36×10^{-4}	2.93×10^{-2}	4.51×10^{-3}	0.965	1.61×10^{-4}	3.46×10^{-2}
2	344	50	0.117	0.117	0.751	0.219	3340	3350	3.87	0.839	4.82	0.459	1.40	3.04	4.41	0.951	1.47	3.17
3	336	50	0.117	0.117	0.748	0.218	3370	3360	4.31	0.935	4.45	0.424	1.43	3.09	4.39	0.955	1.44	3.13
4*	331	30	0.117	0.117	0.750	-	3390	3390	3.91	0.852	3.74	0.357	1.46	3.18	4.26	0.929	1.46	3.18
5	341	30	0.119	0.119	0.759	0.220	3390	3400	3.45	0.746	4.24	0.477	1.42	3.08	3.81	0.821	1.47	3.18
6	346	30	0.118	0.118	0.755	0.220	3330	3360	3.22	0.695	4.44	0.421	1.41	3.04	3.87	0.830	1.52	3.26
7	346	80	0.119	0.119	0.750	0.219	3360	3390	3.12	0.670	5.67	0.535	1.32	2.84	4.85	1.032	1.69	3.59
8	348	80	0.118	0.118	0.750	0.218	3340	3360	3.80	0.816	5.25	0.496	1.39	2.99	4.69	1.004	1.52	3.25
9	344	80	0.117	0.117	0.748	0.218	3330	3340	4.36	0.943	4.90	0.466	1.44	3.12	4.70	1.014	1.47	3.18
10	341	110	0.118	0.118	0.744	0.216	3400	3380	4.59	0.988	5.24	0.495	1.46	3.15	4.90	1.055	1.49	3.21
11	343	110	0.118	0.118	0.745	0.217	3370	3390	3.79	0.814	5.54	0.523	1.40	3.01	4.92	1.051	1.57	3.36
12	344	110	0.119	0.119	0.747	0.218	3370	3410	3.09	0.661	5.82	0.548	1.34	2.86	4.98	1.056	1.76	3.73
April 16-1	422	30	0.119	0.118	0.776	0.228	2940	2970	3.53×10^{-3}	0.735	5.08×10^{-3}	0.466	1.97×10^{-4}	4.11×10^{-2}	4.49×10^{-3}	0.928	2.19×10^{-4}	4.53×10^{-2}
2	415	30	0.118	0.118	0.773	0.226	2960	2970	4.14	0.867	4.36	0.402	2.03	4.25	4.25	0.888	2.05	4.27
3*	412	30	0.118	0.118	0.772	-	2990	2990	4.40	0.918	3.83	0.352	2.08	4.34	4.90	1.021	2.08	4.34
4*	433	50	0.119	0.119	0.775	-	2930	2930	5.20	1.072	4.59	0.425	2.23	4.59	5.52	1.137	2.23	4.59
5	437	50	0.118	0.118	0.777	0.228	2870	2890	4.39	0.911	5.32	0.487	2.09	4.33	5.01	1.035	2.19	4.52
6	435	50	0.119	0.118	0.778	0.228	2880	2920	3.49	0.724	5.85	0.536	1.90	3.94	5.12	1.054	2.31	4.76
7	443	80	0.118	0.118	0.778	0.228	2850	2890	3.45	0.715	6.37	0.582	1.86	3.86	5.56	1.139	2.42	4.96
8	435	80	0.118	0.117	0.774	0.227	2880	2900	4.12	0.857	6.00	0.551	1.95	4.05	5.44	1.125	2.20	4.55
9	430	80	0.117	0.117	0.772	0.226	2890	2910	4.73	0.989	5.68	0.523	2.02	4.22	5.44	1.132	2.11	4.40
10	424	110	0.117	0.117	0.770	0.225	2920	2940	4.68	0.977	5.80	0.533	2.06	4.31	5.51	1.144	2.18	4.54
11	426	110	0.117	0.117	0.772	0.225	2890	2920	4.17	0.873	6.07	0.560	2.02	4.23	5.51	1.146	2.28	4.74
12	423	110	0.118	0.117	0.773	0.226	2910	2940	3.60	0.752	6.38	0.588	1.94	4.05	5.60	1.160	2.45	5.08
April 21-1	503	100	0.116	0.115	0.792	0.234	2540	2580	3.11×10^{-3}	0.639	6.89×10^{-3}	0.629	2.11×10^{-4}	4.34×10^{-2}	6.01×10^{-3}	1.219	3.17×10^{-4}	6.43×10^{-2}
2	501	100	0.117	0.117	0.790	0.233	2600	2630	4.27	0.868	6.63	0.596	2.42	4.92	6.04	1.217	3.84	5.72
3	501	100	0.115	0.114	0.789	0.231	2560	2570	4.65	0.957	6.30	0.571	2.44	5.02	5.91	1.209	2.68	5.48
4	492	80	0.116	0.115	0.788	0.232	2610	2620	4.43	0.908	5.03	0.456	2.38	4.89	4.86	0.993	2.45	5.01
5	505	80	0.115	0.114	0.791	0.232	2540	2570	4.46	0.916	6.22	0.564	2.39	4.92	5.77	1.179	2.66	5.43
6	505	80	0.116	0.116	0.791	0.233	2570	2600	4.04	0.826	6.78	0.613	2.30	4.71	6.09	1.235	2.82	5.72
7	504	80	0.117	0.117	0.793	0.234	2580	2620	3.43	0.701	7.12	0.644	2.21	4.25	6.25	1.259	3.14	6.33

* No mechanism change over occurred - oxygen diffusion rate controlling throughout.

TABLE II (continued)

Run No.	t_g °C	P psia	$(G/M_m)_1$	(G/M_m)	$(Sc)_1$	$(Sc)_2$	$(Re)_1$	Re	K_O	$\frac{K_O(Sc)_1^{2/3}(Re)^{0.41}}{(G/M_m)(1-v)^{0.2}}$	K_H	$\frac{K_H(Sc)_2^{2/3}(Re)^{0.41}}{(G/M_m)(1-v)^{0.2}}$	K_ℓ	$\frac{K_\ell(Sc)_1^{2/3}(Re)^{0.41}}{(G/M_m)(1-v)^{0.2}}$	K_1	$\frac{K_1(Sc)_1^{2/3}(Re)_1^{0.41}}{(G/M_m)_1(1-v)^{0.2}}$	K_{L_1}	$\frac{K_{L_1}(Sc)_1^{2/3}(Re)_1^{0.41}}{(G/M_m)_1(1-v)^{0.2}}$
April 22-1	494	30	0.117	0.116	0.792	0.234	2610	2620	3.89×10^{-3}	0.795	4.98×10^{-3}	0.450	2.38×10^{-4}	4.86×10^{-2}	4.57×10^{-3}	0.928	2.53×10^{-4}	5.13×10^{-2}
2	490	30	0.117	0.117	0.802	0.234	2620	2650	3.32	0.683	5.19	0.470	2.21	4.55	4.53	0.926	2.58	5.26
3	500	30	0.116	0.116	0.792	0.234	2590	2590	4.47	0.910	4.69	0.423	2.53	5.15	4.66	0.947	2.56	5.20
4	511	50	0.116	0.116	0.793	0.234	2550	2560	4.74	0.961	5.36	0.482	2.57	5.22	5.24	1.062	2.65	5.37
5	511	50	0.116	0.116	0.794	0.234	2560	2580	4.16	0.845	5.82	0.523	2.43	4.94	5.33	1.080	2.70	5.47
6	511	50	0.119	0.118	0.795	0.235	2580	2620	3.54	0.715	6.39	0.572	2.32	4.69	5.62	1.124	2.99	5.96
7	501	80	0.116	0.115	0.792	0.234	2560	2610	3.36	0.689	7.12	0.648	2.16	4.43	6.24	1.265	3.12	6.33
8	497	80	0.114	0.114	0.789	0.232	2560	2590	4.30	0.890	6.55	0.600	2.27	4.69	6.00	1.232	2.63	5.40
9	495	80	0.114	0.114	0.787	0.232	2570	2590	4.66	0.964	6.21	0.569	2.31	4.78	5.86	1.207	2.52	5.19
10	488	100	0.116	0.116	0.785	0.231	2640	2650	4.95	1.016	6.21	0.573	2.41	4.94	5.97	1.220	2.57	5.26
11	490	100	0.117	0.117	0.787	0.232	2640	2670	3.83	0.783	6.98	0.632	2.24	4.57	6.20	1.260	2.89	5.84
April 23-1	238	30	0.120	0.120	0.722	0.208	4180	4180	2.12×10^{-3}	0.479	2.68×10^{-3}	0.264	0.609×10^{-4}	1.38×10^{-2}	2.18×10^{-3}	0.491	0.613×10^{-4}	1.38×10^{-2}
2*	233	30	0.120	0.120	0.721	-	4210	4210	2.23	0.505	2.43	0.241	0.601	1.36	2.23	0.504	0.601	1.36
3*	224	30	0.119	0.119	0.719	-	4280	4280	2.30	0.526	2.20	0.219	0.588	1.34	2.30	0.521	0.588	1.33
4*	228	50	0.119	0.119	0.715	-	4250	4250	2.39	0.545	2.31	0.230	0.584	1.33	2.39	0.543	0.584	1.33
5*	231	50	0.120	0.120	0.715	-	4240	4240	2.02	0.457	2.47	0.244	0.554	1.25	2.02	0.457	0.554	1.25
6*	226	80	0.119	0.119	0.715	-	4270	4270	2.08	0.474	2.33	0.232	0.523	1.19	2.08	0.474	0.525	1.20
7*	228	80	0.119	0.119	0.709	-	4210	4210	2.46	0.555	2.21	0.220	0.639	1.44	2.46	0.555	0.639	1.44
8*	233	80	0.119	0.119	0.711	-	4190	4190	2.00	0.451	2.44	0.242	0.584	1.32	2.00	0.451	0.584	1.32
9*	233	100	0.120	0.120	0.707	-	4220	4220	2.13	0.476	2.35	0.232	0.607	1.35	2.13	0.476	0.607	1.36
10	230	100	0.120	0.120	0.705	0.203	4250	4250	1.85	0.413	2.35	0.229	0.582	1.30	1.86	0.415	0.582	1.30
April 24-1*	244	80	0.145	0.145	0.718	-	4950	4950	2.83×10^{-3}	0.562	2.97×10^{-3}	0.258	1.02×10^{-4}	2.01×10^{-2}	2.83×10^{-3}	0.563	1.02×10^{-4}	2.02×10^{-2}
2*	243	80	0.145	0.145	0.717	-	4940	4940	3.05	0.606	2.84	0.248	1.03	2.05	3.05	0.606	1.03	2.05
3*	246	80	0.146	0.146	0.719	-	4940	4940	2.60	0.516	3.06	0.266	0.988	1.96	2.60	0.516	0.988	1.96
4*	254	100	0.147	0.147	0.717	-	4900	4900	2.81	0.549	3.15	0.271	1.05	2.05	2.81	0.549	1.05	2.05
5*	251	100	0.147	0.147	0.717	-	4940	4940	3.13	0.612	3.03	0.261	1.09	2.14	3.13	0.612	1.09	2.14
6*	238	50	0.145	0.145	0.722	-	4970	4970	2.69	0.539	2.79	0.244	0.988	1.98	2.69	0.539	0.988	1.98
7*	229	50	0.144	0.144	0.720	-	5030	5030	2.79	0.564	2.51	0.221	0.964	1.95	2.79	0.564	0.964	1.95
April 28-1*	275	30	0.144	0.144	0.739	-	4550	4550	3.14×10^{-3}	0.620	2.70×10^{-3}	0.231	1.39×10^{-4}	2.75×10^{-2}	3.14×10^{-3}	0.620	1.39×10^{-4}	2.75×10^{-2}
2*	281	30	0.145	0.145	0.741	-	4530	4570	2.93	0.579	3.01	0.259	1.38	2.72	2.93	0.576	1.38	2.71
3*	291	30	0.145	0.145	0.744	-	4460	4460	2.65	0.516	2.93	0.249	1.35	2.63	2.65	0.516	1.36	2.65
4*	300	50	0.145	0.145	0.742	-	4420	4420	3.06	0.594	3.46	0.294	1.39	2.70	3.06	0.594	1.39	2.70
5*	293	50	0.146	0.146	0.740	-	4480	4480	3.39	0.659	3.27	0.278	1.41	2.74	3.39	0.659	1.41	2.75
6*	285	50	0.146	0.146	0.739	-	4510	4510	3.92	0.762	2.79	0.237	1.58	3.07	3.92	0.762	1.58	3.07
7*	296	80	0.144	0.144	0.737	-	4410	4410	3.88	0.753	3.19	0.272	1.50	2.91	3.88	0.753	1.50	2.91
8*	307	80	0.146	0.146	0.740	-	4480	4380	3.42	0.658	3.51	0.296	1.44	2.77	3.42	0.664	1.44	2.79

* No mechanism change over occurred - oxygen diffusion rate controlling throughout.

TABLE II (continued)

Run No.	t_g °C	P psia	$(G/M_m)_1$	(G/M_m)	$(Sc)_1$	$(Sc)_2$	$(Re)_1$	Re	K_O	$\frac{K_O(Sc)_1^{2/3}(Re)^{0.41}}{(G/M_m)(1-v)^{0.2}}$	K_H	$\frac{K_H(Sc)_1^{2/3}(Re)^{0.41}}{(G/M_m)(1-v)^{0.2}}$	K_ℓ	$\frac{K_\ell(Sc)_1^{2/3}(Re)^{0.41}}{(G/M_m)(1-v)^{0.2}}$	K_1	$\frac{K_1(Sc)_1^{2/3}(Re)_1^{0.41}}{(G/M_m)_1(1-v)^{0.2}}$	K_{L_1}	$\frac{K_{L_1}(Sc)_1^{2/3}(Re)_1^{0.41}}{(G/M_m)_1(1-v)^{0.2}}$
April 30-1	411	35	0.143	0.143	0.774	0.227	3590	3610	5.52×10^{-3}	1.031	5.38×10^{-3}	0.443	2.74×10^{-4}	5.11×10^{-2}	4.84×10^{-3}	0.900	2.50×10^{-4}	4.66×10^{-2}
2*	420	35	0.144	0.144	0.778	-	3540	3540	5.44	1.003	4.06	0.329	2.81	5.19	5.44	1.003	2.81	5.18
3*	428	50	0.144	0.144	0.776	-	3530	3530	6.02	1.105	4.72	0.383	2.82	5.18	6.02	1.105	2.82	5.18
4	429	50	0.143	0.143	0.775	0.228	3520	3530	4.60	0.855	5.61	0.461	2.34	4.34	6.59	1.219	2.43	4.49
5	426	80	0.142	0.142	0.772	0.227	3530	3550	4.43	0.825	6.57	0.542	2.18	4.06	5.77	1.071	2.45	4.55
6	429	80	0.142	0.142	0.772	0.226	3520	3520	5.40	1.004	5.78	0.475	2.40	4.46	5.67	1.053	2.43	4.51
7	427	100	0.142	0.142	0.771	0.227	3520	3550	4.83	0.899	6.84	0.563	2.26	4.21	6.19	1.147	2.51	4.66
8	432	100	0.141	0.141	0.770	0.226	3500	3500	6.01	1.115	5.82	0.478	2.53	4.69	6.07	1.126	2.53	4.70
May 19-1	336	50	0.0868	0.0866	0.747	0.218	2520	2540	2.06×10^{-3}	0.537	4.02×10^{-3}	0.462	0.699×10^{-4}	1.82×10^{-2}	3.41×10^{-3}	0.882	0.940×10^{-4}	2.43×10^{-2}
2	336	50	0.0862	0.0861	0.746	0.218	2520	2530	2.71	0.709	3.87	0.445	0.751	1.96	3.43	0.893	0.830	2.16
3*	338	50	0.0856	0.0856	0.745	-	2510	2510	3.62	0.947	3.43	0.397	0.810	2.12	3.62	0.947	0.810	2.12
4	336	50	0.0860	0.0859	0.745	0.218	2520	2520	3.02	0.790	3.72	0.428	0.771	2.02	3.44	0.898	0.806	2.10
5	335	50	0.0858	0.0857	0.742	0.217	2520	2520	3.32	0.866	3.60	0.415	0.791	2.06	3.51	0.916	0.802	2.09
6*	332	50	0.0856	0.0856	0.744	-	2520	2520	4.02	1.055	3.05	0.353	0.863	2.26	4.02	1.055	0.863	2.26
7*	332	50	0.0857	0.0857	0.746	-	2510	2510	4.73	1.248	2.53	0.291	0.988	2.59	4.73	1.238	0.988	2.59
8*	332	50	0.0856	0.0856	0.744	-	2520	2520	4.14	1.085	3.00	0.347	0.881	2.31	4.14	1.085	0.881	2.31
9	329	50	0.0871	0.0868	0.747	0.218	2550	2580	1.86	0.485	4.17	0.480	0.678	1.77	3.52	0.913	1.19	3.10
10†	330	50	0.0888	0.0882	0.750	0.220	2560	2610	1.19	0.310	4.21	0.482	0.623	1.62	3.72	0.951	1.41	3.61
May 11-1	386	50	0.0810	0.0807	0.763	0.224	2150	2180	1.92×10^{-3}	0.510	3.95×10^{-3}	0.464	0.833×10^{-4}	2.22×10^{-2}	3.37×10^{-3}	0.888	1.17×10^{-4}	3.10×10^{-2}
2	390	50	0.122	0.122	0.765	0.225	3230	3250	3.16	0.657	4.93	0.452	1.39	2.88	4.24	0.875	1.60	3.30
3	386	50	0.153	0.152	0.763	0.225	4050	4080	3.38	0.615	5.50	0.443	1.59	2.89	4.63	0.838	1.86	3.38
4	390	50	0.179	0.178	0.765	0.225	4700	4730	3.91	0.649	5.75	0.422	1.86	3.09	4.84	0.800	2.05	3.39
5	376	50	0.210	0.210	0.761	0.224	5640	5670	4.44	0.670	6.17	0.412	2.21	3.34	5.18	0.779	2.35	3.52
May 12-1	374	100	0.0788	0.0785	0.755	0.222	2130	2160	1.78×10^{-3}	0.481	4.13×10^{-3}	0.494	0.756×10^{-4}	2.04×10^{-2}	3.53×10^{-3}	0.944	1.18×10^{-4}	3.16×10^{-2}
2	378	100	0.109	0.109	0.757	0.222	2940	2970	2.65	0.588	5.20	0.510	1.17	2.59	4.43	0.977	1.58	3.49
3	382	100	0.145	0.144	0.758	0.223	3860	3900	3.34	0.629	6.51	0.541	1.51	2.84	5.53	1.032	2.08	3.88
4	386	100	0.168	0.167	0.760	0.223	4440	4480	3.61	0.623	7.09	0.540	1.69	2.91	5.98	1.024	2.29	3.91
5	382	100	0.186	0.185	0.758	0.223	4960	5010	3.99	0.649	7.40	0.531	1.85	3.00	6.23	1.004	2.39	3.85
6	385	100	0.208	0.207	0.760	0.223	5510	5560	4.23	0.686	7.76	0.520	2.16	3.28	6.53	0.983	2.59	3.90
May 5-1	389	100	0.194	0.194	0.763	0.224	5090	5120	5.20×10^{-3}	0.818	7.56×10^{-3}	0.525	2.61×10^{-4}	4.10×10^{-2}	6.56×10^{-3}	1.026	2.89×10^{-4}	4.52×10^{-2}
2	389	100	0.147	0.146	0.763	0.224	3840	3870	3.59	0.668	6.00	0.493	1.82	3.40	5.12	0.946	2.19	4.06
3	385	100	0.114	0.113	0.761	0.223	3000	3030	3.09	0.668	5.11	0.488	1.48	3.21	4.42	0.949	1.78	3.83
4	378	100	0.0739	0.0735	0.758	0.223	1970	2000	1.71	0.480	4.20	0.521	0.819	2.30	3.60	1.001	1.34	3.74
May 7-1	394	100	0.132	0.132	0.765	0.224	3430	3460	3.46×10^{-3}	0.682	5.59×10^{-3}	0.487	1.80×10^{-4}	3.54×10^{-2}	4.81×10^{-3}	0.942	2.12×10^{-4}	4.15×10^{-2}
2	385	100	0.107	0.107	0.762	0.223	2820	2850	2.74	0.614	4.95	0.489	1.43	3.20	4.24	0.942	1.82	4.05
3	389	100	0.162	0.161	0.764	0.224	4230	4270	3.76	0.661	6.54	0.506	2.01	3.54	5.53	0.964	2.48	4.32
4	382	100	0.0720	0.0717	0.760	0.223	1910	1940	1.63	0.467	4.03	0.507	0.805	2.29	3.45	0.972	1.33	3.74

* No mechanism change over occurred - oxygen diffusion rate controlling throughout.

† Hydrogen diffusion rate controlling throughout.

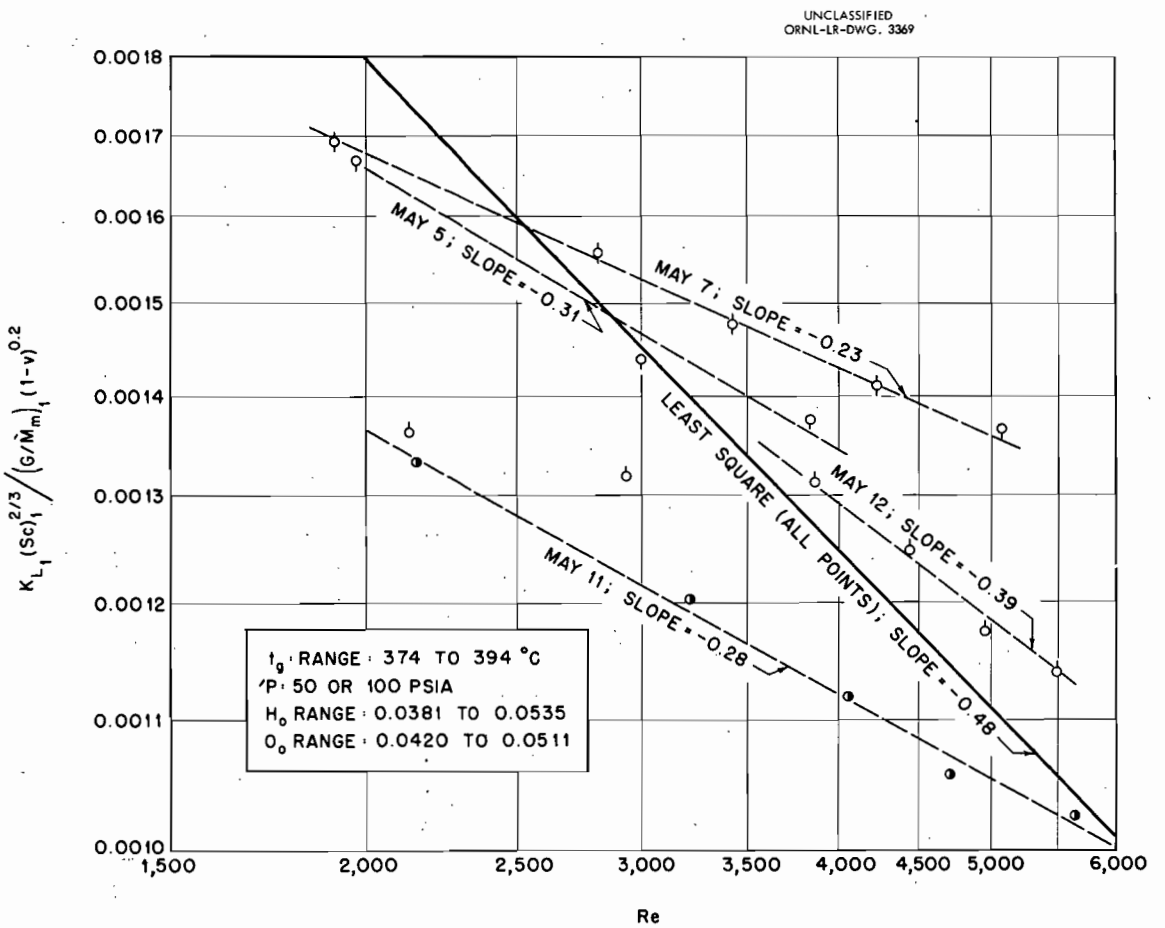

Figure 2

Justification Of The Reynolds Number Dependence Of The Dual-Langmuir Mechanism Mass Transfer Coefficient; Logarithmic Plots Of The Data Of Experiments Of May 5, 7, 11, and 12.

it turns out for Case III that

$$\ln \frac{(2O_0-H_0)(1-0.5H_2)}{(1-0.5H_0)\,H_2} \approx -\frac{\delta^n}{2}\left[\frac{\delta H_0-2O_0}{(1-H_0)(\delta-1)} + \frac{2(1-O_0)}{(1-H_0)}\ln\frac{2O_0}{2O_0-H_0}\right] + \left[\delta^n \frac{K_1 JaL}{2V_0(1-H_0)} + \ln(\delta-1)\left[\frac{\delta}{\delta-1}\right]^{\delta^n}\right] \qquad (46)$$

and for Case V that

$$(2O_0-H_0)\ \ln \frac{(2O_0-H_0)(1-0.5H_2)}{(\delta-1)(1-0.5H_0)H_2} \approx -\delta^n\left[\frac{2(\delta H_0-2O_0)}{\delta-1} - (2O_0-H_0)\ln\frac{2O_0}{2O_0-H_0}\,\frac{\delta-1}{\delta}\right] + \delta^n\left[\frac{K_{L_1}\ JaL}{V_0}\right] \qquad (47$$

The implication is that when the left hand members of equations (46) and (47) are plotted versus the first bracketed terms (for a series of runs made with identical Schmidt and Reynolds numbers, but with different O_0/H_0 ratios), two straight lines should result and the slopes of these should be

$-0.5\delta^n$ and $-\delta^n$ respectively.

Figures 3 and 4 are plots of the data for the runs of April 21-22 and May 19 respectively that result when the procedure described is carried out for the dual-Langmuir case represented by equation (47). Values of $n = 1.01$ and 0.75 apply for the data of April 21 and 22 separately, whereas a lumped treatment of these yields 0.88, and the May 19 data give $n = 0.89$. The same data treated for Case III in accordance with equation (46) give $n = 0.79$ for the April 21-22 data and 0.62 for the May 19 set of experiments. Using a similar but more highly approximated approach, Ransohoff and Spiewak had extricated a value of $n = 0.605$ for the May 19 data. In view of the approximate character of equations (46) and (47) themselves, the non-conformity of the experimental conditions with respect to isothermality, failure to maintain constant Re, among others, the agreement of the estimated n with the 2/3 anticipated value is considered adequate justification for application of the Gamson correlation.

The May data delineated in Figure 4 show a feature previously pointed out by Ransohoff and Spiewak in their comparable plot. According to the development leading to this method of representing the data, the linear portion should exist only for those ranges of operation which develop two diffusion zones in the bed; outside of this range on either side, the plot should lose its linearity. The data confirm this. Of the ten experiments conducted in the May 19 series, four are for a completely oxygen diffusion controlled bed, five are for a two-zone bed, and one (run 10) is on the verge of being completely hydrogen diffusion controlled. The fact that the observed data indicate the curvature changes at the proper locations on Figure 4 is taken as substantiation of the conjecture that a mechanism change-over occurs when hydrogen becomes the less abundant component at the catalyst.

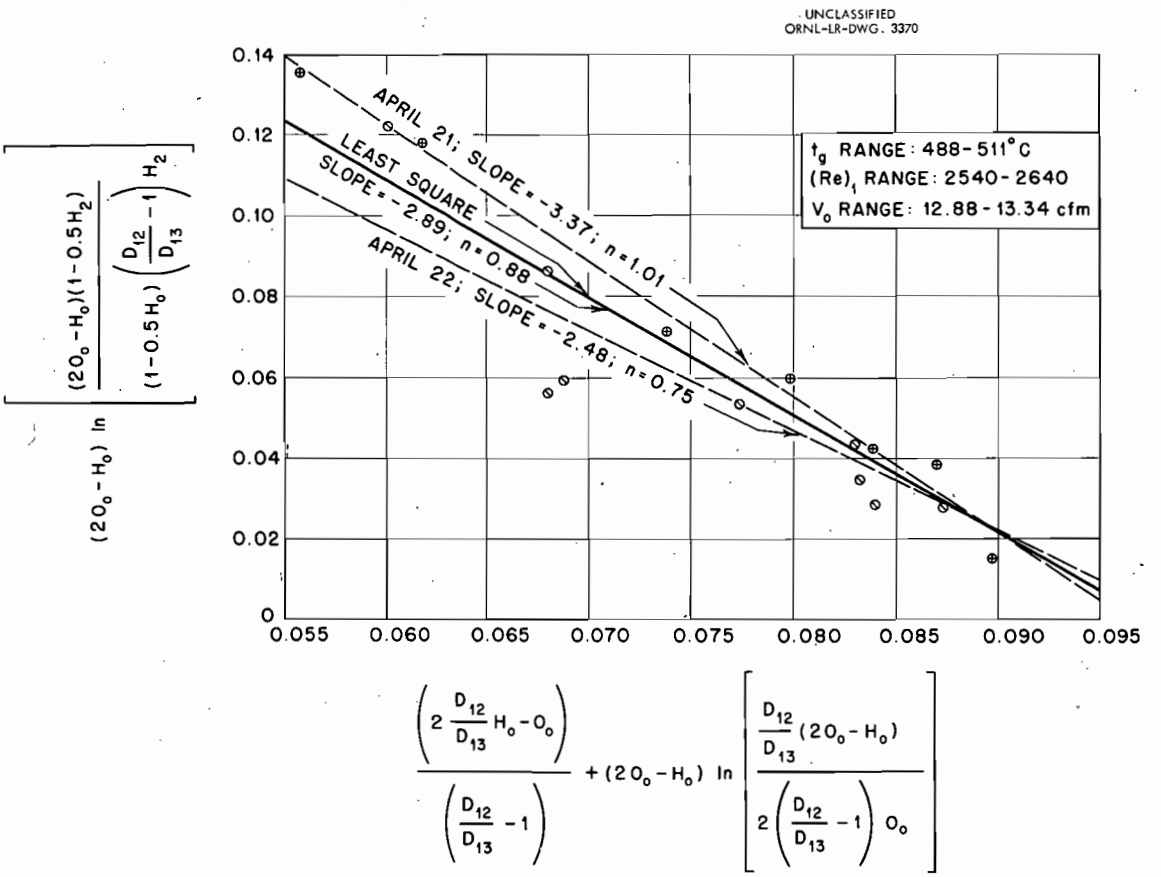

Figure 3

Justification Of The Schmidt Number Dependence Of The Dual-Langmuir Mechanism Mass Transfer Coefficient; Data Of Experiments Of April 21 and 22.

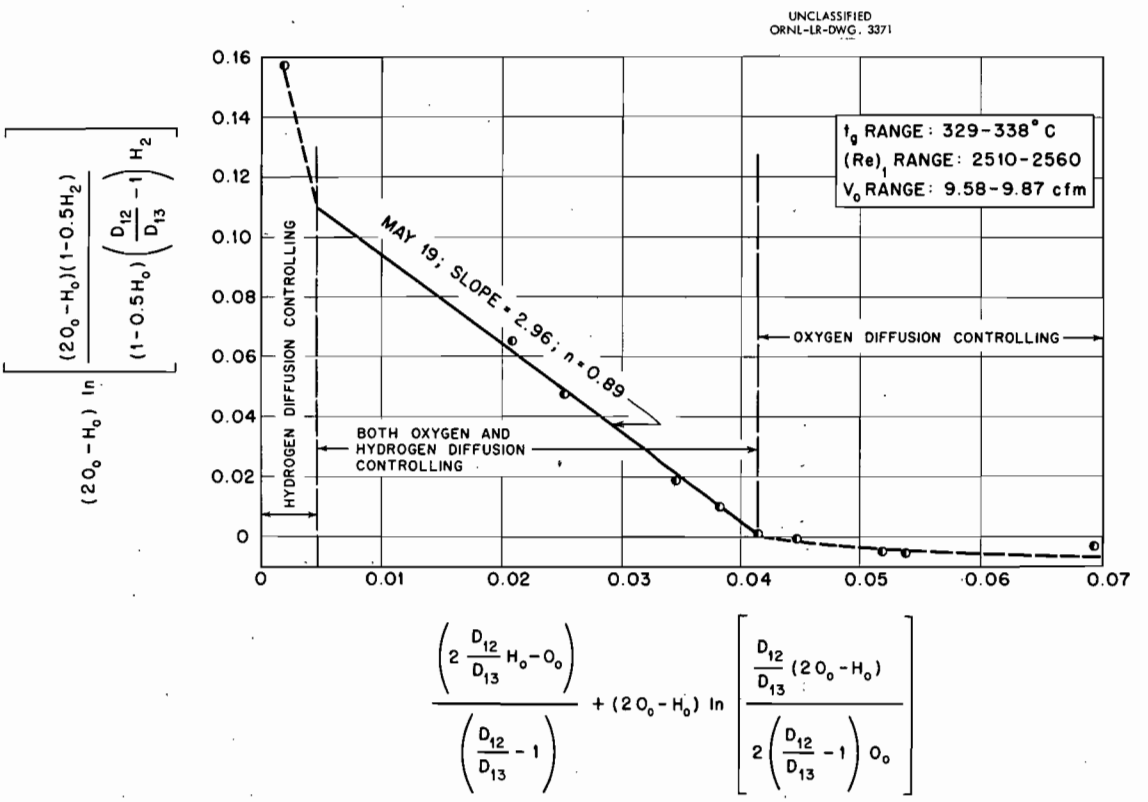

Figure 4

Justification Of The Schmidt Number Dependence Of The Dual-Langmuir Mechanism Mass Transfer Coefficient; Data Of Experiments Of May 19.

Characteristics Of The Recombiner Bed

To evaluate the various mass transfer coefficients described, the magnitudes of the parameters involved are necessary, and these are tabulated in this section. The observation of some inconsistencies concerning the catalytic bed in ORNL Report 1583 prompted one of the authors (HJG) to request Mr. Spiewak to check the doubtful points. The revised information resulting from this check (13) are stated here and supersede the previously reported values.

The important geometrical features of the recombiner used are indicated in Figure 5. The pertinent details are:

1. The converter shell is packed with 424 right cylinder catalyst pellets having a mean diameter of 0.1287 inch and 0.1408 inch length, exposing a superficial surface of 0.08295 sq in per pellet and a total (JaL) superficial surface of 0.2442 sq ft.

2. The cover shell is a 1.705 inch length of standard 1-inch schedule 40 pipe with an internal diameter of 1.009 inch. The thermocouple well is a cylinder with external diameter 0.510 inch with a hemispherical end having a radius of 0.255 inch, and the maximum axial dimension of this well is 0.640 inch.

3. The volume of one catalyst pellet is 0.001832 cu in and the total volume occupied by the 424 pellets is 0.7766 cu in.

4. The internal unpacked volume of the catalyst shell, uncorrected for the well, is 1.3633 cu in, and the volume occupied by the thermocouple well is 0.1088 cu in, resulting in an unpacked internal volume for the shell of 1.2545 cu in. The void space for gas flow is 0.4779 cu in and the void fraction is $v = 0.3809$. The catalyst superficial specific surface is $J = 336.4$ sq ft/cu ft.

5. The equivalent spherical diameter of the catalyst pellets is $D_p = 0.1625$ inch, and insofar as flow is concerned, the area effectiveness factor (correction for non-point contact between pellets) of $\phi = 0.91$, resulting in a Reynolds number based upon the superficial mass velocity, as defined by equation (43b) of $Re = 0.02404G/\mu$, with G stated as lb/(sec)(sq ft) and μ as lb/(ft)(sec).

6. The presence of the thermocouple well raises a question regarding the proper value to use for a (the cross-sectional area of the bed) in calculating the superficial mass velocity. The final decision was to employ a weighted mean cross-sectional area. The cross-sectional area of the portion fore and aft of the well is 0.7996 sq in, each with a length of 0.5975 inch, whereas the thermocouple section has a mean unrestricted flow channel of 0.6110 sq in and a length of 0.510 inch, so the value of a is $(0.7996 \cdot 0.5975 + 0.6110 \cdot 0.510)/1.705 = 0.7432$ sq in, or $a = 0.005161$ sq ft.

UNCLASSIFIED
ORNL-LR-DWG. 3372

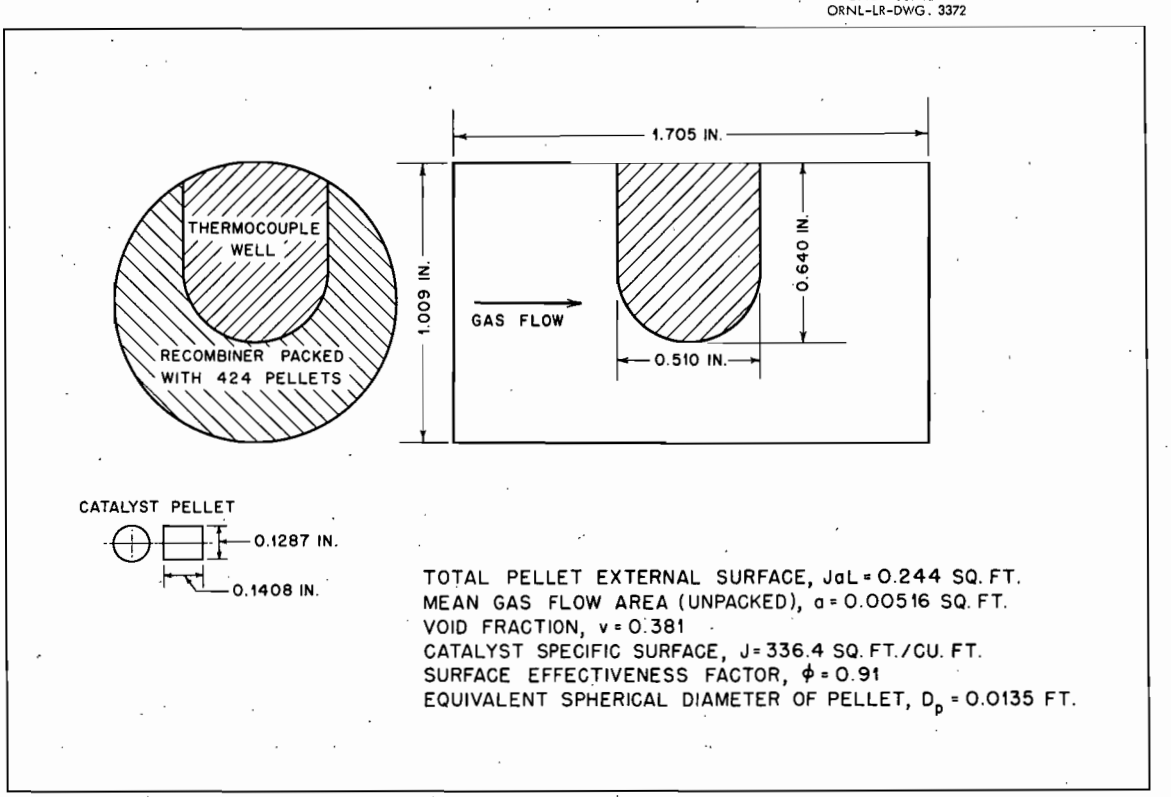

Figure 5

Significant Details Of The Catalytic Recombiner

7. The possibility that a "blind zone" might exist behind the thermocouple well, making this zone unavailable for entry of new gas and catalysis, was considered, but the calculations presented are made assuming complete availability of all of the bed. If the "blind zone" had been employed, the values of a and JaL would have been readjusted to 0.004360 sq ft and 0.2072 sq ft respectively.

Calculated Mass Transfer Coefficients And Dimensionless Groups

The defined mass transfer coefficients K_O, K_H, K_ℓ, K_1, and K_{L_1} for the five cases outlined previously were evaluated for the 104 experiments of Ransohoff and Spiewak using equations (16), (19), (34), (44a), and (44b) and the original data summarized in Table I. The results of these calculations are given in Table II. This table also gives the values of the "grand" dimensionless group $(KM_m/G)(Sc)^{2/3}(Re)^{0.41}/(1-v)^{0.2}$ that apply for each experiment for the five cases considered.

An inspection of Table II shows that the maximum value encountered for the dimensionless groups is 1.27 for run No. 7 of April 22 for Case III. Inasmuch as this is for the oxygen diffusion regulated portion of the bed this value should be halved before comparing this result with the 1.46 magnitude specified by the Gamson correlation. The resulting maximum value of 0.64 (actually the K_H group for this run of 0.65 is slightly higher) as compared to 1.46 indicates that the recombination rate constants at best approach but 44 per cent of the value that would be predicted from the correlation for purely physical diffusion controlled processes. It appears that if the possible influence of severe channeling (induced by the thermocouple well) is ruled out, and the fact that the bed always operated in the hydrodynamic entrance region is overlooked, the conclusion is that the recombination reaction is not a purely diffusion regulated process. The surface chemistry evidently plays a major role. This conclusion is given further support by the fact that the data show an unmistakable temperature dependence, approximately tripling during a temperature increase of 270° C.

Since the attitude taken here is primarily Edisonian, the question of deciding which of the mechanisms suggested best fits the observed data is answered by plotting the various "grand" dimensionless groups versus a characteristic operating temperature. The mean gas stream temperature, t_g, defined as the average of the gas discharge temperature (t_2) and the thermocouple value (t_b) is used as the independent variable. The averages for the same pressure runs for each day, as summarized in Table III, rather than the values of the individual runs, are indicated on Figures 6, 7, 8, 9, and 10. Because of the excessive scattering of the points, no correlation curve is indicated on Figures 6, 7, 8, and 9. The dual-Langmuir mechanism values give the strongest indication for a valid correlation with temperature. Since these findings are essentially in agreement with the original postulates, the dual-Langmuir is considered to be the most suitable basis for designing recombiners.

TABLE III

MEAN VALUES OF THE MASS TRANSFER DIMENSIONLESS GROUPS

Designation	Run Nos.	t_b mean °C	t_g mean °C	P psia	$\frac{K_O(Sc)_1^{2/3}(Re)^{0.41}}{(G/M_m)(1-v)^{0.2}}$	$\frac{K_H(Sc)_2^{2/3}(Re)^{0.41}}{(G/M_m)(1-v)^{0.2}}$	$\frac{K_\ell(Sc)_1^{2/3}(Re)^{0.41}}{(G/M_m)(1-v)^{0.2}}$	$\frac{K_1(Sc)_1^{2/3}(Re)^{0.41}}{(G/M_m)_1(1-v)^{0.2}}$	$\frac{K_{L_1}(Sc)_1^{2/3}(Re)^{0.41}}{(G/M_m)_1(1-v)^{0.2}}$
⊖	April 15; 1- 3	347	343	50	0.822	0.460	3.022×10^{-2}	0.957	3.252×10^{-2}
	4- 6	342	339	30	0.764	0.418	3.099	0.860	3.207
	7- 9	348	346	80	0.810	0.499	2.982	1.017	3.340
	10-12	351	343	100	0.821	0.522	3.006	1.054	3.431
⦶	April 16; 1- 3	423	416	30	0.840	0.407	4.232×10^{-2}	0.946	4.382×10^{-2}
	4- 6	438	435	50	0.902	0.483	4.289	1.075	4.625
	7- 9	439	436	80	0.854	0.552	4.042	1.132	4.635
	10-12	427	424	110	0.867	0.560	4.198	1.150	4.788
⊕	April 21; 1- 3	516	502	100	0.821	0.599	4.760×10^{-2}	1.215	5.878×10^{-2}
	4- 7	516	502	80	0.838	0.569	4.692	1.166	5.622
⊗	April 22; 1- 3	507	495	30	0.796	0.448	4.854×10^{-2}	0.934	5.196×10^{-2}
	4- 6	522	511	50	0.840	0.526	4.952	1.071	5.602
	7- 9	509	498	80	0.848	0.606	4.632	1.235	5.637
	10-11	508	489	100	0.900	0.603	4.755	1.240	5.547
⊘	April 23; 1- 3	233	232	30	0.503	0.241	1.353×10^{-2}	0.505	1.356×10^{-2}
	4- 5	231	230	50	0.501	0.237	1.291	0.500	1.289
	6- 8	229	229	80	0.493	0.231	1.316	0.493	1.318
	9-10	230	232	100	0.444	0.230	1.326	0.445	1.327
⊗	April 24; 1- 3	232	244	80	0.561	0.258	2.006×10^{-2}	0.562	2.007×10^{-2}
	4- 5	243	253	100	0.581	0.266	2.094	0.581	2.094
	6- 7	222	234	50	0.552	0.233	1.966	0.552	1.965
◓	April 28; 1- 3	285	282	30	0.572	0.246	2.700×10^{-2}	0.571	2.704×10^{-2}
	4- 6	296	293	50	0.672	0.270	3.836	0.672	2.839
	7- 8	303	302	80	0.706	0.284	2.840	0.709	2.852
◒	April 30; 1- 2	426	416	35	1.017	0.386	5.152×10^{-2}	0.952	4.922×10^{-2}
	3- 4	435	429	50	0.980	0.422	4.760	1.162	4.836
	5- 6	432	428	80	0.914	0.508	4.262	1.062	4.528
	7- 8	435	430	100	1.007	0.520	4.452	1.137	4.677
◐	May 19; 1-10	350	334	50	0.803	0.410	2.153×10^{-2}	0.978	2.578×10^{-2}
◑	May 11; 1- 5	395	386	50	0.620	0.439	2.885×10^{-2}	0.836	3.342×10^{-2}
○	May 12; 1- 6	398	381	100	0.609	0.523	2.777×10^{-2}	0.994	3.698×10^{-2}
○	May 5; 1- 4	398	385	100	0.659	0.507	3.253×10^{-2}	0.980	4.038×10^{-2}
○	May 7; 1- 4	402	388	100	0.606	0.497	3.145×10^{-2}	0.955	4.067×10^{-2}

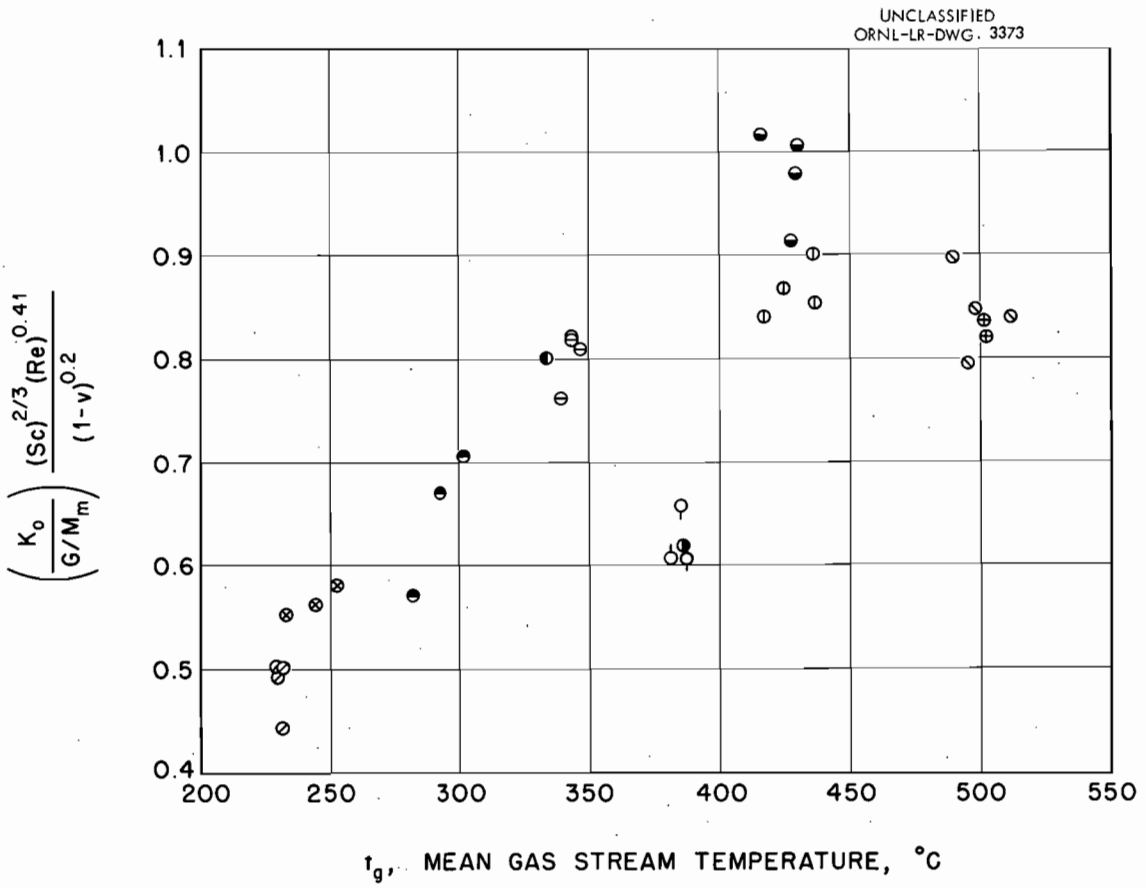

Figure 6

Temperature Dependence Of The Mass Transfer Dimensionless Group For Case I; Oxygen Diffusion Rate Controlling Over Entire Bed.

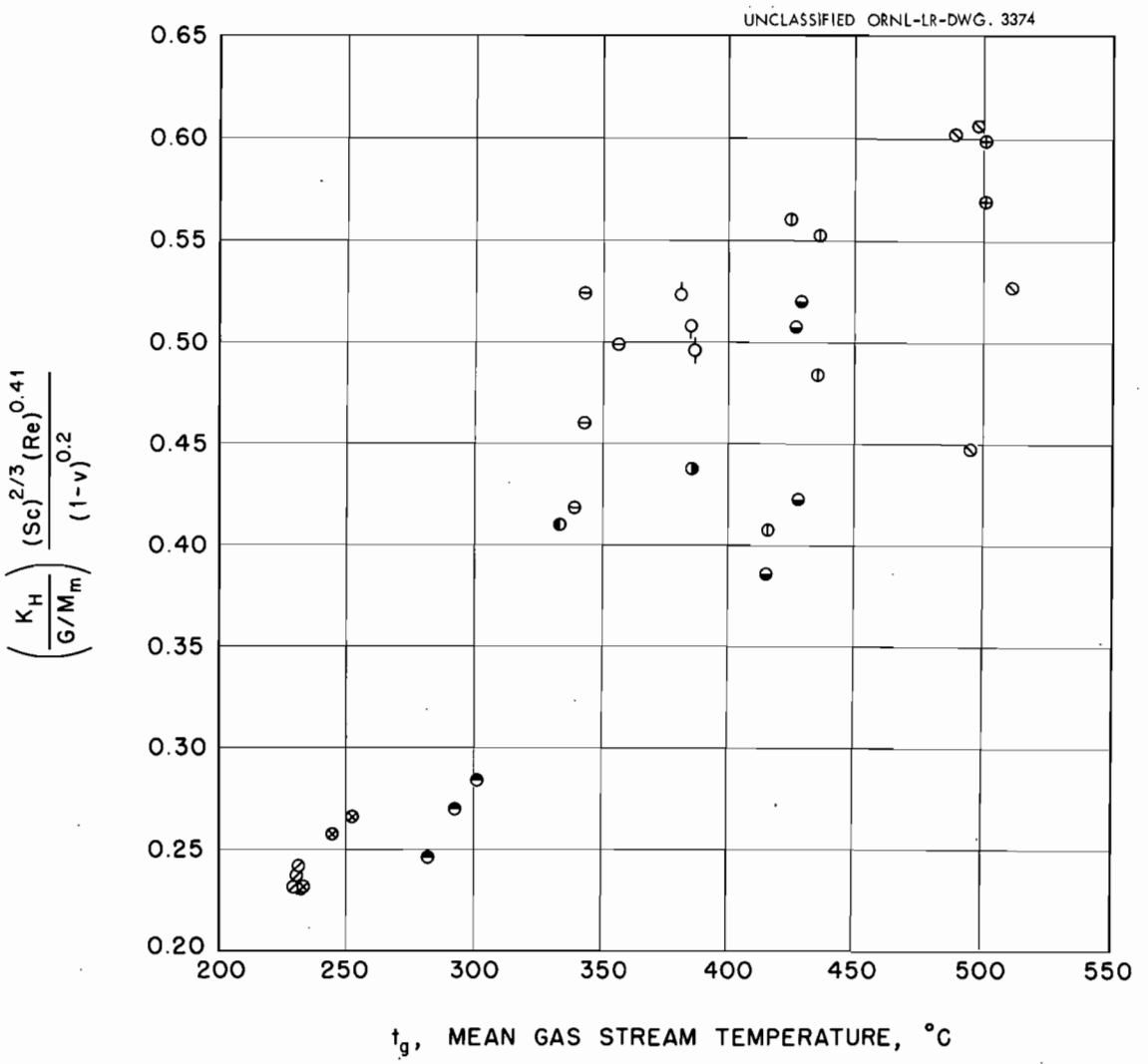

Figure 7

Temperature Dependence Of The Mass Transfer Dimensionless Group For Case II; Hydrogen Diffusion Rate Controlling Over Entire Bed.

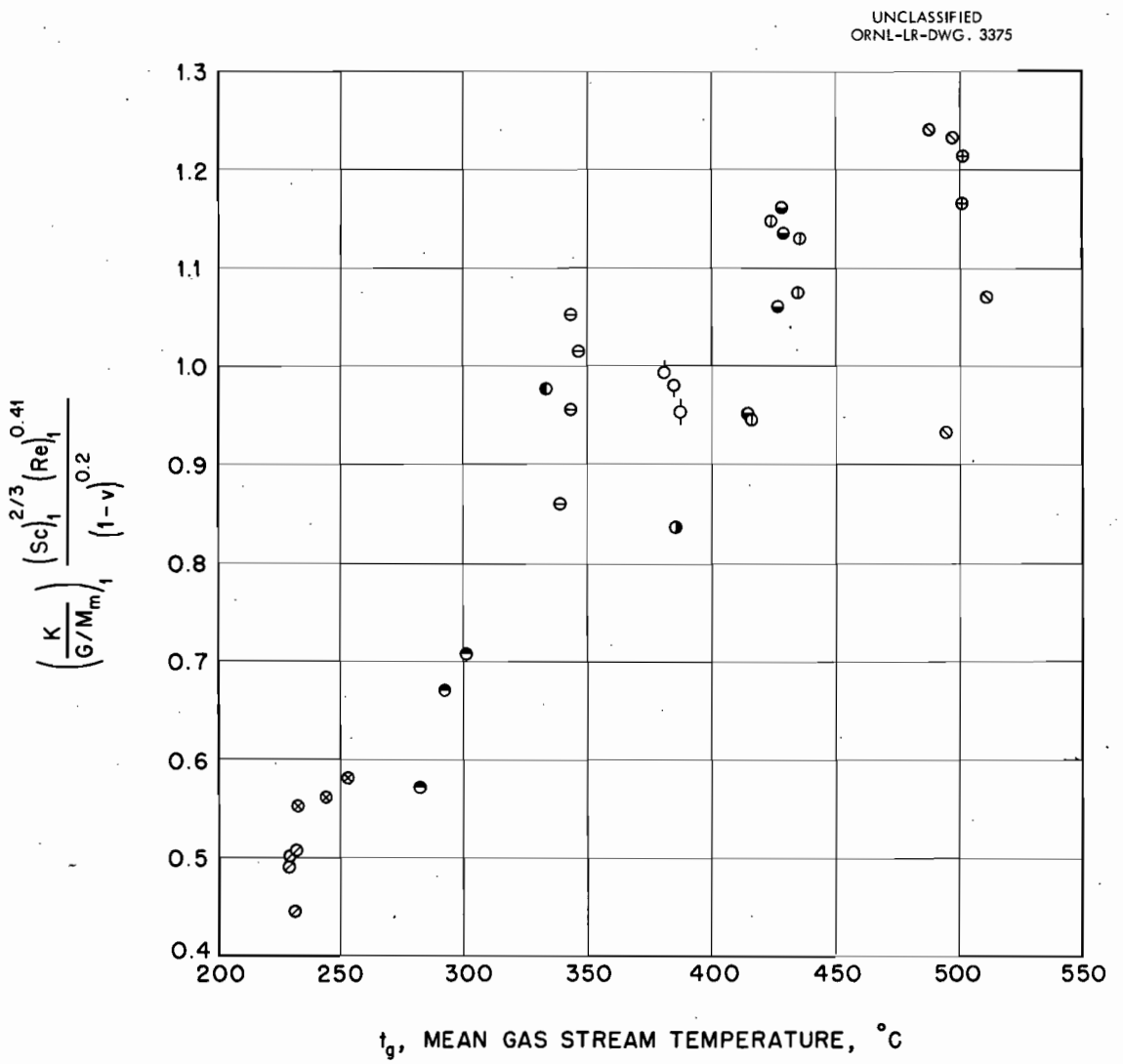

Figure 8

Temperature Dependence Of The Langmuir Mass Transfer Dimensionless Group For Case III; Oxygen Diffusion Rate Controlling Over Entire Bed With Catalytic Surface Restricted.

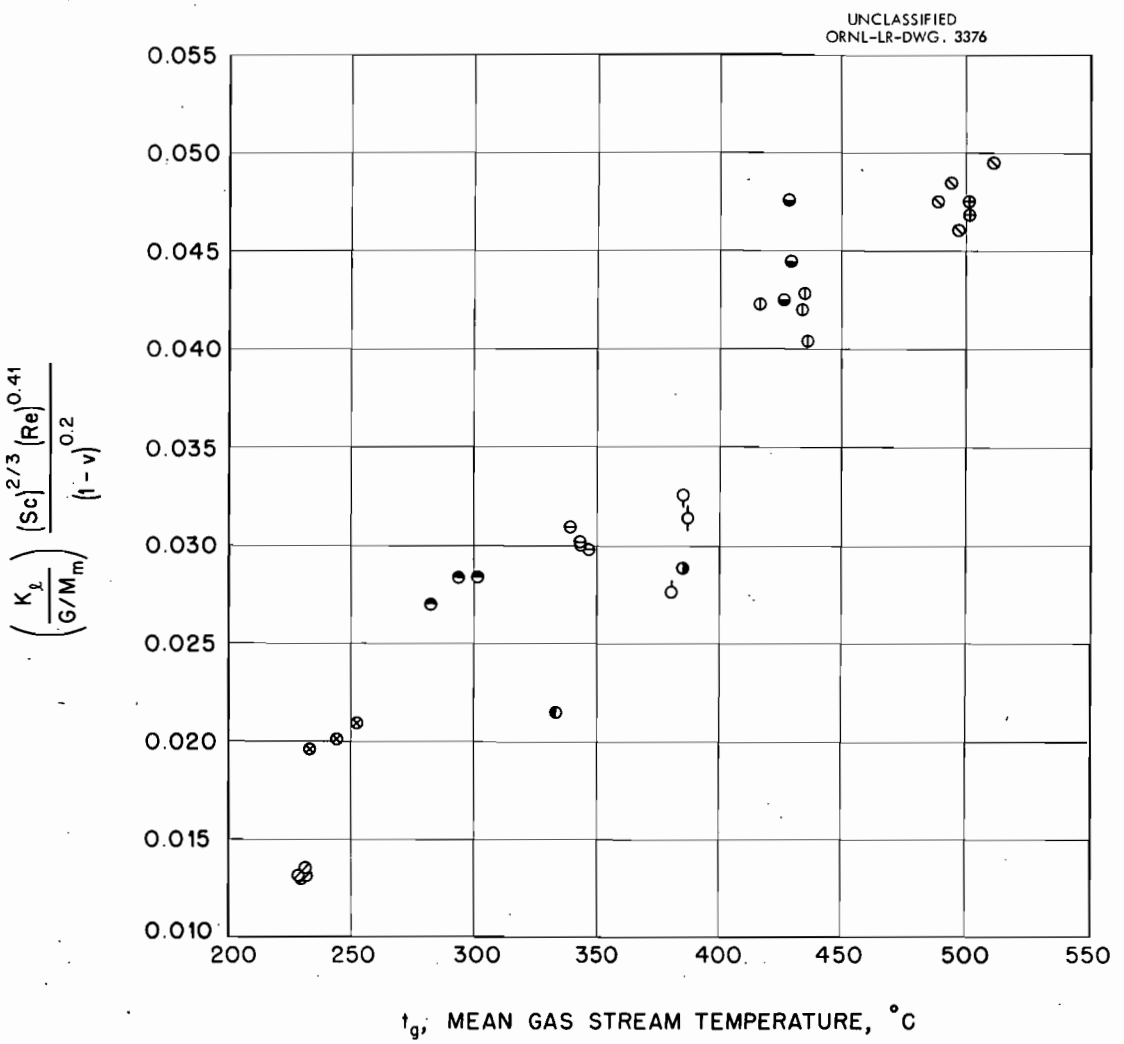

Figure 9

Temperature Dependence Of The Mass Transfer Dimensionless Group For Case IV; Oxygen And Hydrogen Diffusion Rates Controlling For Separate Portions Of The Bed.

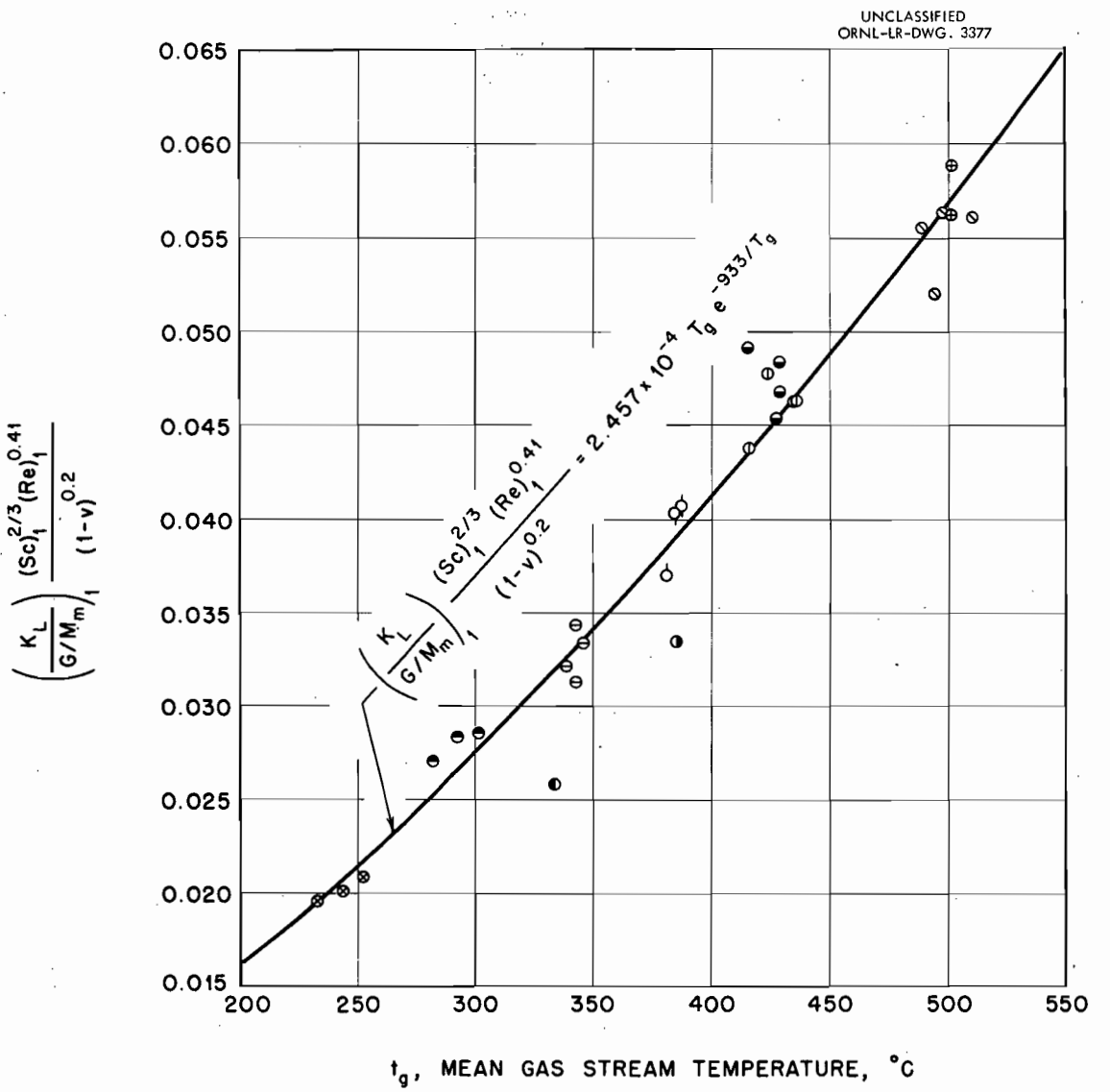

Figure 10

Temperature Dependence Of The Dual-Langmuir Mass Transfer Dimensionless Group For Case V; Oxygen And Hydrogen Diffusion Rates Controlling For Separate Portions Of The Bed With Catalytic Surface Restricted. Curve Shows Correlation According To Eyring Equation.

The curves indicated on Figures 10 and 11 are the correlations that apply when the Eyring (4) and Arrhenius equations respectively are used to develop the temperature dependence of the dual-Langmuir dimensionless groups. These curves are generated by the "least-square" lines of the natural logarithm of the appropriate argument versus reciprocal absolute temperature plots applying for the two modes of treatment, as shown in Figures 12 and 13. Five of the obviously bad points (13), the runs of April 23 and May 19, have been omitted in this curve-fitting process. The correlations that result are

$$\frac{K_{L_1}}{(G/M_m)_1} \cdot \frac{(Sc)_1^{2/3}\,(Re)_1^{0.41}}{(1-v)^{0.2}} = 2.46 \times 10^{-4} T_g \; e^{-933/T_g} \tag{48}$$

and

$$\frac{K_{L_1}}{(G/M_m)_1} \cdot \frac{(Sc)_1^{2/3}\,(Re)_1^{0.41}}{(1-v)^{0.2}} = 0.426\; e^{-1560/T_g} \tag{49}$$

where T_g is the mean gas stream temperature in °K.

A comparison of the observed values of the dual-Langmuir mass transfer dimensionless groups with those predicted by equations (48) and (49) is given in Table IV. The average mean deviations of the predicted values from the observed values is 3.76 per cent for the Eyring-correlation of equation (48) as compared to 3.81 per cent for the Arrhenius-correlation of equation (49), indicating an insignificant preference for the former.

In developing a basis for the Langmuir mechanism postulated in Case IV it was pointed out that the activation energy involved should be the heat of evaporation of adsorbed hydrogen molecules. The quantity 1560 in equation (49) implies that the activation energy as deduced from the recombiner data is 3100 calories per mole. This figure is of the same order of magnitude as that alluded to by some authorities as a reasonable energy of evaporation of hydrogen molecules from metallic surfaces (e. g. see J. H. de Boer, "The Dynamical Character of Adsorption", Oxford University Press 1953, pp. 32-36).

The correlations of the mass transfer dimensionless groups with temperature given in equations (48) and (49) employ the arbitrarily defined mean gas stream temperature t_g as the independent variable rather than the measured catalyst bed temperature t_b or the discharge gas temperature t_2, where

$$t_g = 0.5\,(t_b + t_2) \tag{50}$$

Some explanation of this choice may be in order. The argument is based upon the energetics and heat transfer feature of the bed operation.

The recombination reaction involves a large exothermicity, the energy released heating up the bed, raising the temperature of the flowing gas stream, and supplying the heat losses of the system to the surroundings. Continued

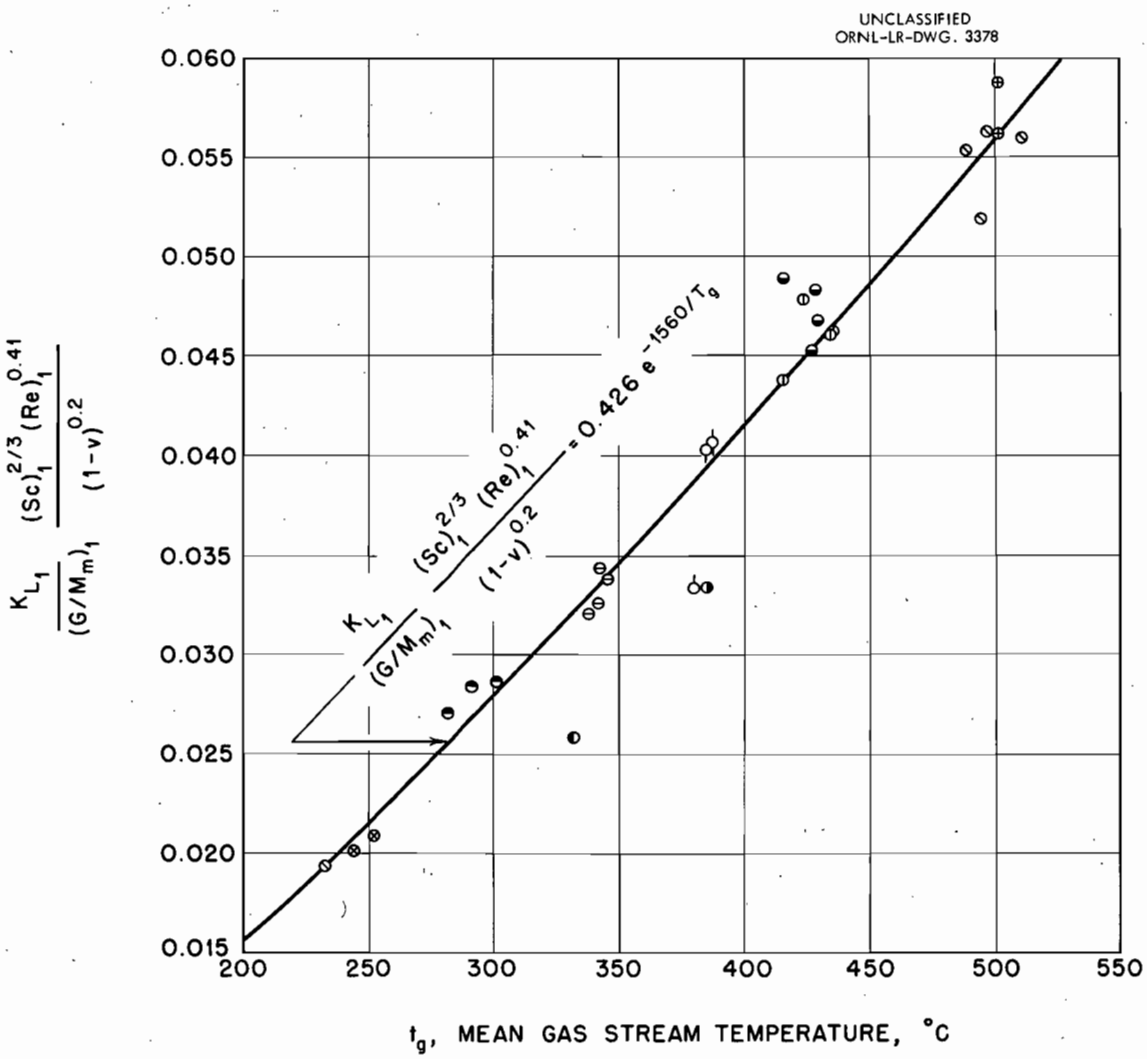

Figure 11

Correlation Of Dependence Of The Dual-Langmuir Mass Transfer Dimensionless Group On Temperature According To Arrhenius Equation.

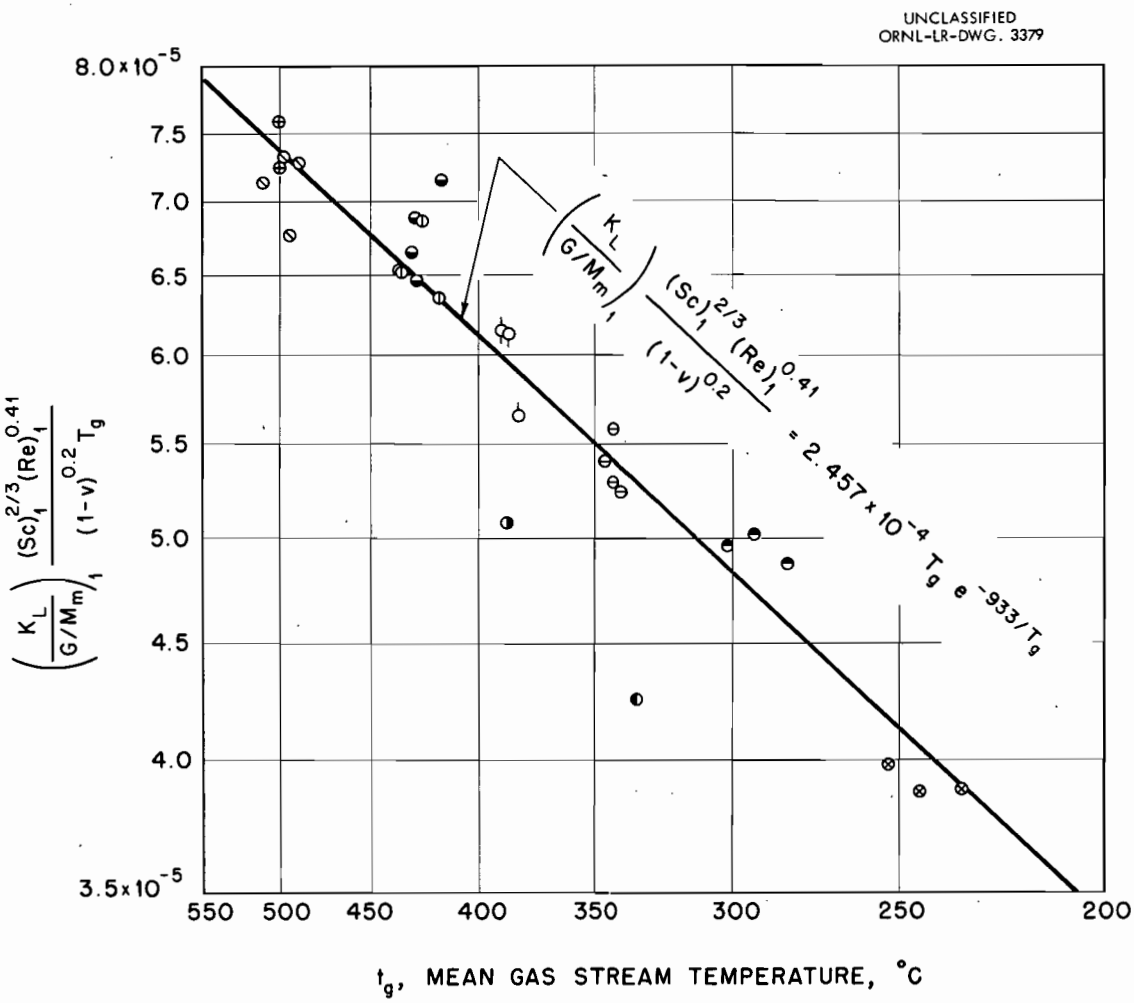

Figure 12

Rectification Of The Dual-Langmuir Mass Transfer Dimensionless Group Data In Accordance With The Eyring Equation; Logarithmic Plot Of The Dimensionless Group Divided By Absolute Temperature Versus Reciprocal Of Absolute Temperature.

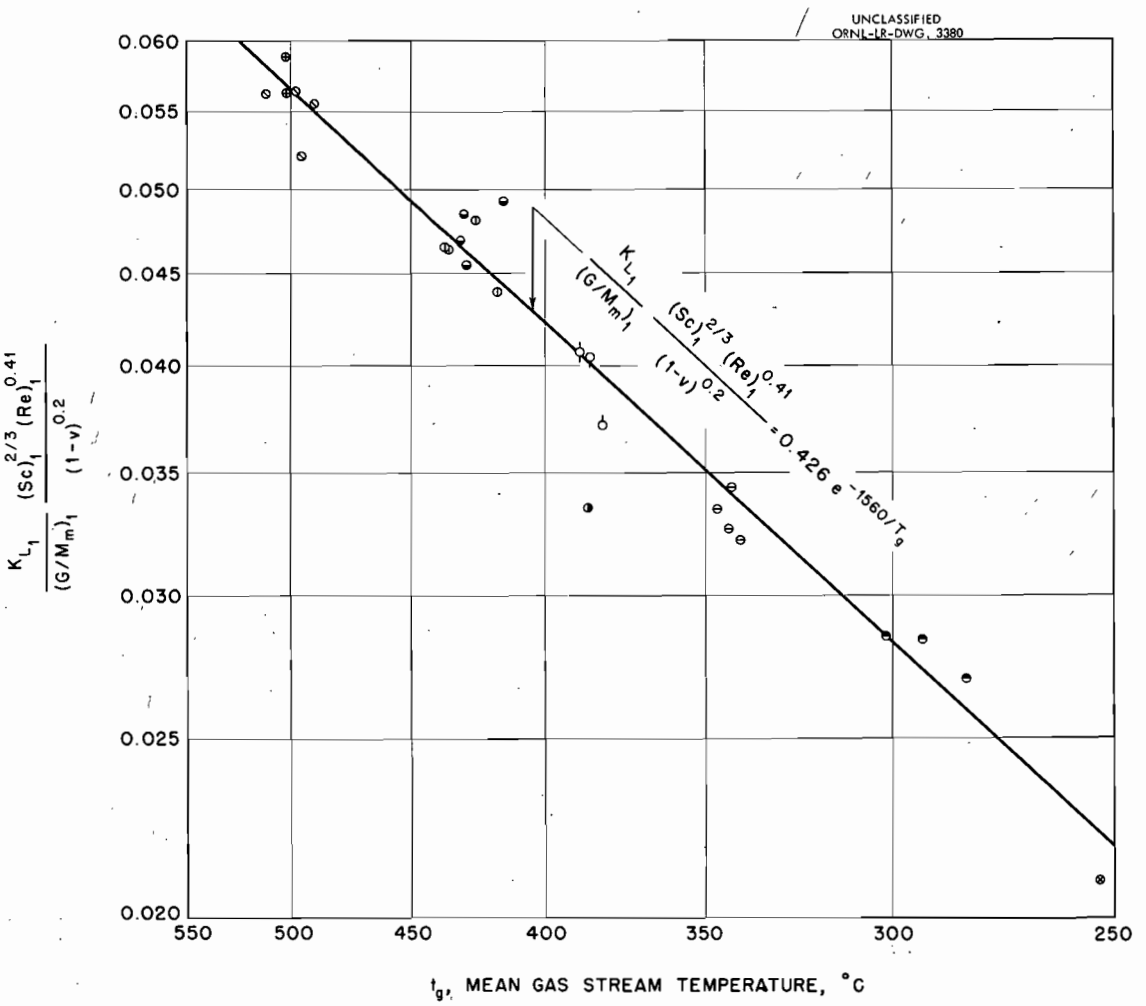

Figure 13

Rectification Of The Dual-Langmuir Mass Transfer Dimensionless Group Data In Accordance With The Arrhenius Equation; Logarithmic Plot Of The Dimensionless Group Versus Reciprocal Of Absolute Temperature.

TABLE IV

COMPARISON OF THE OBSERVED AND CALCULATED VALUES OF THE DUAL-LANGMUIR MECHANISM MASS TRANSFER DIMENSIONLESS GROUPS

Run Nos.	t_g mean °C	P psia	$\frac{K_{L_1}(Sc)_1^{2/3}(Re)_1^{0.41}}{(G/M_m)_1(1-v)^{0.2}}$	$2.46 \times 10^{-4}\ T_g e^{-933/T_g}$	% Deviation	$0.426\ e^{-1560/T_g}$	% Deviation
April 15; 1- 3	343	50	3.25×10^{-2}	3.33×10^{-2}	2.51	3.36×10^{-2}	3.37
4- 6	339	30	3.21	3.28	2.38	3.31	3.21
7- 9	346	80	3.34	3.38	1.05	3.40	4.98
10-12	343	100	3.43	3.33	-2.96	3.36	-2.15
April 16; 1- 3	416	30	4.38×10^{-2}	4.38×10^{-2}	-0.02	4.40×10^{-2}	0.48
4- 6	435	50	4.62	4.66	0.90	4.68	1.15
7- 9	436	80	4.64	4.68	0.95	4.69	1.19
10-12	424	110	4.79	4.50	-6.09	4.52	-5.71
April 21; 1- 3	502	100	5.88×10^{-2}	5.72×10^{-2}	-2.77	5.65×10^{-2}	-3.82
4- 7	502	80	5.62	5.71	1.60	5.65	0.51
April 22; 1- 3	495	30	5.20×10^{-2}	5.60×10^{-2}	7.77	5.55×10^{-2}	6.80
4- 7	511	50	5.60	5.87	4.73	5.79	3.39
7- 9	498	80	5.64	5.65	0.23	5.60	-0.75
10-11	489	100	5.55	5.51	-0.68	5.47	-1.45
April 23; 1- 3	232	30	1.36×10^{-2}	-	-	-	-
4- 5	230	50	1.29	-	-	-	-
6- 8	229	80	1.32	-	-	-	-
9-10	232	100	1.33	-	-	-	-
April 24; 1- 3	244	80	2.01×10^{-2}	2.10×10^{-2}	4.54	2.07×10^{-2}	3.21
4- 5	253	100	2.09	2.19	4.68	2.17	3.70
6- 7	234	50	1.97	1.98	0.57	1.94	-1.19
April 28; 1- 3	282	30	2.70×10^{-2}	2.55×10^{-2}	-5.78	2.55×10^{-2}	-5.79
4- 6	293	50	2.84	2.68	-5.73	2.68	-5.51
7- 8	302	80	2.85	2.79	-2.28	2.80	-1.89
April 30; 1- 2	416	35	4.92×10^{-2}	4.37×10^{-2}	-11.23	4.39×10^{-2}	-10.77
3- 4	429	50	4.84	4.56	-5.62	4.58	-5.29
5- 6	428	80	4.53	4.55	0.48	4.57	0.84
7- 8	430	100	4.68	4.58	-2.07	4.59	-1.77
May 19; 1-10	334	50	2.58×10^{-2}	-	-	-	-
May 11; 1- 5	386	50	3.34×10^{-2}	3.93×10^{-2}	17.60	3.96×10^{-2}	18.53
May 12; 1- 6	381	100	3.70×10^{-2}	3.87×10^{-2}	4.54	3.90×10^{-2}	5.37
May 5; 1- 4	385	100	4.04×10^{-2}	3.93×10^{-2}	-2.78	3.96×10^{-2}	-2.02
May 7; 1- 4	388	100	4.07×10^{-2}	3.96×10^{-2}	-2.69	3.99×10^{-2}	-1.94
				Mean Deviation 3.76%		Mean Deviation 3.81%	

operating with relatively cold feed gases eventually results in a virtually steady state of affairs for the bed, the catalyst pellet temperature gradient along the bed being dictated by the operating conditions. The catalyst pellets, at which the heat release occurs, themselves serve as heat recuperators. Thus the temperature of the cold gas feed stream is elevated rapidly at the entrance, as a consequence of heat transfer to it from the bed and energy released by the combustion. Insofar as the gas is concerned, the process is not isothermal. However, to avoid the extreme difficulties that would be introduced in attempting to treat the process rigorously, the analysis has been conducted as though the process is actually isothermal. It is not entirely clear what interpretation is to be given to the bed temperature as indicated by the thermocouple, whereas the gas discharge temperature t_2 is presumably the mixed mean temperature of the recombined gas stream. The latter is possibly too low a figure to employ as a mean reaction temperature in that the ratio of heat losses from the system to heat generated by reaction is greater for the tail end of the apparatus. Thus, to attempt a compensation, instead of using either t_b or t_2 as the temperature of the system, their mean is employed.

Temperature Rise Accompanying The Recombination Reaction

It is of interest to examine the energetics of the recombination reaction and estimate the temperature elevation to be anticipated. In this connection the thermodynamic data tabulated by Thacker, Folkins, and Miller (14) are employed:

1. Heat of formation at 298.1° K

$$\Delta H_0 = -57,798 \text{ cal/mole of hydrogen}$$

2. Molal Heat Capacities

Steam: $C_p = 7.187 + 2.373 \cdot 10^{-3} T$ cal/mole °K

Hydrogen: $C_p = 6.62 + 0.81 \cdot 10^{-3} T$

Oxygen: $C_p = 8.27 + 0.258 \cdot 10^{-3} T - 1.877 \cdot 10^{5} T^{-2}$

where T is the absolute temperature in °K. Application of Kirchoff's law to these data gives the temperature dependence of the heat of combustion as

$$\Delta H = -56,481 - 3.568T + 0.717 \cdot 10^{-3} T^2 - 0.944 \cdot 10^{5} T^{-1} \text{ cal/mole}$$

which leads to exothermicities of 58,280 and 58,990 calories per mole of hydrogen at 500 and 800° K respectively, and a mean of 58,600 over this range. Over this same range the mean molal heat capacities of steam, hydrogen, and oxygen are 8.72, 7.16, and 7.92 calories per °K respectively. The mean values are used rather than the point values to avoid subsequent computational difficulties.

If the recombination process is assumed to occur adiabatically (the actual bed operation is not adiabatic), the temperature elevation that accompanies the combustion can be obtained from the differential energy balance

$$58,600\ H_0 df \approx \left\{8.72[1-O_0-H_0(1-f)] + 7.16H_0(1-f) + 7.92(O_0-0.5H_0f)\right\}dT$$

Solution of this for the temperature rise ΔT that occurs as a result of the combination of f_2 fraction of the hydrogen fed leads to

$$\Delta T \approx 24,420 \ln \frac{8.72 - 1.56H_0 - 0.80\ O_0}{8.72-1.56\ H_0-0.80\ O_0 -2.40\ H_0f_2} \tag{51}$$

This adiabatic temperature elevation can be stated slightly more approximately and simply as

$$\Delta T \approx \frac{58,600\ H_0f_2}{8.72-1.56\ H_0-0.80\ O_0} \tag{51a}$$

which indicates that the expected temperature rise at various points in the bed should be almost directly proportional to the fraction of completion of combination.

The application of equation (51a) to the experimental data reveals some pertinent information concerning the operation of the bed. Consider as an example run No. 1 of April 22 for which $H_0 = 0.0747$, $O_0 = 0.0593$, $f_2 = 0.869$, $V_0 = 6.11 \times 10^{-4}$ lb mole/sec, $t_0 = 141°$ C, $t_b = 508°$ C, and $t_2 = 480°$ C. The anticipated adiabatic temperature rise is 445° C or a final gas temperature of 586° C would have been expected, whereas the observed value of t_2 is 480° C, some 106° below the theoretical value; further, the thermocouple bed temperature of $t_b = 508°$ C is 78° below this value. The actual power rate for this run amounts to 1060 calories per second, whereas the observed power increase acquired by the gases in passing through the bed and now residing in the discharge gas is 790 calories per second. This means that 270 calories per second are being dissipated as heat losses or that about 25 per cent of the energy released in the recombiner is lost to the surroundings.

EVALUATION OF TRANSPORT AND RELATED PROPERTIES

In the course of extricating the mass transfer coefficients K_1 and K_{L_1} and setting up the various mass transfer dimensionless groups given in Table II, values of Reynolds numbers for the gas stream and Schmidt numbers for the film regions are needed. To accomplish this task the following specific items have to be calculated:

1. Viscosities of the gas stream for zone 1 (μ_{m_1}), the entire recombiner bed (μ_m), and the diffusion film for zones 1 and 2 (μ_{f_1} and μ_{f_2}).

2. Diffusivity of oxygen in the diffusion film for zone 1 $(D_{3f})_1$ and the entire bed (D_{3f}), and the diffusivity of hydrogen in the diffusion film for zone 2 $(D_{2f})_2$ and the entire bed (D_{2f}).

3. Density of the gas mixture in the diffusion film for zone 1 $(\rho_f)_1$ and zone 2 $(\rho_f)_2$ and for the entire bed (ρ_f).

The methods used to calculate these quantities in this investigation are outlined in the following sections.

Calculation Of Viscosities Of Gas Mixtures

The basis for determining accurate viscosities of gas mixtures is a simplification devised from the excellent method disclosed recently by Hirschfelder (1, 6, 7) and his co-workers. For a pure gas Hirschfelder has shown that the viscosity is predicted very accurately by the expression

$$\mu = 2.6693 \times 10^{-5} \; (MT)^{1/2} \; r_0^{-2} \frac{\psi}{W^{(2)}(2;kT/\epsilon)} \text{ poise} \tag{52}$$

where

k = Boltzmann constant, $1.38 \cdot 10^{-16}$ erg/°K
r_0 = low velocity head-on molecular collision diameter, Angstrom units
$W^{(2)}(2;kT/\epsilon)$ = collision integral which is a function of kT/ϵ
ϵ = low velocity maximum interaction energy, ergs
ψ = a correction factor near unity which is a function of kT/ϵ

The situation for multicomponent mixtures is considerably more complicated, involving interaction effects for the various types of two-molecule encounters that can occur. According to Hirschfelder, the most compact way for expressing the viscosity of a three component mixture precisely is

$$\mu_m \times 10^7 = - \frac{\begin{vmatrix} N_{11} & N_{12} & N_{13} & 1 \\ N_{12} & N_{22} & N_{23} & 1 \\ N_{13} & N_{23} & N_{33} & 1 \\ 1 & 1 & 1 & 0 \end{vmatrix}}{\begin{vmatrix} N_{11} & N_{12} & N_{13} \\ N_{12} & N_{22} & N_{23} \\ N_{13} & N_{23} & N_{33} \end{vmatrix}} \text{ poise} \tag{53}$$

where the elements of the determinants are given by

$$N_{11} = 2Z_{11} + x_2(Y_{12} + M_2 Z_{12}/M_1)/x_1 + x_3(Y_{13} + M_3 Z_{13}/M_1)/x_1$$
$$N_{12} = -Y_{12} + Z_{12}$$

$$N_{13} = -Y_{13} + Z_{13}$$

$$N_{22} = 2Z_{22} + x_1(Y_{12} + M_2Z_{12}/M_1)/x_2 + x_3(Y_{23} + M_2Z_{23}/M_2)/x_2$$

$$N_{23} = -Y_{23} + Z_{23}$$

$$N_{33} = 2Z_{33} + x_1(Y_{13} + M_3Z_{13}/M_1)/x_3 + x_2(Y_{23} + M_2Z_{23}/M_3)/x_3$$

and

$$Y_{ij} = 0.017663\ (r_{ij})^2\ \frac{(M_iM_j)^{1/2}}{T^{1/2}\ (M_i + M_j)^{3/2}}\ W^{(1)}\ (1;kT/\epsilon)$$

$$Z_{ij} = 0.0052988\ (r_{ij})^2\ \frac{(M_iM_j)^{1/2}}{T^{1/2}\ (M_i + M_j)^{3/2}}\ W^{(2)}\ (2;kT/\epsilon)$$

$$r_{ij} = 0.5(r_i + r_j)$$

$$\epsilon_{ij}/k = \sqrt{\frac{\epsilon_i}{k} \cdot \frac{\epsilon_j}{k}}$$

and where the terms not previously defined have the meanings:

M_i = molecular weight of the i-th component (1 ~ H_2O; 2 ~ H_2; 3 ~ O_2)

r_{ij} = low velocity head-on collision diameter for an i-j type of encounter

$W^{(1)}(1;kT/\epsilon)$ = collision integral which is a function of kT/ϵ

x_i = mole fraction of the i-th component in the mixture

ϵ_{ij} = low velocity maximum molecular interaction energy for an i-j cluster

To facilitate computations with equation (53) Table V and Figure 14 are useful for selecting values of the collision integrals $W^{(1)}$ and $W^{(2)}$. Table VI identifies the values of the pertinent transport parameters, and Figures 15 and 16 summarize the values of the various Y_{ij} and Z_{ij} combinations. The values of r_{ii} and ϵ_{ii} listed in Table VI for hydrogen and oxygen are taken from Hirschfelder (6) and the values for steam are taken from the dissertation of Ercan (2). Values of ψ, as given by Hirschfelder (6) are given in Table VII.

The precise evaluation of the viscosity of about the 1000 ternary mixtures needed in this investigation via equation (53) would represent an overwhelming amount of drudgery. Consequently, a sufficiently accurate (for the case at hand) but short-cut procedure was evolved, making use of equations (52) and (53) to devise the procedure. Several possible schemes were examined. The one adopted involves a comparison of the value of the viscosity of steam as computed from equation (52) with the viscosity of representative mixtures as evaluated from equation (53), making use of the observation that the accurately

TABLE V

VALUES OF THE COLLISION INTEGRALS $W^{(1)}(1; kT/\epsilon)$ AND $W^{(2)}(2; kT/\epsilon)$

kT/ϵ	$W^{(1)}(1; kT/\epsilon)$	$W^{(2)}(2; kT/\epsilon)$	kT/ϵ	$W^{(1)}(1; kT/\epsilon)$	$W^{(2)}(2; kT/\epsilon)$
0.30	1.331	2.785	2.60	0.4939	1.081
0.35	1.238	2.628	2.70	0.4885	1.069
0.40	1.159	2.492	2.80	0.4836	1.058
0.45	1.092	2.368	2.90	0.4788	1.048
0.50	1.033	2.257	3.00	0.4745	1.039
0.55	0.9829	2.156	3.10	0.4703	1.030
0.60	0.9383	2.065	3.20	0.4664	1.022
0.65	0.8991	1.982	3.30	0.4628	1.014
0.70	0.8644	1.908	3.40	0.4593	1.007
0.75	0.8335	1.841	3.50	0.4560	0.9999
0.80	0.8058	1.780	3.60	0.4529	0.9932
0.85	0.7809	1.725	3.70	0.4499	0.9870
0.90	0.7585	1.675	3.80	0.4471	0.9811
0.95	0.7382	1.629	3.90	0.4444	0.9755
1.00	0.7197	1.587	4.00	0.4418	0.9700
1.05	0.7028	1.549	4.10	0.4394	0.9649
1.10	0.6873	1.514	4.20	0.4370	0.9600
1.15	0.6731	1.482	4.30	0.4347	0.9553
1.20	0.6601	1.452	4.40	0.4326	0.9507
1.25	0.6479	1.424	4.50	0.4305	0.9464
1.30	0.6367	1.399	4.60	0.4284	0.9422
1.35	0.6263	1.375	4.70	0.4265	0.9382
1.40	0.6166	1.353	4.80	0.4246	0.9343
1.45	0.6075	1.333	4.90	0.4228	0.9305
1.50	0.5991	1.314	5.00	0.4211	0.9269
1.55	0.5912	1.296	6.00	0.4062	0.8963
1.60	0.5837	1.279	7.00	0.3948	0.8727
1.65	0.5767	1.264	8.00	0.3856	0.8538
1.70	0.5701	1.248	9.00	0.3778	0.8379
1.75	0.5639	1.234	10.00	0.3712	0.8242
1.80	0.5580	1.221	20.00	0.3320	0.7432
1.85	0.5523	1.209	30.00	0.3116	0.7005
1.90	0.5471	1.197	40.00	0.2980	0.6718
1.95	0.5421	1.186	50.00	0.2878	0.6504
2.00	0.5373	1.175			
2.10	0.5284	1.156	60.00	0.2798	0.6335
2.20	0.5203	1.138	70.00	0.2732	0.6194
2.30	0.5129	1.122	80.00	0.2676	0.6076
2.40	0.5061	1.107	90.00	0.2628	0.5973
2.50	0.4998	1.093	100.00	0.2585	0.5882

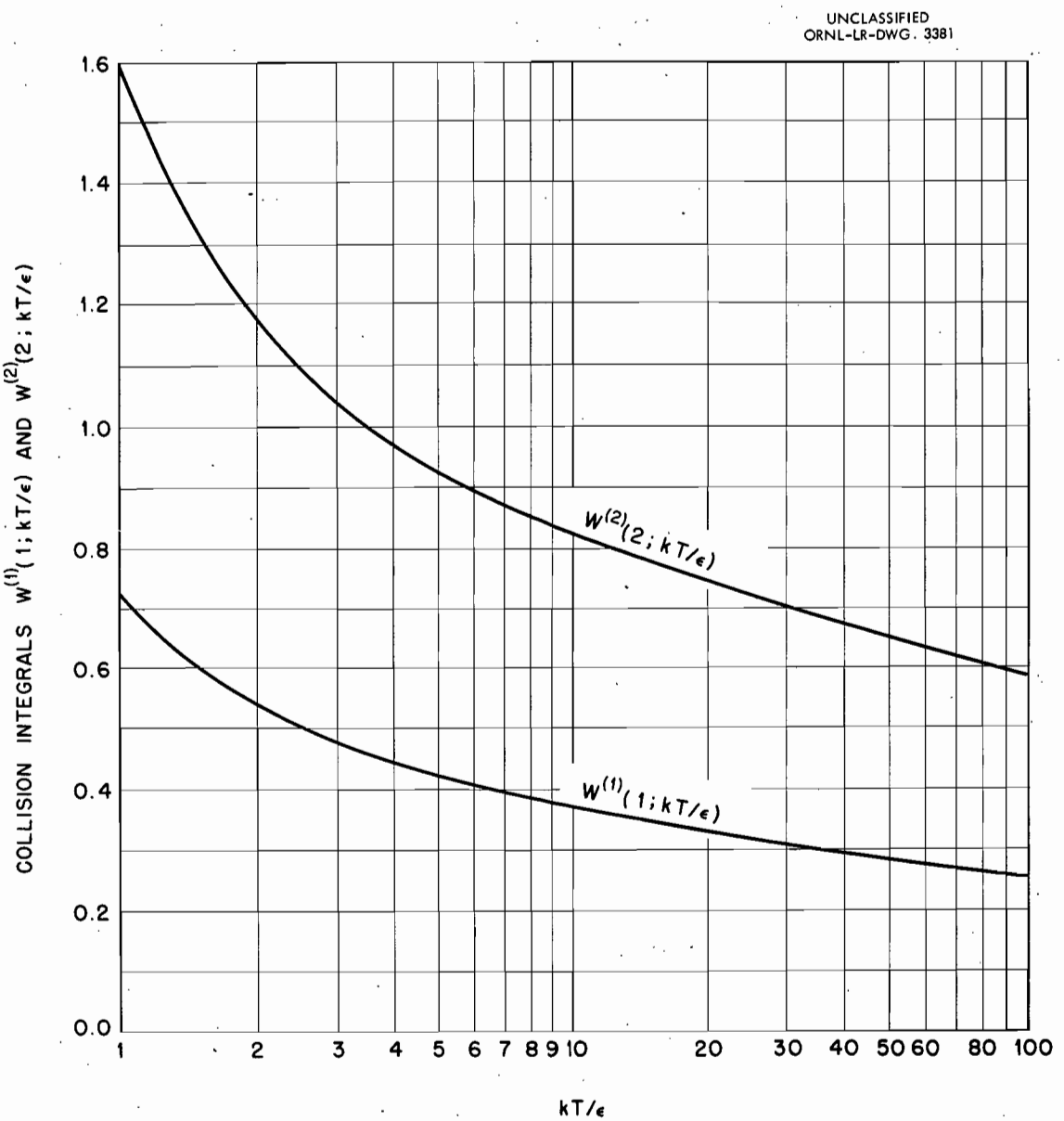

Figure 14

Values Of The Collision Integrals $W^{(1)}(1;kT/\epsilon)$ And $W^{(2)}(2;kT/\epsilon)$ As A Function Of kT/ϵ.

TABLE VI

SUMMARY OF PERTINENT QUANTITIES USED
FOR
CALCULATING TRANSPORT PROPERTIES

Quantity	H_2O	H_2	O_2	H_2O-H_2	H_2O-O_2	H_2-O_2
	Values of ij					
	11	22	33	12	13	23
M_i	18.016	2.016	32.000	-	-	-
ϵ_{ij}/k, °K	486	33.3	113.2	127.2	234.6	61.40
r_{ij} A°	3.050	2.986	3.433	3.009	3.242	3.201
r_{ij}^2	9.303	8.881	11.786	9.054	10.511	10.246
$(M_i M_j)^{1/2}$	18.016	2.016	32.000	6.028	24.014	8.032
$(M_i + M_j)^{1/2}$	-	-	-	4.476	7.072	5.832
$\left[\frac{M_i + M_j}{M_i M_j}\right]^{1/2}$	-	-	-	0.7426	0.2945	0.7261
$\frac{(M_i M_j)^{1/2}}{(M_i + M_j)^{3/2}}$	0.08329	0.2490	0.06250	0.06723	0.06788	0.04049
$\frac{1}{r_{ii}^2}\sqrt{\frac{M_i \epsilon_i}{k}}$	10.04	0.9301	5.107	-	-	-
Y_{ij} Coefficient	0.01376	0.03896	0.01308	0.01081	0.01267	0.007369
Z_{ij} Coefficient	0.004105	0.01162	0.003903	0.003225	0.003781	0.002198
$\left[\frac{M_i + M_j}{M_i M_j}\right]^{1/2} (r_{ij})^{-2}$	-	-	-	0.08201	0.02802	0.07087

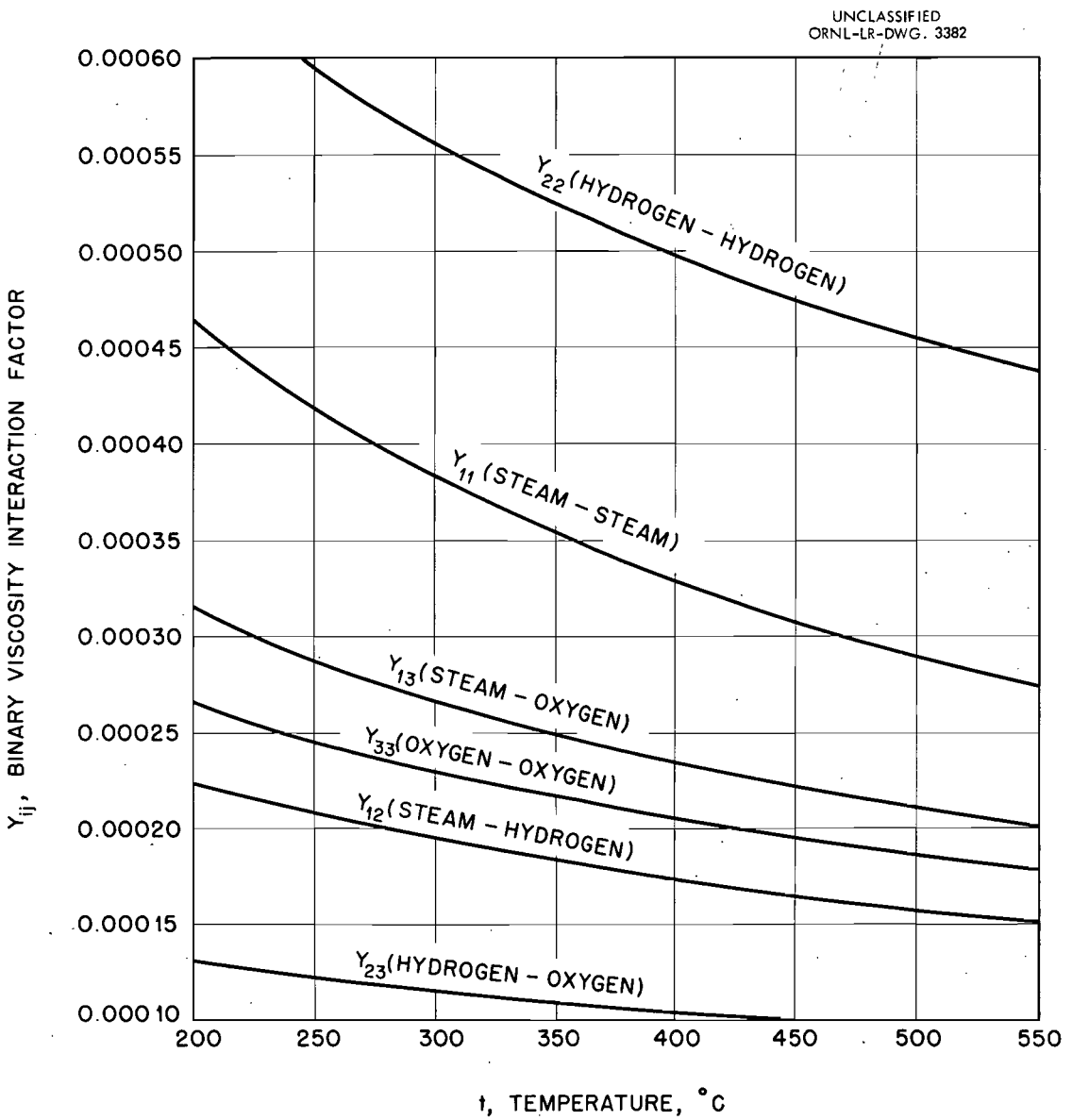

Figure 15

Variation Of Y_{ij} With Temperature For The System Steam-Hydrogen-Oxygen.

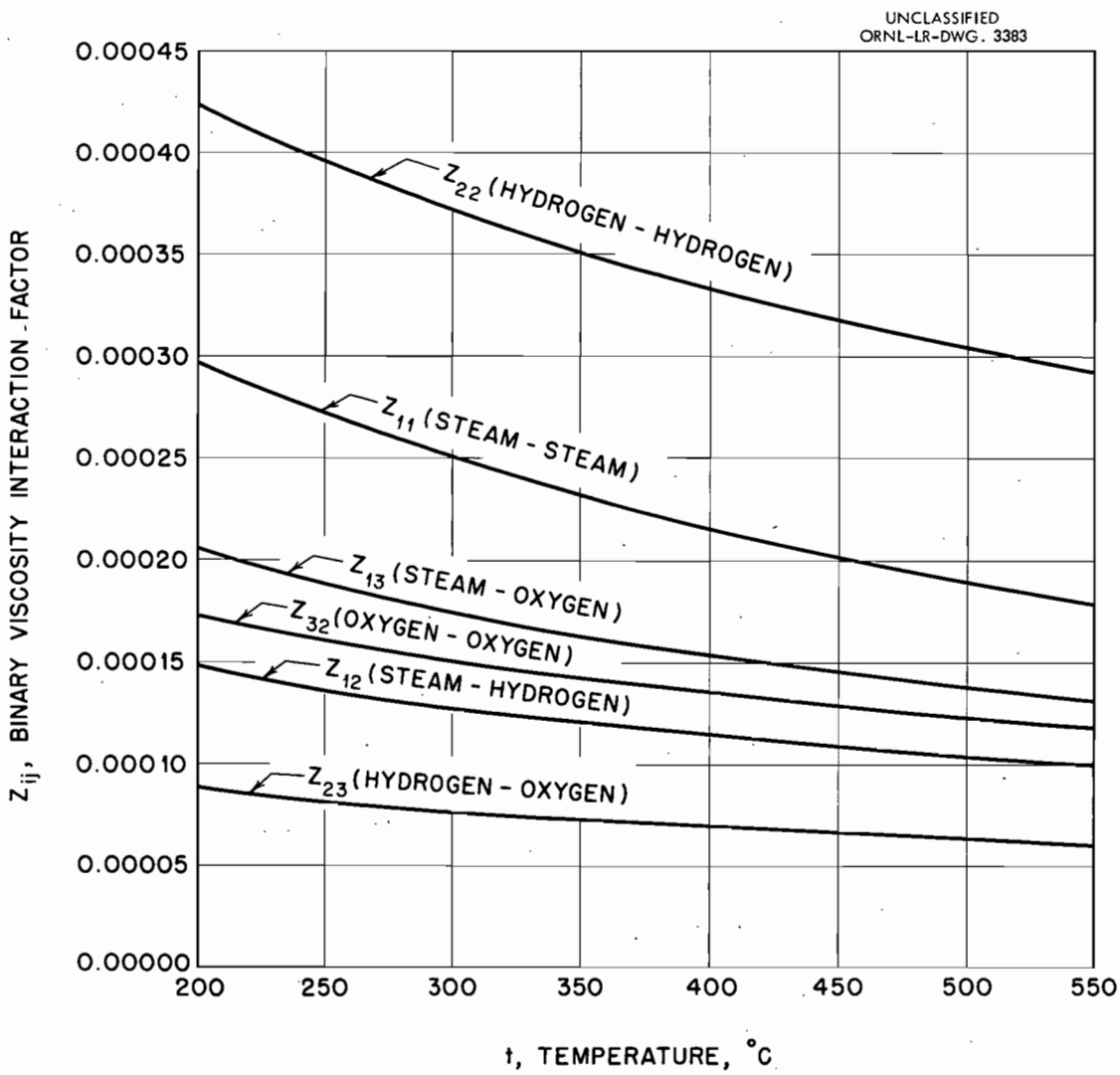

Figure 16

Variation Of Z_{ij} With Temperature For The System Steam-Hydrogen-Oxygen.

calculated viscosity of the mixture is virtually the calculated steam viscosity multiplied by the factor one plus the sum of the hydrogen and oxygen mole fractions, i. e.

$$\mu_m = \mu_1(1 + H + O) \tag{54}$$

This was established by making computations for the mean gas and film stream compositions for all 104 of the Ransohoff-Spiewak data for the three situations involved, i. e., grouped as to whether the entire operation is oxygen diffusion controlled, part of the bed is oxygen diffusion controlled, and part of the bed is hydrogen diffusion controlled. The results of these calculations are summarized in Table VIII, where the compositions indicated are the mean values.

TABLE VII

VALUES OF THE FUNCTION ψ

kT/ϵ	ψ
0.30	1.0014
0.50	1.0002
0.75	1.0000
1.00	1.0000
1.25	1.0001
1.50	1.0004
2.00	1.0014
2.50	1.0025
3.00	1.0034
4.00	1.0049
5.00	1.0058
10.00	1.0075
50.00	1.0079
100.00	1.0080

TABLE VIII

COMPARISON OF CALCULATED VERSUS ESTIMATED VISCOSITIES OF STEAM-HYDROGEN-OXYGEN MIXTURES

Diffusant	t_g, °C	Zone	H	O	μ calc	$\mu_1(1+H+O)$	% Dev.
					Poise × 10^4		
Oxygen	282.1	g	0.0231	0.0231	2.0324	2.0198	-0.62
Oxygen	282.1	f	0.0115	0.0116	1.9859	1.9753	-0.53
Oxygen	407.6	1-g	0.0353	0.0374	2.5075	2.5203	0.51
Oxygen	407.6	1-f	0.0177	0.0187	2.4402	2.4349	-0.02
Hydrogen	407.6	2-g	0.0115	0.0257	2.4070	2.4368	1.24
Hydrogen	407.6	2-f	0.0057	0.0129	2.3798	2.3932	0.56
					Mean Deviation		0.58%

The small mean deviation of 0.58 per cent coupled with the simplicity of the calculation made this an adequate procedure for estimating viscosities of gas mixtures in this investigation. It should be emphasized that equation (54) applies only to mixtures that are relatively lean with respect to oxygen and hydrogen.

To facilitate the use of equation (54) the computed viscosities of steam as derived from equation (52) are useful. Table IX gives the computed steam viscosities in more useful engineering units.

TABLE IX

CALCULATED VISCOSITIES OF SUPERHEATED STEAM AT RELATIVELY LOW PRESSURES

t, °C	μ_1 lb/(ft)(sec)
225	1.165×10^{-5}
250	1.224
275	1.282
300	1.339
325	1.395
350	1.451
375	1.507
400	1.562
425	1.617
450	1.671
475	1.724
500	1.776
525	1.828
550	1.880

For the relatively low operating pressures encountered in this work, equation (52), which does not appear to account explicitly for the influence of pressure on viscosity, is entirely satisfactory. However, for relatively high pressure operations, the low velocity head-on collision diameters given in Table VI no longer apply. Ercan (2) has investigated this point and has shown that equation (52) can also be applied to compute viscosities at even super pressures (e. g. 800 atm) by considering r_0 to be a single valued function of the pressure. His dissertation includes plots which show the decrease in r_0 with increase of pressure as a series of isothermal curves for 10 substances.

Calculation of Diffusivities

Hirschfelder's (1, 6, 7) developments were also used to calculate binary diffusion coefficients (D_{ij}) and the diffusivity of hydrogen and oxygen in ternary gas mixtures (D_{ig}). The binary diffusion coefficient is given by

$$D_{ij} = 9.2916 \times 10^{-4} \frac{T^{3/2}\left[(M_i+M_j)/M_iM_j\right]^{1/2}}{P\,(r_{ij})^2\,W^{(1)}(1;kT/\epsilon)} \quad \text{sq cm/sec} \qquad (55)$$

where the sumbols used have the same meanings as before, with the exception that here P is in atmospheres.

Equation (11), previously used in estimating the location of the mechanism change-over point, gives the diffusivity of component i as a multicomponent mixture containing n species as

$$D_{ig} = \frac{1 - x_i}{\sum_{\substack{j=1 \\ j \neq i}}^{n} (x_j/D_{ij})} \qquad (11)$$

Specifically, the diffusivities of hydrogen (D_{2g}) and oxygen (D_{3g}) in steam rich gas mixtures containing H and O mole fractions of hydrogen and oxygen are given by

$$D_{2g} = \frac{1 - H}{\frac{O}{D_{23}} + \frac{1-H-O}{D_{12}}} \qquad (56a)$$

$$D_{3g} = \frac{1 - O}{\frac{H}{D_{23}} + \frac{1-H-O}{D_{13}}} \qquad (56b)$$

All of the diffusivities used in making the calculations for this investigation were obtained by inserting the appropriate arithmetic mean compositions of the gas streams and film regions of interest into equations (56a) and (56b).

Figure 17 shows the variation of the three binary diffusion coefficients with temperature for a pressure of 10 psia. The selection of 10 psia as an arbitrary reference pressure, considering the inverse relationship between D_{ij} and P, is a more convenient choice than 1 atmosphere. Table X, which summarizes the calculated values of the binary diffusion coefficients in more useful engineering units for various temperatures, facilitates computations with these transport properties.

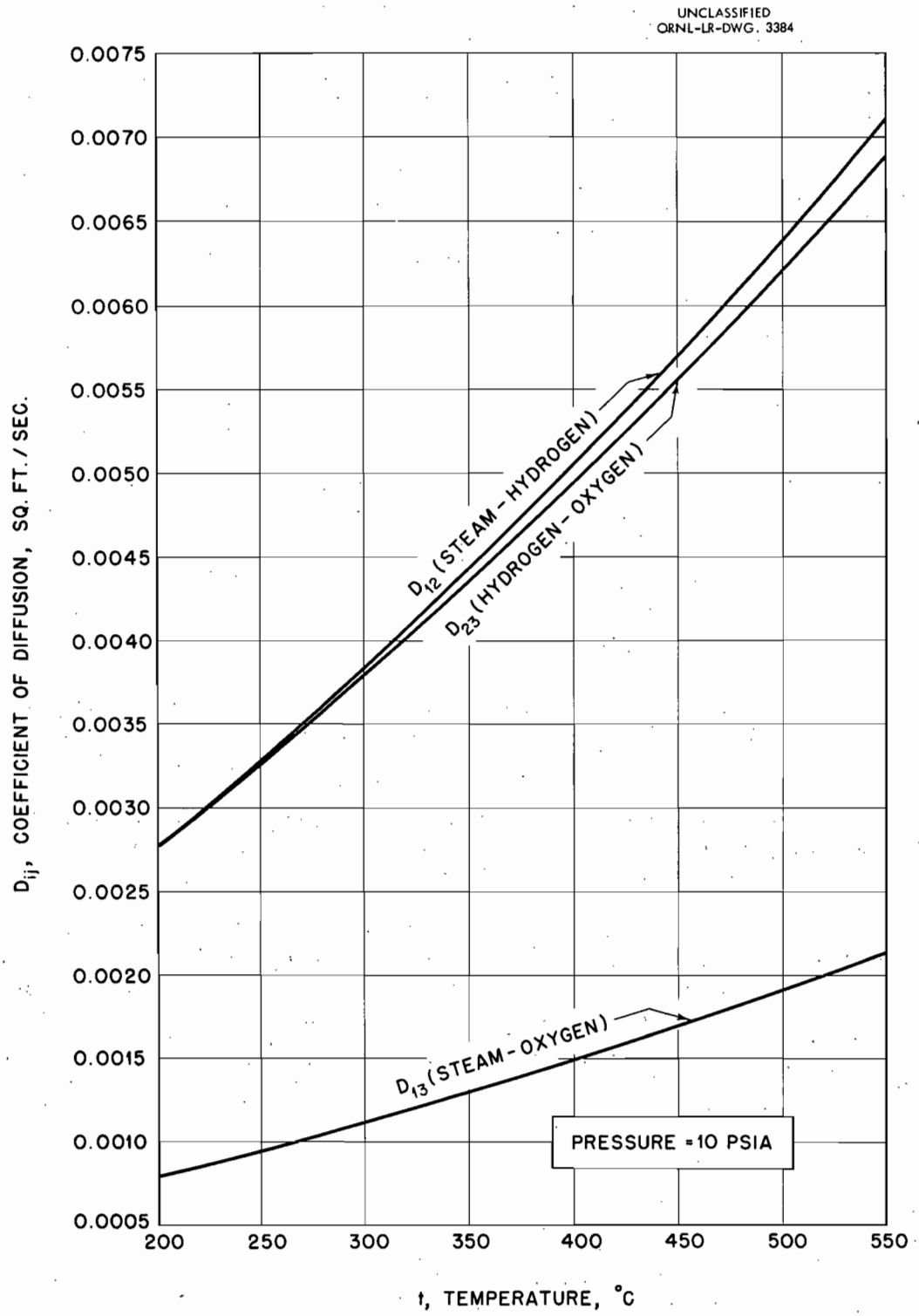

Figure 17

Variation Of The Binary Diffusion Coefficients For The System Steam-Hydrogen-Oxygen At 10 Psia With Temperature.

TABLE X

CALCULATED BINARY DIFFUSION COEFFICIENTS AT 10 PSIA

Values are expressed as sq ft/sec

t, °C	D_{12}	D_{13}	D_{23}
225	3.019×10^{-3}	0.870×10^{-3}	3.010×10^{-3}
250	3.285	0.951	3.267
275	3.560	1.036	3.533
300	3.843	1.123	3.805
325	4.135	1.213	4.086
350	4.435	1.305	4.372
375	4.739	1.400	4.658
400	5.051	1.498	4.951
425	5.374	1.598	5.253
450	5.705	1.701	5.562
475	6.046	1.806	5.878
500	6.394	1.913	6.203
525	6.743	2.022	6.535
550	7.103	2.135	6.875

Calculation Of Gas Mixture Densities

Since steam is the principal component of the stream flowing through the recombiner and its behavior departs significantly but not greatly from that of an ideal gas in the temperature and pressure range of the Ransohoff-Spiewak investigations, use of the ideal gas law for calculating gas densities is deemed unsatisfactory. However, the incorporation of a compressibility coefficient into the ideal gas law to express the pressure-density-temperature relationships for the mixture is adequate for the case at hand.

The method adopted presumes that the compressibility coefficients for steam, as derived from the superheat portion of the vapor tables of Keenan and Keyes (8) may be applied directly to the ternary mixtures. With steam contents in the gas stream in excess of 90 mole per cent, this should be a valid assumption. Accordingly, gas stream and diffusion film densities used in the calculations were estimated from

$$\rho = \frac{PM_m}{(zB)T} \tag{57}$$

where

B = gas constant, psi (cu ft)/(lb mole)(°K)
M_m = mean molecular weight, lb/lb mole
P = pressure of the system, psia
T = absolute temperature, °K
z = compressibility coefficient
ρ = gas density, lb/cu ft

Values of the compressibility factor, the product zB, as derived from the Keenan and Keyes tables are summarized in Table XI and are plotted versus temperature in Figure 18 as a series of isobars for the pressure used in the Ransohoff-Spiewak investigations.

TABLE XI

ESTIMATED COMPRESSIBILITY FACTORS OF STEAM-HYDROGEN-OXYGEN MIXTURES

Values of zB in (psi)(cu ft)/(lb mole)(°K)

	Pressure, psia					
t, °C	30	35	50	80	100	110
200	19.11	19.08	18.97	18.75	18.59	18.51
225	19.15	19.12	19.12	19.04	18.87	18.68
250	19.18	19.16	19.09	18.95	18.85	18.80
275	19.21	19.19	19.13	19.01	18.94	18.89
300	19.22	19.21	19.16	19.06	18.99	18.96
350	19.25	19.24	19.20	19.13	19.08	19.06
400	19.27	19.25	19.23	19.18	19.14	19.13
450	19.28	19.27	19.25	19.21	19.19	19.17
500	19.29	19.29	19.27	19.23	19.21	19.20

CONSIDERATION OF THE GAS FLOW VELOCITY PROFILE

The treatment of the data resulting from the recombiner experiments of Ransohoff and Spiewak has been based upon the assumption that the gas flows "slugwise" through the catalyst bed. The unknown disturbances created by the protrusion of the thermocouple well into such a large portion of the recombiner flow channel raises doubt concerning the validity of this assumption. Moreover, considering the small diameter of the bed, even if there had been no thermocouple well in the system, the velocity profile would have been far from uniform. The experimental evidence for this conclusion is contained in a paper published recently by Schwartz and Smith (12). Their investigations on the flow distribution of gases through packed beds indicates a decided increase in the flow velocity with increase in radial distance from the centerline of the bed. Eventually the velocity passes through a maximum and then drops off rapidly as the containing wall is approached. They also found that the velocity distribution becomes more uniform with increase in bed diameter and decrease in pellet size. In summarizing their work they found it advantageous to show the results in dimensionless form, i. e., ratios of the point to mean stream velocities were plotted against the ratio of radial distance to bed radius.

Figure 19, which has been duplicated directly from the curve presented by Schwartz and Smith for a 2 inch diameter bed packed with 1/4 inch cylinders (geometrically similar to the recombiner bed with a diameter of 1 inch

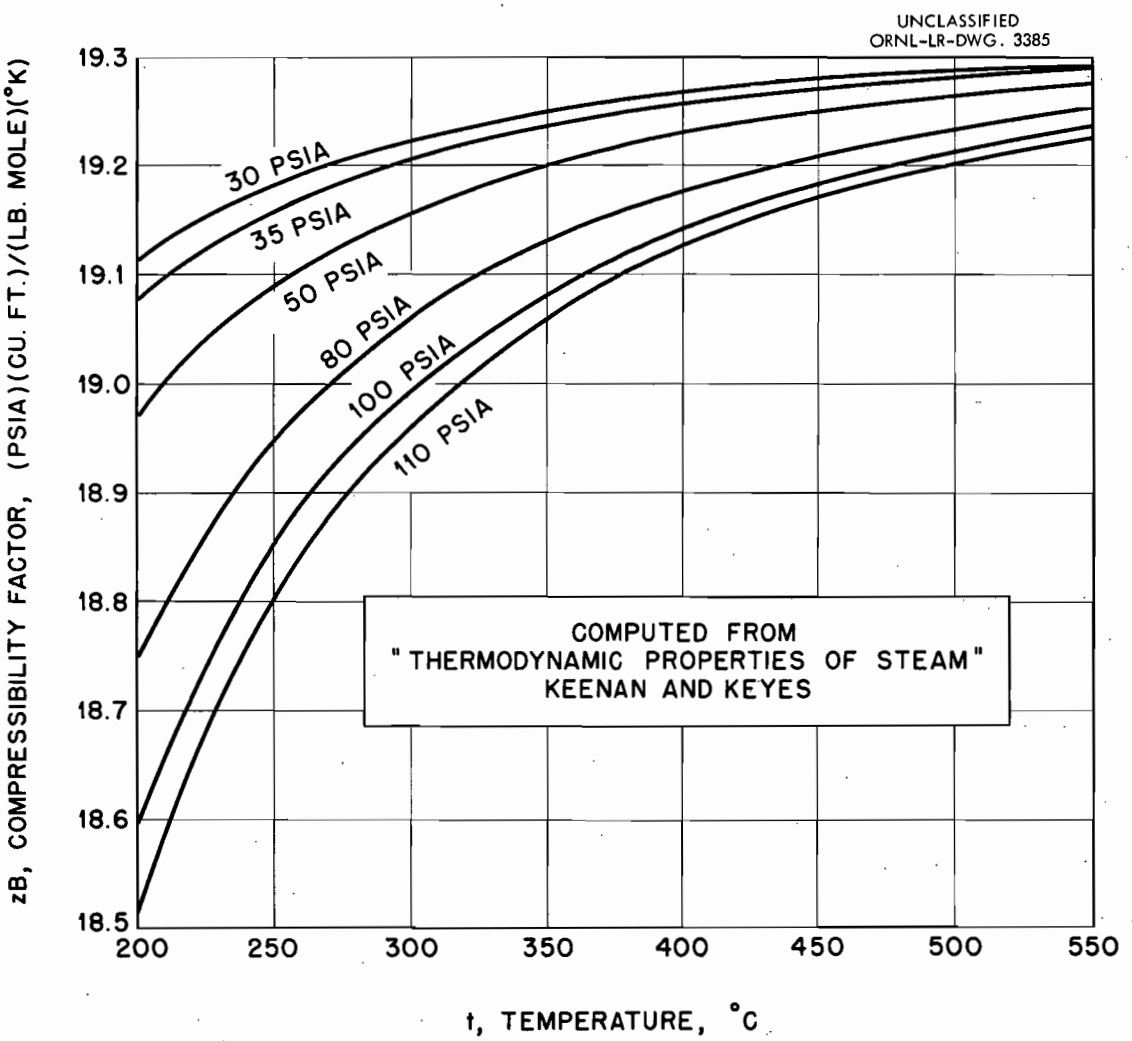

Figure 18

Compressibility Factor For The System Steam-Hydrogen-Oxygen As A Function Of Temperature And Pressure.

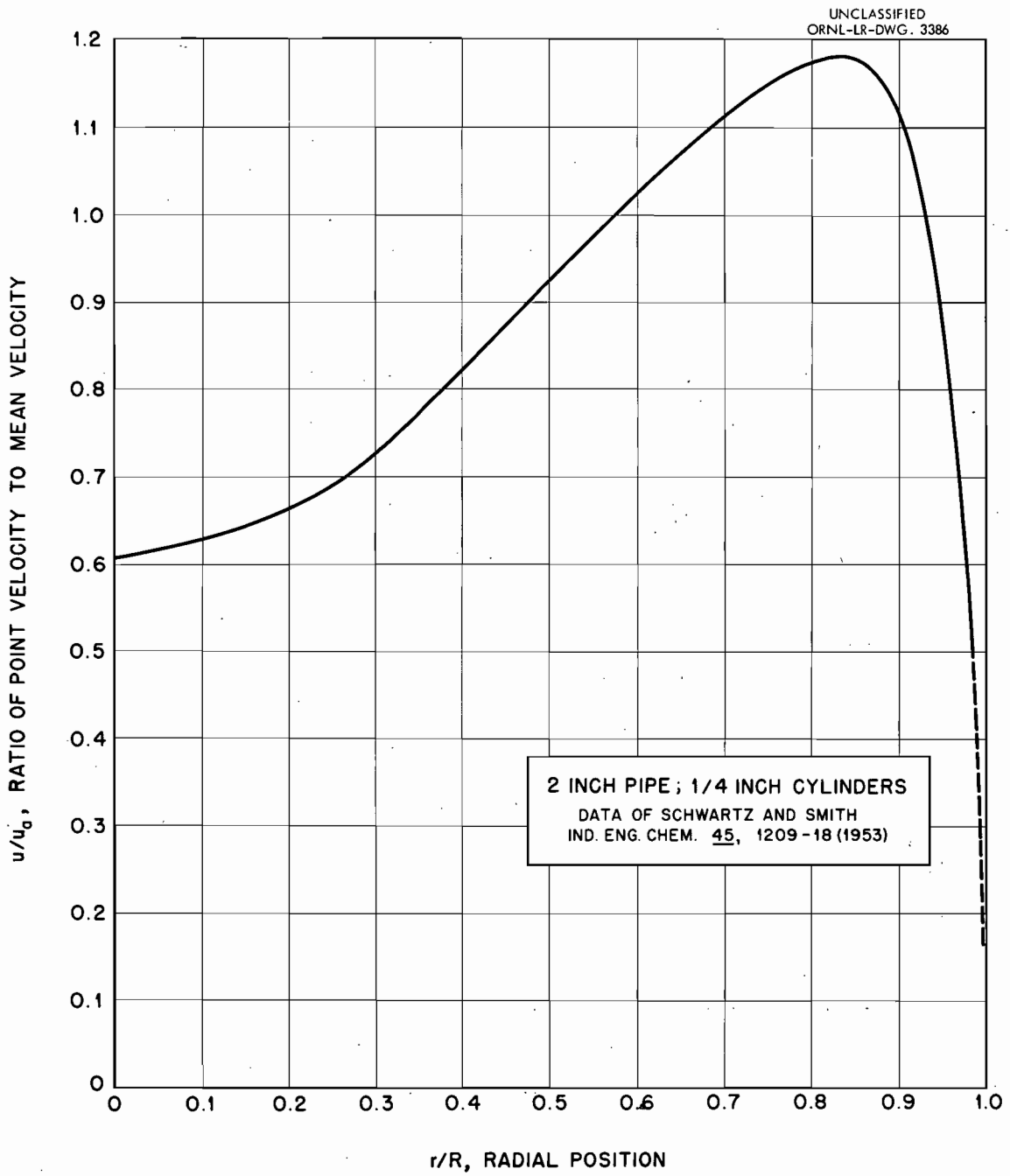

Figure 19

Variation Of The Ratio Of Point To Mean Velocity As A Function Of Radial Position Ratio In A 2 Inch Pipe Packed With 1/4 Inch Cylinders.

and packed with 1/8 inch cylinders), is representative of the flow distribution that would prevail in the recombiner experiments if the velocity profile were permitted to become fully developed. When the consequences of such a drastically non-uniform velocity profile are considered, some serious doubts may arise concerning the validity of the interpretations that have been made from the data. For example, if Figure 19 is a true representation of the recombiner velocity profile and a form similar to equation (48 or 49), but with altered constants, applies as a point rather than overall relationship for stating magnitudes of mass transfer coefficients, the conclusion is that the rate of recombination varies with the radial position as well as axial distance along the bed. This means that across a plane perpendicular to the flow the fraction of recombination will vary with radial distance instead of being constant. Further, because of the varying mass transfer rates and residence times it is even conceivable for a situation to arise where some annular sections of the bed are operating as two zones whereas other annular sections in the same bed are operating as one zone. Even more disturbing is the possible circumstance wherein a casual overall treatment of the data for a run indicates that the bed operation is entirely oxygen diffusion controlled, yet some portions of the bed actually involve a mechanism change-over, and exhibit two zones. It is now apparent that the assumption of a uniform velocity profile is quite bold. The question that arises at this point is how much confidence can be placed in the derived mass transfer coefficients and the analysis that has been made from them. The more immediate practical question is what modifications are necessary to apply the findings of this investigation to the design of large recombiner units wherein flat velocity profiles are encountered.

One immediate conclusion is that any of the derived mass transfer coefficients is actually an equivalent or mean quantity. Thus the result of a detailed computation for a particular experiment which treats the recombiner as a set of annular reaction beds should lead to the same value as the simple overall treatment. A numerical example makes this argument more convincing, and also demonstrates the variation of bed performance with radial position. For this purpose, run No. 3 of April 16 is taken as an example. For this run the pertinent quantities are:

$H_0 = 0.0647$; $O_0 = 0.0433$; $V_0 = 6.19 \times 10^{-4}$ lb mole/sec;

$T_g = 685°$ K; $P = 30$ psia; $H_2 = 0.0143$; ($H_1 = 0.0097$)

An overall treatment of the experimental data indicates that the recombiner is operating <u>entirely within the oxygen diffusion controlled region</u>.

The bed is first broken down into a set of 20 zones, each having a cross-sectional area designated as Δa. Using the value of $K_{L_1} = 4.34 \cdot 10^{-2} (G/M_m)_1 (1-v)^{0.2} (Sc)_1^{-2/3} (Re)_1^{-0.41}$ as derived from the data, this expression, coupled with the Schwartz-Smith data shown in Figure 19, is used to calculate the point mass transfer coefficients for the various annular zones. Corresponding values of V_0 are calculated for each of these zones and are designated as V_r. Now, to develop the operating details it is necessary

to use equation (41a) for predicting the performance of annular beds operating entirely in the oxygen diffusion controlled zone and equation (44b) for those which include both zones. For the case at hand, the specific formulations that apply are

$$\frac{J\Delta aLK_{L_1}}{V_r} = 2\,\frac{0.0647-H_2}{1-0.5H_2} - 0.0220 \ln \frac{1}{\dfrac{1-0.115(0.0647-H_2)}{(1-0.5H_2)}} \quad \text{for } H_2 > 0.0097 \tag{58}$$

$$\frac{J\Delta aLK_{L_1}}{V_r} = 0.0883 + 0.448\left[\frac{0.0973(0.0097-H_2)}{(1-0.5H_2)} + 0.0220 \ln \frac{0.0097(1-0.5H_2)}{H_2}\right] \quad \text{for } H_2 < 0.0097 \tag{59}$$

To simplify the solution of these for H_2, the curves given in Figure 20 are convenient, in that they permit a direct calculation. The value of the argument $J\Delta aLK_{L_1}/V_r$ for a specific annular portion determines the value of H_2, and this value can be read from Figure 20 for each of the annular zones, which process develops the radial hydrogen concentration profile in the recombined stream. Taking into account the various mole flow rates, when the final H_2 values are averaged, this computation leads to a mean discharge gas hydrogen concentration slightly less than the observed figure of 0.0143. On the other hand, when 98 per cent of the derived K_{L_1} (i. e. $0.98 \cdot 4.34 \times 10^{-2} = 4.25 \times 10^{-2}$) is used to estimate the point mass transfer coefficients, the calculated mean discharge hydrogen mole fraction agrees with the observed value of 0.0143. The results of the estimates are summarized in Figure 21 where the expected variation of discharge stream hydrogen mole fraction and point mass transfer coefficients as a function of radial position are delineated. This chart indicates the complex character of the operation occurring in a well behaved small catalytic recombiner. Because of the presence of the thermocouple well and lack of hydrodynamic profile development in the experimental recombiner unit, the conditions pictured probably do not describe the actual operations too closely.

The conclusion to be drawn from these speculations is that mass transfer coefficients developed from small scale experimental equipment are entirely reliable and can be used without modification for designing large recombiners. This presumes, however, that the flow channel and entrance sections of these test units are properly arranged to avoid the presence of "blind zones" and unusual lop-sided velocity profiles. In this connection the 98 per cent factor mentioned stems from a defect in the Schwartz-Smith curve. Integration of their velocity profile data to calculate the total volumetric flow rate indicates that their curve has been drawn so as to involve an inherent error of approximately 3 per cent in the calculated total flow, and it is this which eventually generates the 98 per cent factor.

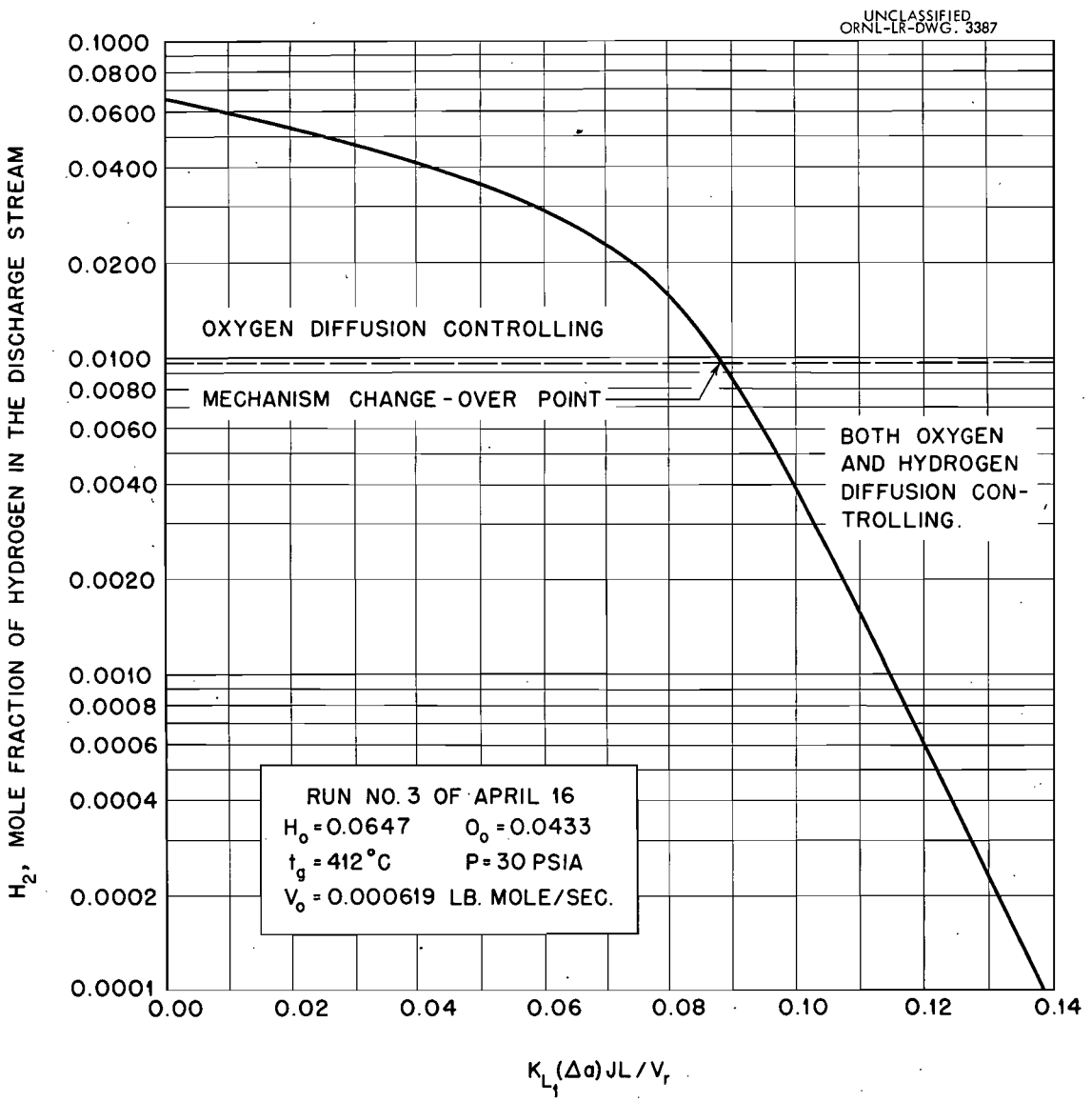

Figure 20

Numerical Solution Of The Catalytic Bed Equation For Run No. 3 Of April 16.

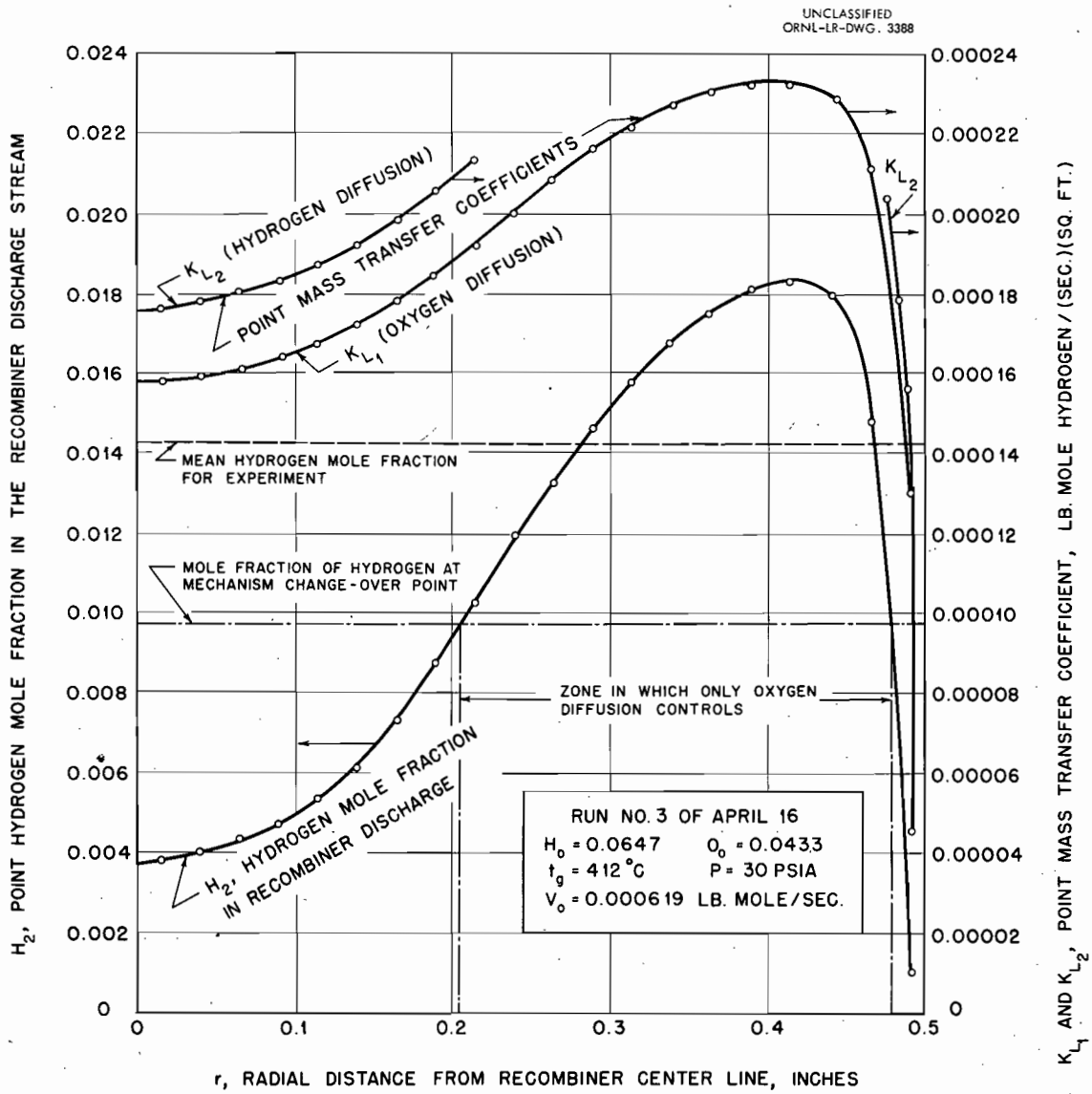

Figure 21

Calculated Variation Of Discharge Stream Hydrogen Mole Fraction And Dual-Langmuir Point Mass Transfer Coefficient With Radial Position For Run No. 3 Of April 16.

RECOMMENDATIONS FOR FUTURE EXPERIMENTATION

It is to be emphasized that the investigations of Ransohoff and Spiewak, which were carried out primarily to gather experience on the operation of a catalytic recombiner, contribute very much to our understanding of the mechanisms involved in the platinum catalyzed oxidation of hydrogen. Compared to similar mass transfer and reaction kinetics studies on catalyzed exothermic reactions that have been reported, their data are quite excellent, and their investigations constitute a significant technical contribution.

Some improvements of the experimental setup in future investigations have been alluded to, and are virtually self evident. Future catalytic experimental recombiners should be more differential in character to make their operation more nearly isothermal, and temperature measurements should be made in the gas streams rather than by incorporating relatively large thermocouples into the catalytic section. This would tend to reduce channeling in the system and make all of the catalyst equally available to the feed stream. This would also tend to increase the confidence in the data observed insofar as "scale-up" procedures are concerned. Finally, future beds should be provided with adequate fore-sections of packed but uncatalyzed straight-runs of sufficient length to insure operation with fully developed velocity profiles in the test recombiner unit. This would aid materially in making more satisfactory analyses of the data.

As has been pointed out, the present justification for the use of the 2/3 power on the Schmidt number in the correlations is not completely satisfactory. This power was used primarily because the confidence in the Gamson correlation was somewhat greater than it was in the reported recombiner data. Several carefully controlled and executed experiments would clarify this point. Two series of runs comprising about 15 runs for each series should be carried out at constant Reynolds numbers in the neighborhodd of 500 and 5000 with initial mixtures containing varied ratios of initial oxygen to hydrogen in the range $O_0/H_0 = 0.5$ to 3, with a substantial number of runs conducted so as to reduce the final hydrogen concentration well below the mechanism change-over point. This would necessitate operation with several bed lengths instead of merely one. Such operations would require scrupulous care in making sure that the activity level of the catalyst used in these runs is maintained constant. The data obtained from such a study would be tested by equation (47) to develop the proper Schmidt number exponent. The value of 2/3 is indicated from other considerations and probably will be vindicated. Such an analysis would also lend more justification to the assumed diffusional nature of the process.

The assumed 0.41 exponent on the Reynolds number should also be tested. To do this, two series of runs, each at a constant Schmidt number, are recommended. Each of the series should comprise about 12 runs over the Reynolds number range 200 to 8000, one series being for a bed operated entirely within the oxygen diffusion controlling range (suggested $O_0/H_0 = 0.5$, $Sc \approx 0.78$), The other being entirely within the hydrogen diffusion controlling zone (suggested $O_0/H_0 = 3$, $Sc \approx 0.23$). The Reynolds number variation preferably should be obtained by regulating the flow rate rather than by varying the temperature level of operations. This is to minimize the masking of

diffusional effects by the surface chemical aspects, the chemical features being quite temperature sensitive as indicated by the previous discussion. The maintenance of virtually isothermal conditions and constant flow rate over the wide range of operation suggested makes this quite a task to carry out.

As indicated in the discussions dealing with the dual-Langmuir mechanism proposed, the analysis indicates a possible pressure dependence of the recombiner bed. Further, if some scatter in the values for the runs of April 22, 23, and 30 are overlooked, the data of Ransohoff and Spiewak show a small regular pressure dependence of the derived mass transfer coefficients. The effect is negligible for the pressure range 30-110 psia investigated insofar as design considerations for this range are concerned, but it may be sufficiently important as to invalidate extrapolation of the recommended design procedure to extreme pressures. For this reason this question should be settled by performing additional experiments. Since the pressure sensitivity is suspected on theoretical counts as well as from experimental evidence for the hydrogen diffusion controlled portion, the work may be confined to gas mixtures with $O_0/H_0 > 3$, so as to study the influence of pressure on operations entirely in the second zone. The data resulting from such tests could be treated directly and more confidently than data derived from a bed operating within both zones, for the various effects can be isolated from each other with greater certainty. The suggested pressure range for this study is 30-1200 psia.

REFERENCES CITED

1. Bird, R. B., Hirschfelder, J. O., and Curtiss, C. F., "Survey Of The Equation Of State And Transport Properties Of Gases and Liquids", Proceedings Of The Third Midwestern Conference On Fluid Mechanics, University Of Minnesota Book Store 1953, pp. 1-84.

2. Ercan, S. A., "Viscosity Of Gases And Gas Mixtures", M. S. Ch. E. Thesis, University of Tennessee, December 1953, pp. 46, 62, 68, 74.

3. Gamson, B. W., "Heat And Mass Transfer-Fluid Solid Systems", Chemical Engineering Progress 47, 19-28 (1951).

4. Glasstone, S., Laidler, K. J., and Eyring, H., "The Theory Of Rate Processes", McGraw Hill Book Co., Inc., New York 1941, pp. 14.

5. Hinshelwood, C. N., "Kinetics Of Chemical Change", Oxford University Press 1940, pp. 198-201.

6. Hirschfelder, J. O., Bird, R. B., and Spotz, E. L., "Viscosity And Other Physical Properties Of Gases And Gas Mixtures", Transactions Of The American Society Of Mechanical Engineers 71, 921-37 (1949).

7. Hirschfelder, J. O., Curtiss, C. F., and Bird, R. B., "Molecular Theory Of Gases And Liquids", John Wiley and Sons, Inc., New York 1954, pp. 528-533 (viscosities), 538-539 and 566-573 (diffusivities), 1110-1111 (force constants), 1126-1127 (collision integrals).

8. Keenan, J. H., and Keyes, F. G., "Thermodynamic Properties Of Steam", John Wiley and Sons, Inc., New York 1936, pp. 42-53.

9. Langmuir, I., "The Mechanism Of The Catalytic Action Of Platinum In The Reactions $2CO + O_2 = 2CO_2$ and $2H_2 + O_2 = 2H_2O$", Transactions Of The Faraday Society 17, 621-54 (1921-22).

10. Ransohoff, J. A., Personal communication, May 12, 1953.

11. Ransohoff, J. A., and Spiewak, I., "Development Of Hydrogen Oxygen Recombiners", Progress Report Oak Ridge National Laboratory 1583, October 12, 1953, SECRET, pp. 24-47, 64-76.

12. Schwartz, C. E., and Smith, J. M., "Flow Distribution In Packed Beds", Industrial And Engineering Chemistry 45, 1209-18 (1953).

13. Spiewak, I., Personal communication, May 19, 1954.

14. Thacker, C. M., Folkins, H. O., and Miller, E. L., "Free Energies Of Formation Of Gaseous Hydrocarbons And Related Substances", Industrial And Engineering Chemistry 33, 584-90 (1941).

TABLE OF SYMBOLS

Symbol	Meaning
a	Cross-sectional area of catalyst bed, sq ft
Δa	Cross-sectional area of an annular portion of the catalyst bed, sq ft
B	Ideal gas law constant, (psi)(cu ft)/(lb mole)(°K)
C_p	Molal heat capacity at constant pressure, cal/(mole)(°K)
D	Diffusion coefficient, sq ft/sec or sq cm/sec
D_p	Equivalent spherical diameter of catalyst pellets, ft
D_{ig}	Diffusivity of component i in the gas mixture, sq ft/sec
D_{if}	Diffusivity of component i in the film mixture, sq ft/sec
D_{ij}	Diffusion coefficient for the binary system i-j, sq ft/sec
e	Natural logarithm base
f	Fraction of completion of recombination of hydrogen, considered variable
f_2	Fraction of completion of recombination of hydrogen in the recombiner discharge stream
F	Volumetric gas feed rate to the recombiner, standard conditions cfm
G	Superficial mass velocity of gas flow through the recombiner lb/(sec)(sq ft)
H	Variable hydrogen mole fraction in the gas stream
H_0	Mole fraction of hydrogen in the feed stream
H_1	Mole fraction of hydrogen in the gas stream at the mechanism change-over point
H_2	Mole fraction of hydrogen in the recombiner discharge stream
H_m	Mean mole fraction of hydrogen in the diffusion film
ΔH	Heat of combustion of hydrogen, cal/mole
ΔH_0	Standard heat of combustion of hydrogen at 298.1° K, cal/mole
J	Catalyst superficial specific surface, sq ft/cu ft
k	Boltzmann constant, 1.38×10^{-16} erg/°K
K	Mass transfer coefficient, generalized connotation, lb mole hydrogen/(sec)(sq ft)(driving force)
K_1	Mass transfer coefficient for zone 1 for Case III, lb mole hydrogen/(sec)(sq ft)(mole fraction of oxygen)
K_2	Mass transfer coefficient for zone 2 for Case III, lb mole hydrogen/(sec)(sq ft)(mole fraction of hydrogen)
K_H	Mass transfer coefficient for Case II, lb mole hydrogen/(sec)(sq ft)(mole fraction of hydrogen)
K_ℓ	Mass transfer coefficient for Case IV, lb mole hydrogen/(sec)(sq ft)(oxygen mole fraction/hydrogen mole fraction)
K_{L_1}	Mass transfer coefficient for zone 1 for Case V, lb mole hydrogen/(sec)(sq ft)(oxygen mole fraction/hydrogen mole fraction)

Symbol	Meaning
K_{L_2}	Mass transfer coefficient for zone 2 for Case V, lb mole hydrogen/(sec)(sq ft)(hydrogen mole fraction/oxygen mole fraction)
K_O	Mass transfer coefficient for Case I, lb mole hydrogen/(sec)(sq ft)(mole fraction of oxygen)
L	Length of packed section of recombiner, ft
L_1	Length of recombiner bed operating in zone 1, ft
L_2	Length of recombiner bed operating in zone 2, ft
M	Molecular weight, general connotation
M_i	Molecular weight of the i-th component
M_m	Mean molecular weight of the gas stream
M_0	Mean molecular weight of the gas fed to the recombiner
n	Exponent
N_{ij}	Elements in the determinants used in evaluating viscosities of multicomponent mixtures
O	Variable oxygen mole fraction in the gas stream
O_m	Mean mole fraction of oxygen in the diffusion film
O_0	Mole fraction of oxygen in the feed stream
P	Pressure of the system, psia (or atm)
r	Radial distance from center-line of the recombiner, ft
r_{ii}	Low velocity head-on collision diameter for an i-i encounter, Angstrom units
r_{ij}	Low velocity head-on collision diameter for an i-j encounter, Angstrom units
r_0	Low velocity head-on collision diameter, Angstrom units
R	Radius of the recombiner bed, ft
Re	Reynolds number, generalized connotation
Re_1	Reynolds number for zone 1
Re_2	Reynolds number for zone 2
Sc	Schmidt number, generalized connotation
Sc_1	Schmidt number for the diffusion film for zone 1
Sc_2	Schmidt number for the diffusion film for zone 2
t	Temperature, °C
t_b	Catalyst bed temperature read by thermocouple, °C
t_g	Mean gas stream temperature, $0.5(t_b + t_2)$, °C
t_0	Temperature of the feed stream, °C
t_2	Temperature of recombined gases, °C
T	Temperature, °K
ΔT	Calculated adiabatic process temperature rise, °K
T_g	Mean gas stream temperature, °K
u	Variable velocity of the gas stream, ft/sec
u_a	Mean gas stream velocity, ft/sec
v	Fraction of voids in the catalyst bed for gas flow
V	Variable gas mole flow rate through the recombiner, lb mole/sec
V_0	Feed gas mole flow rate into the recombiner, lb mole/sec

Symbol	Meaning
V_r	Variable gas mole flow rate through an annular section of the bed having an area Δa and located at a radial distance r from the bed center-line, lb mole/sec
$W^{(1)}(1;kT/\epsilon)$	Collision integral
$W^{(2)}(2;kT/\epsilon)$	Collision integral
x_i	Mole fraction of component i in the gas mixture
x_j	Mole fraction of component j in the gas mixture
Y_{ij}	Transport parameter used in evaluating gas viscosities
z	Compressibility coefficient
Z_{ij}	Transport parameter used in evaluating gas viscosities
α	Characteristic constant, determined by feed stream composition, $(O_0-0.5H_0)/(1-0.5H_0)$
β	Characteristic constant, determined by feed stream composition, $(H_0-H_1)/(1-0.5H_1)$
γ	Characteristic constant, determined by feed and discharge stream composition, $(H_0-H_2)/(1-0.5H_2)$
δ	Diffusivity coefficient ratio, D_{12}/D_{13}
ϵ	Low velocity maximum interaction energy, ergs
ϵ_{ii}	Low velocity maximum interaction energy for an i-i encounter, ergs
ϵ_{ij}	Low velocity maximum interaction energy for an i-j encounter, ergs
η	Surface reaction factor, fraction of hydrogen-surface-adsorbed-oxygen collisions that result in recombination
Θ	Fraction of catalyst surface that is bare
Θ_i	Fraction of catalyst surface that is occupied by component i
λ_i	Moles of species i impinging on the catalyst, lb moles/(sec)(sq ft)
μ	Gas viscosity, generalized connotation, lb/(ft)(sec)
μ_i	Viscosity of the i-th component, lb/(ft)(sec)
μ_f	Viscosity of the diffusion film, lb/(ft)(sec)
μ_m	Viscosity of the gas stream, lb/(ft)(sec)
ν_i	Surface evaporation rate of the i-th component when completely covering the catalyst surface, lb moles/(sec)(sq ft)
ξ_i	Surface factor for condensation of the i-th component, fraction of molecules of component i that adhere to the catalyst surface out of the total of those that impinge on the surface
π	3.14159
ρ	Gas density, generalized connotation, lb/(cu ft)
ρ_f	Density of the diffusion film, lb/(cu ft)
ϕ	Surface effectiveness factor for gas flow, 0.91 for cylinders packed in random fashion

Symbol	Meaning
Φ	Driving force, generalized connotation
Ψ	Transport property correlation factor, used in computing viscosities
ω	Recombination speed of reaction, lb mole hydrogen/(sec) (sq ft catalyst)

Subscript Notation

1	For component, refers to water or steam; also refers to zone 1 of the recombiner bed
2	For component, refers to hydrogen; also refers to zone 2 of the recombiner bed
3	Refers to oxygen
f	Refers to diffusion film
g	Refers to gas mixture
m	Refers to mean value, or to gas stream